The Role and Regulation of the Slc38a3 (SNAT3) Glutamine Transporter in the Mouse

Dissertation

zur

Erlangung der naturwissenschaftlichen Doktorwürde

(Dr. sc. nat.)

vorgelegt der Mathematisch-naturwissenschaftlichen Fakultät

der Universität Zürich

von

Stephanie Marie Busque

aus den USA

Promotionskomitee:

Prof. Dr. Carsten A. Wagner

Prof. Dr. Jürg Biber

Prof. Dr. Johannes Loffing

Prof. Dr. Hannelore Daniel

Zürich, 2009

TABLE OF CONTENTS

Summary……2

Deutsche Zusammenfassung der Doktorarbeit……..6

I. Introduction: Renal ammoniagenesis……....10

II. Regulation of renal ammonium production…….…..12

III. Renal ammonium handling……....14

III.1. The Proximal Tubule……....14

III.2. The Loop of Henle……....15

III.3. The Collecting Duct……..16

IV. AIM I: Potassium restriction, high protein intake and metabolic acidosis increase expression of the glutamine transporter SNAT3 (Slc38a3) in mouse kidney

IV.1. Dietary effecters of acid-base homeostasis……...18

IV.2. Amino acid transporters involved in acid-base balance……....19

IV.3. Publication related to AIM I……23

V. AIM II: Dysregulation of the glutamine transporter SNAT3 (Slc38a3) and ammoniagenic enzyme in obese, insulin-resistance mice

V.1. Diabetes mellitus and uric acid nephrolithiasis……....49

V.2. Insulin action in the kidney……..50

V.3. Manuscript submitted related to AIM II……..51

VI. AIM III: Characterization of a novel ENU-mutated mouse model of SNAT3 (Slc38a3)

VI.1. Introduction……..83

VI.2. Materials and methods……....85

VI.3. Preliminary results……...90

VI.4. Discussion……94

VI.5. Figures legends..……...97

VII. Dissertation discussion……101

VIII. References……103

IX. Acknowledgements……..119

X. Curriculum Vitae……..120

XI. List of publications……...122

Summary

Ammoniagenesis occurs at the site of renal proximal tubule and is essential for correcting disturbances in acid-base homeostasis. These disturbances can manifest with changes in diet, physical activity or during various disease states. Glutamine is the critical substrate for renal ammoniagenesis and gluconeogenesis; each molecule of glutamine transported into the proximal tubule cell is ultimately converted into ammonium and bicarbonate, restoring systemic acid-base balance. The sodium-coupled, neutral amino acid transporter, Slc38a3 (SNAT3) has been localized to the basolateral membrane of the proximal tubule cell and is purported to be the transport mechanism that allows glutamine entry into the cell to generate ammonium. We have shown that SNAT3, as well as two important enzymes involved in renal ammoniagenesis and gluconeogenesis, namely phosphate-dependent glutaminase (PDG) and phosphoenolpyruvate carboxykinase (PEPCK) exhibit increased mRNA expression and protein levels after a dietary acid challenge. Along this line, recent clinical studies have identified a link between type II diabetes mellitus and an increased prevalence of uric acid nephrolithiasis in humans. These subjects have reduced renal ammonium excretion; however the etiology of these defects is unknown and may be related to defective ammoniagenesis and SNAT3 function or regulation.

In lieu of these observations, the aim of this dissertation was thus three-fold. First, we sought to elucidate the role of SNAT3 in ammoniagenesis during potassium restriction or excess protein intake; two known effecters of acid-base homeostasis. Second, we created a murine model of diet-induced obesity to determine if an ensuing insulin-resistant state could alter renal ammoniagenesis, which could explain the development of nephrolithiasis and reported urinary changes in diabetic individuals. Third, we developed an ENU mutagenesis mouse model for SNAT3 in order to clarify the role of this transporter *in vivo.*

Both potassium depletion and high dietary protein intake are known to elevate renal ammonium excretion. For our first experimental aim, we examined SNAT3, phosphate-dependent glutaminase (PDG), and phosphoenolpyruvate carboxykinase (PEPCK) regulation during a control (0.36%) or low K^+ (0.02%) diet for 7 or 14 days; or

a control (20%) or high protein (50%) diet for 7 days. Metabolic acidosis was induced in control and low K^+ groups by administration of NH_4Cl to the drinking water. We observed that urinary ammonium excretion increased during metabolic acidosis, K^+ restriction alone after 14 days, and during high protein intake. SNAT3, PDG and PEPCK mRNA abundance was elevated in metabolic acidosis and 14 day K^+ restriction but not during high protein intake. SNAT3 protein abundance was enhanced during metabolic acidosis (both control and low K^+), 14 day low K^+ treatment alone, and during high protein intake. Seven day dietary K^+ depletion alone had no effect. Immunohistochemical studies showed SNAT3 staining in earlier parts of the proximal tubule during 14 day K^+ restriction with or without NH_4Cl treatment and during high protein intake. In sum, chronic dietary K^+ restriction, high protein intake and metabolic acidosis enhance ammoniagenesis paralleled by increased SNAT3 expression.

To further investigate the role of SNAT3 during renal ammoniagenesis, we employed a murine model of diet-induced obesity for our second aim. The study design was based on reports that the prevalence of uric acid nephrolithiasis among patients with type 2 diabetes and metabolic syndrome is highly correlated with a more acidic urine and lower urinary ammonium excretion; the etiology is likely associated with insulin resistance. Insulin has been shown to stimulate ammoniagenesis in renal cell lines, possibly via increased phosphate-dependent glutaminase (PDG) activity and glutamine metabolism. We placed C57BL6 mice on either a control (standard mouse chow) or "cafeteria" style diet for 10 weeks to induce obesity and insulin resistance. Intraperitoneal glucose tolerance tests (IPGTT) were performed and animals were subsequently assigned to various groups: control with normal IPGTT; **o**bese, **g**lucose-**i**ntolerant animals with abnormal IPGTT (O-GI); or moderate weight animals with normal IPGTT (**N**on-**R**esponders, NR). Groups were divided into subgroups and NH_4Cl was added to the food for the final 48 h. We found that basal urinary ammonium excretion was unremarkable among groups. Providing an acid challenge with NH_4Cl increased urinary ammonium excretion in all groups, but to a lesser extent in the O-GI group. SNAT3 mRNA expression was remarkably enhanced in both cafeteria-diet treated groups. PDG expression was strongly elevated only in the O-GI group given NH_4Cl, whereas PEPCK was enhanced in both O-GI and NR groups given NH_4Cl.

Na^+/H^+ Exchanger (NHE) activity in the brush border membrane of the proximal tubule was strongly reduced in the O-IR group indicative of a lower capacity to excrete ammonium. These data suggest that obesity and insulin resistance impairs renal ammonium excretion in response to NH_4Cl feeding through reduced NHE3 activity. Upregulation of SNAT3 and ammoniagenic enzymes suggest a possible compensatory mechanism involved in O-GI mice.

Our interest in characterizing the role of SNAT3 during renal ammoniagenesis and metabolic acidosis led us to develop a novel genetic mouse model to clarify the role of SNAT3 *in vivo*. Male mice were treated with the potent mutagen *N*-ethyl-*N*-nitrosourea (ENU), resulting in offspring carrying a single nucleotide polymorphism ("C" to "T" mutation) known as "SLC38a3-Q263X". This mutation creates a premature stop codon deleting the second half of the SNAT3 protein. A total of 52 pups from five litters have been analyzed for this study. Pups were sacrificed between postnatal-day 15-18, since mutant mice died shortly thereafter. Tissues, serum and urine were collected and analyzed.

SNAT3 protein abundance in both kidney and liver was undetectable in mutant mice using antibodies directed towards both the C- and N-terminus of the SNAT3 protein, demonstrating that the mutation indeed leads to ablation of the protein. Mutant mice weighed less than littermates, exhibited reduced urinary NH_4^+ and urea excretion and had elevated serum urea. Renal SNAT3 mRNA expression was significantly lower in mutants, while PDG and PEPCK mRNA expression remained unchanged. Mutant mice showed enhanced PDG protein levels, while PEPCK remained unchanged in kidney.

Interestingly, heterozygous mice showed reduced renal and hepatic SNAT3 protein levels in comparison to wildtype mice; this prompted further investigation. After an NH_4Cl acid challenge, heterozygous mice showed enhanced SNAT3, PDG and PEPCK mRNA expression, however no changes were observed in NHE3 activity, the apical NH_4^+ efflux pathway in the proximal tubule.

These data suggest that the absence of functional SNAT3 is lethal in mice. Mutant mice are smaller, display abnormal neurological behavior, and have altered regulation of renal ammoniagenic/gluconeogenic enzymes as well as reduced urinary ammonium and

urea excretion. Heterozygous mice showed regulatory changes in SNAT3, PDG and PEPCK, perhaps as a compensatory mechanism to account for the partial defect in SNAT3.

In conclusion, the data presented herein show strong evidence that SNAT3 is likely the glutamine influx mechanism in renal proximal tubule cells for the production of ammonia.

Deutsche Zusammenfassung der Doktorarbeit

Der proximale Tubuls synthetisiert Ammonium, das essentiell für die Korrektur von Säure-Basenstörungen ist. Solche Störungen treten auf infolge Veränerungen in der Diät, der körperlichen Aktivität oder während verschiedener Erkrankungen. Glutamin dient als Substrat für die renale Ammoniagenese und auch Glukoneogenese, aus jedem Molekül Glutamin, das in die Zellen des proximalen Tubulus aufgenommen worden ist, kann nach Ammonium und Bikarbonat enstehen und damit die Säure-Basenbalance wiederhergestellt werden.

Der Natrium-gekoppelte Aminosäuretransporter Slc38a3 (SNAT3) wurde an der basolateralen Membran des proximalen Tubulus lokalisiert und gilt als Kandidat für die Aufnahme von Glutamin in die Zelle für Ammoniagenese. Wir haben bereits gezeigt, dass SNAT3 und zwei wichtige Enzyme der Ammoniagenese und Glukoneogenese, die Phosphat-abhängige Glutaminase (PDG) und die Phosphoenolpyruvatkarboxykinase (PEPCK), verstärkt exprimiert werden unter einer Säurebelastung. In die gleiche Richtung gehend, haben verschiedene neuere klinische Studien gezeigt, dass es eine Korrelation zwischen Typ II Diabetes und dem erhöhten Auftreten von Uratnierensteinen bei Patienten besteht. Diese Patienten haben eine verminderte Ammoniumausscheidung im Urin, allerdings ist die Ursache für diesen Defekt nicht bekannt, ein Zusammenhang mit veränderter Ammoniagenese und SNAT3 Funktion oder Regulation ist möglich. Aufgrund dieser Beoachtungen hatte die vorliegende Dissertation drei Ziele. Erstens versuchten wir die Rolle von SNAT3 während vermehrter Ammoniagenese stimuliert durch Kaliumrestriktion oder vermehrter Eiweisszufuhr zu klären. Zweitens, wollten wir ein Mausmodell für Diät-induzierte Adipositas etablieren um zu testen, inwiefern ein Insulin-resistenter Zustand die renale Ammoniagenese beeinflusst um zu sehen, ob dies das vermehrte Auftreten von Uratnierensteinen bei Diabetikern miterklären könnte. Als drittes Ziel, charakterisierten wir ein durch NEU-Mutagenese enstandenes Mausmodell defizient für SNAT3 um die Funktion dieses Transporters in vivo zu untersuchen. Sowohl Kaliumrestriktion als auch Proteinzufuhr verusachen erhöhte Ammoniumausscheidung. Im ersten Teilprojekt untersuchten wir SNAT3, PDG und PEPCK während einer Kontrolldiät (0.36% Kalium) oder einer Niedrigkaliumdiät

(0.02% Kalium) für 7 oder 14 Tage. Ausserdem wurde noch in einer Subgruppe metabolische Azidose durch die Gabe von NH_4Cl im Trinkwasser verursacht. Die renale Ammoniumausscheidung wurde stimuliert während metabolischer Azidose und Kaliumreskrition für 14 Tage, sowie durch Proteinzufuhr. SNAT3, PDG und PEPCK mRNA Expression wurde erhöht durch metabolische Azidose und Kaliumrestriktion, nicht aber durch Proteinzufuhr. Die Proteinexpression von SNAT3 war vermehrt während metabolischer Azidose, 14 Tage Kaliumrestriktion und durch proteinzufuhr. Eine 7-tägige Kaliumrestriktion hatte keine Wirkung. Immunhistochemie zeigte, dass SNAT3 auch in den früheren Anteilen des proximalen Tubulus exprimiert wurde während dieser Maneuver. Zusammenfassend lässt sich sagen, dass die erhöhte Ammoniagenese und Ausscheidung in diesen Situation mit der erhöhten SNAT3 Expression korreliert.

Um die Rolle von SNAT3 in der renalen Ammoniagenese im zweiten Teilprojekt weiter zu untersuchen, entwickelten wir ein Mausmodell für Diät-induzierte Adipositas. Diese Studie basiert auf der Beobachtung, dass das Auftreten von Uratnierensteinen bei Patienten mit Typ II Daibetes und metabolischem Syndrom sehr stark korreliert mit einem sauren Urin pH und niedriger Ammoniumausscheidung. Die Ursache ist vermutlich Insulinresistenz. Insulin stimuliert in renalen Zelllinien die Ammoniagenese, vermutlich via vermehrte PDG Aktivität und erhöhten Glutaminmetabolismus. C57BL6 Mäuse erhielten entweder eine Standarddiät oder eine “Cafeteria” Diät für 10 Wochen um Adipositas und Insulinresistenz zu induzieren. Ein intraperitonealer Glukosetoleranztest (IPGTT) wurde durchgeführt und die Tiere anschliessend in verschiedene Gruppen eingeteilt: Kontrolltiere mit normalen IPGTT; **o**bese, **g**lucose-**i**ntolerant (adipöse, Glukose-intolerante) Tiere mit pathologischem IPGTT (O-GI); oder Tiere mit moderatem Gewichtsanstieg und normalen IPGTT (**N**on-**R**esponders, NR). Diese drei Gruppen wurden weiter unterteilt und jeweils die eine Hälfte noch zusätzlich mit NH_4Cl im Futter für die letzten 48 Stunden behandelt. Die basale Ammoniumausscheidung war in allen Gruppen gleich. Jedoch die Gabe von NH4Cl verusachte in der O-GI Gruppe einen geringeren Ammoniumanstieg im Urin. SNAT3 mRNA Expression war deutlich erhöht in den Cafeteria-Diät Gruppen. PDG mRNA Expression war deutlich erhöht, aber nur in der O-GI Gruppe, während PEPCK erhöht

war in beiden O-GI und NR Gruppen unter NH_4Cl Gabe. Na^+/H^+ Austauscher (NHE) Aktivität in der Bürstensaummembran des proximalen Tubulus war deutlich reduziert in der O-IR Gruppe, ein Hinweis auf einer verminderte Kapazität Ammonium auszuscheiden. Diese Daten deuten darauf hin, dass Adipositas und Insulinresistenz die renale Ammoniumausscheidung bei NH_4Cl Beladung vermindert. Die erhöhte Expression von SNAT3 und der Ammonigeneseenzyme deuten auf einen kompensatorischen Mechanismus hin.

Im dritten Teilprojekt charakterisierten wir eine neue genetisch veränderte Maus um die Rolle von SNAT3 in der renalen Ammoniagenese und während metabolsicher Azidose zu untersuchen. Männliche Mäuse wurden mit dem potenten Mutagen *N*-ethyl-*N*-nitrosourea (ENU) behandelt. Dies führte dazu, dass die Nachfahren einen „single nucleotide polymorphism“ (“C” zu “T”) tragen, auch “SLC38a3-Q263X” benannt. Diese Mutation führt zu einem vorzeitigen Stopkodon, das die zweite Hälfte des SNAT3 Protein entfernt. Wir untersuchten insgesamt 52 junge Mäuse aus 5 Würfen. Die jungen Mäuse wurden zwischen dem 15. Und 18. postnatalen Tag getötet, da die mutierten Mäusen kurze Zeit spatter starben. Gewebe, Urin und Blut wurde gesammelt und untersucht. Das SNAT3 Protein konnte in Niere und Leber mittels Antikörper gegen den Karboxy oder Amino-terminus nicht entdeckt werden, ein Nachweis, das die Mutation zum Verlust des SNAT3 Proteins führt. Mutierte Mäuse hatten ein niedrigeres Gewicht als Geschwister, eine niedrigere Ammonium- und Harnstoffausscheidung im Urin und erhöhte Serumharnstoffwerte. Die renale SNAT3 mRNA Expression war reduziert, während PDF und PEPCK mRNA Expression normal waren. Allerdings hatten mutierte Mäuse eine erhöhte PDG Proteinexpression, die PEPCK Proteinexpression blieb normal.

Interessanterweise hatten heterozygote Mäuse eine reduzierte renale und hepatische SNAT3 Proteinexpression. Daher untersuchten wir die Folgen einer Säurebeladung mit NH_4Cl. Heterozygote Mäuse hatten eine erhöhte SNAT3, PDG und PEPCK mRNA Expression, die NHE3 Aktivität war jedoch unverändert.

Unsere Daten zeigen, dass das Fehlen von SNAT3 in Mäusen lethal ist. SNAT3 defiziente Mäuse haben ein vermindertes Wachstum, neurologische Störungen und eine veränderte renale Ammoniagenese und Gluconeogenese sowie eine reduzierte

Ammonium- und Harnstoffauscheidung. Heterozygote Mäuse haben vermutlich kompensatorischen Aenderungen in SNAT3, PDG und PEPCK Expression.

Zusammenfassend deuten unsere Daten sehr stark darauf hin, dass SNAT3 vermutlich die Aufnahme von Glutamin für die renale Ammoniagenese vermittelt.

I. Introduction: Renal ammoniagenesis

Control of acid-base balance is a homeostatic mechanism that involves a highly intricate balance of organ systems. Diet composition can largely influence the control of acid-base balance. For example, excess protein intake associated with a western-type diet, results in a nonvolatile acid load secondary to the increased intake of sulphur-containing amino acids (51). On the other hand, volatile weak acids such as carbonic acid can dissociate to carbon dioxide (CO_2) and water, or, in the presence of carbonic anhydrase, be readily converted to protons (H^+) and bicarbonate (HCO_3). The CO_2 produced is removed through exhalation by the lungs, but nonvolatile acids cannot be excreted in this manner, so another regulatory mechanism must be in place.

The kidney is the major organ responsible for removal of nonvolatile acid loads, which is accomplished by the generation and secretion of ammonium (NH_4^+, bicarbonate (HCO_3) and H^+ from the amino acid substrate, glutamine. Regulation of acid-base homeostasis is highly dependent upon circulating concentrations of glutamine. Glutamine is a conditionally essential amino acid that is found in abundant quantities in the blood and cerebrospinal fluid. It is critical for central nervous system neurotransmission, hepatic detoxification of ammonia into urea, and renal ammoniagenesis. During metabolic acidosis, glutamine is released from various organs and shunted to the kidney in order to produce the ammonium required to buffer physiological acids.

Ammoniagenesis occurs principally in the proximal tubule cell, which houses all of the necessary transport mechanisms involved in NH_4^+, HCO_3 and H^+ production and excretion. The process of ammoniagenesis begins with glutamine entry from the blood into the proximal tubule cell cytosol. A mitochondrial glutamine transporter, which is in fact an electroneutral uniporter, shuttles glutamine into the mitochondrial matrix, where it is rapidly converted to glutamate following an enzymatic reaction involving phosphate-dependent glutaminase (PDG) (58, 122). This process results in the liberation of one molecule of NH_4^+. Glutamate is then further metabolized either through transamination or via glutamate dehydrogenase to yield α-ketoglutarate (31, 97). This metabolic substrate can be shuttled into the tricarboxylic acid cycle or the gluconeogenic pathway

whereby cytosolic phosphoenolpyruvate carboxykinase (PEPCK), a key enzyme of gluconeogenesis, converts α-ketoglutarate to glucose and two bicarbonate molecules (31, 97). Thus, PDG and PEPCK are important regulators of ammoniagenesis during metabolic acidosis (3, 32, 38). The bicarbonate molecules generated from these processes help to partially alleviate acidosis after release into the blood, while the NH_4^+ is excreted into the urine, ultimately restoring systemic pH.

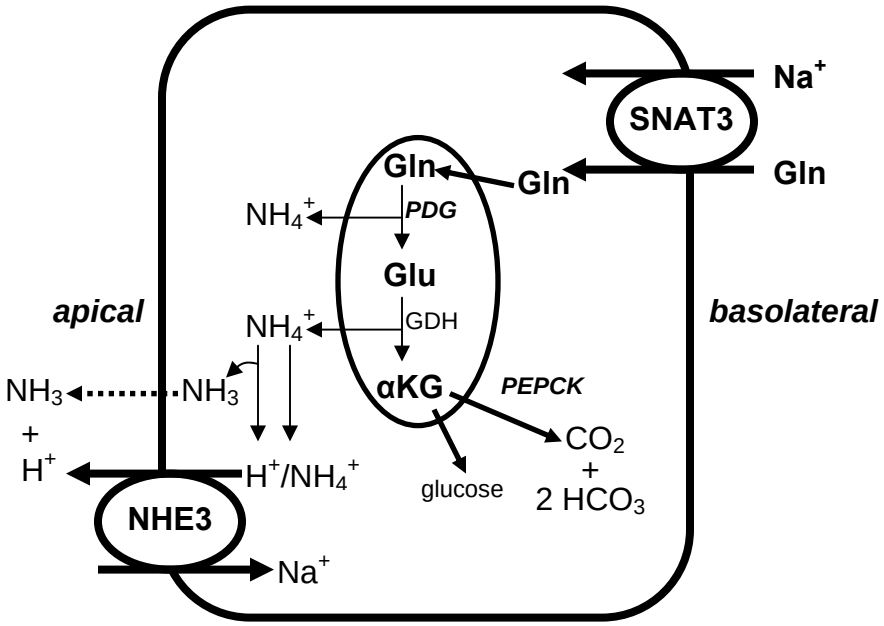

Figure 1. Renal proximal tubule cell model. SNAT3 is localized to the basolateral aspect and participates in glutamine influx. Mitochondrial PDG, glutamate dehydrogenase and PEPCK are involved in conversion of glutamine to CO_2 or glucose. These enzymatic reactions generate two molecules of NH_4^+ and HCO_3. α-ketoglutarate (αKG); Glutamine (Gln); Glutamate (Glu); Glutamate dehydrogenase (GDH); phosphate-dependent glutaminase (PDG); phosphoenolpyruvate carboxykinase (PEPCK); Na^+/H^+ Exchanger isoform 3 (NHE3).

II. Regulation of renal ammonium production

Regulation of ammoniagenesis is indeed complex and involves several different mechanisms. Both acute and chronic acidosis and alkalosis, potassium restriction, changes in luminal flow rate, and hormones such as angiotensin II, insulin, parathyroid hormone and prostaglandins can alter ammoniagenesis.

Metabolic acidosis is one important pathological driving force for increased renal ammonium production. Glutamine is shunted to the kidney rather than visceral organs leading to a substantial increase in renal glutamine extraction from blood and uptake into the proximal tubule cell during chronic acidosis (35, 125, 149). Transport of glutamine into the proximal tubule cell cytosol is purported to occur via the basolaterally-located, sodium-coupled, neutral amino acid transporter Slc38a3 (SNAT3). Protein and mRNA abundance of SNAT3 increases substantially in response to an acid challenge given as NH_4Cl (68, 91, 102, 127).

Along this line, renal catabolism of glutamine is also enhanced during metabolic acidosis. This occurs primarily via enhanced ammoniagenic and gluconeogenic enzyme activity, namely PDG and PEPCK (34, 57, 112, 113, 152) PDG is responsible for the catabolism of glutamine to glutamate, while PEPCK converts α-ketoglutarate into glucose and bicarbonate. The mechanism by which these enzymes exert their effects, however, differs greatly. PDG has been shown to increase in response to metabolic acidosis as a result of increased stabilization of its mRNA secondary to the binding of ξ-crystallin/NADPH:quinone reductase to a pH responsive AU-rich region in the 3' untranslated region of its mRNA (52, 78, 79). PEPCK, on the other hand, shows increased enzyme activity via increases in PEPCK transcription as well as mRNA stabilization (57, 59, 60).

Alkalosis, in contrast to acidosis, exerts an inhibitory effect on ammonia production and excretion. The effects appear to be primarily associated with a reduction in ammoniagenic and gluconeogenic enzyme activity, affecting ammonia production (80, 81, 108).

Hormones can also regulate renal ammonia production. Parathyroid hormone (PTH) has been shown to inhibit HCO_3 absorption in the proximal tubule, as well as

inhibit Na^+/H^+ Exchanger isoform 3 (NHE3) activity, ultimately reducing luminal NH_4^+ transport (11, 64, 109). Insulin administration has been shown to increase NHE3 activity and stimulate ammoniagenesis and excretion (26, 77). Angiotensin II can stimulate renal ammoniagenesis, which may involve changes in intracellular calcium concentration and activation of a calcium-calmodulin dependent pathway (27, 93, 95, 98). Glucocorticoids play a role in the response to acidosis by increasing glutamine fluxes to the kidney as well as enhancing NHE3 activity via increases in mRNA expression (75, 148). Activation of NHE3 activity has been shown to occur prior to changes on the protein level and involves trafficking to the apical membrane in opossum kidney cells (OKP) (14, 146). Additionally, there is evidence suggesting that glucocorticoid levels increase during metabolic acidosis (85, 147). A recent study by Karinch et al. demonstrated the effect of glucocorticoids on SNAT3 regulation. They showed that adrenalectomized rats exhibited a reduction in SNAT3 mRNA during metabolic acidosis which was partially compensated for by dexamethasone administration. In contrast, sham-operated rats given the glucocorticoids inhibitor RU486 attenuated the increase in SNAT3 mRNA normally associated with metabolic acidosis (67).

III. Renal ammonium handling

The nephron is organized in a series of segments that have different functions and transport properties in terms of ammonium excretion and absorption. This chapter will summarize the various transport mechanisms involved in renal ammonium handling.

III. 1 *The Proximal Tubule*

The proximal tubule is the principal site of ammoniagenesis, occurring primarily in the proximal tubule cell mitochondria, with excretion into the tubular lumen. In the presence of glutamine, metabolic acidosis increases ammonia production in the S1, S2, and S3 segments of the proximal tubule. Metabolic alkalosis, on the other hand, produces a reduction in ammoniagenesis (43). Since the intracellular proximal tubule cell pH is roughly 7.2, most of the ammonia produced combines with H^+ to form NH_4^+, due to the high pK_a of this molecule (~pH 9), and subsequently this NH_4^+ must be secreted into the tubular lumen in order to buffer acids. A once widely accepted theory of ammonium excretion is largely derived from the work done by Pitts et al. and is so coined the "diffusion trapping" theory (107). This theory explains that in fact, there are no NH_3 gradients, such that NH_3 concentrations do not change within the nephron. Further, this model suggests that NH_4^+ cannot readily permeate cells and that its concentration is equal to that of circulating H^+. Pitts hypothesized that NH_3 synthesized from glutamine diffuses into the proximal tubule lumen, only to combine with H^+ in the luminal fluid; no mention of alternative transport mechanisms were inferred from his work.

The current body of data suggests that indeed proximal tubule NH_4^+ handling is much more complex. Although NH_3 diffusion is still widely accepted, NH_4^+ can also be transported into the lumen of the proximal tubule. The apical Na^+/H^+ Exchanger (NHE) isoform 3 has been shown to transport NH_4^+ in exchange for Na^+. Evidence for this is based on work in rabbit renal microvillus membrane vesicles, whereby ^{22}Na uptake was stimulated by NH_4^+ administration, suggesting that NH_4^+ can be transported by NHE, perhaps in place of H^+ (74). Further, apical ammonia secretion is inhibited when luminal Na^+ concentrations are reduced and with the addition of a specific inhibitor of NHE

activity in isolated perfused mouse proximal tubules (92, 96). Conditions that enhance ammoniagenesis, such as metabolic acidosis, potassium depletion and changes in the hormone, angiotensin II, have been shown to alter NHE3 expression and activity, providing more evidence in support of NHE3-mediated, proximal tubular NH_4^+ secretion (4, 94, 99).

Apical membrane K^+ channels are also present in the proximal tubule, and it has been observed that NH_4^+ can bind in place of K^+ (28), suggesting that perhaps these channels could function in NH_4^+ secretion. However, it is more likely that these channels have a greater role in the maintenance of proximal tubule cell membrane potential than NH_4^+ excretion (140).

III.2 *The Loop of Henle*

The loop of Henle, particularly the thick ascending limb (TAL) is the site of most of the NH_4^+ reabsorption, amounting to nearly 80% of all NH_4^+ delivered to this nephron segment (18, 119). Ammonium reabsorption by this segment is necessary in order to establish an equilibration between luminal and medullary interstitial NH_4^+, which is subsequently transported into the collecting ducts and ultimately into the final urine. In the TAL, the apical Na^+-K^+-$2Cl^-$ cotransporter (NKCC2) is responsible for most of the NH_4^+ reabsorption, and occurs via competition of NH_4^+ for K^+ (42). During metabolic acidosis, enhanced medullary TAL NH_4^+ reabsorption occurs via increased NKCC2 mRNA and protein expression, and this increase is secondary to stabilization of NKCC2 mRNA (9, 66).

Apical NHE3 activity has also been detected in this segment, however, since the primary function of the TAL is to reabsorb NH_4^+, NHE3 activity is probably not related to NH_4^+ reabsorption, but may play a role in regulation of intracellular pH secondary to greater influxes of NH_4^+ (44). Metabolic acidosis also enhances NHE3 mRNA and protein levels in the TAL, however the reason for this upregulation has not been elucidated but may involve concomitant HCO_3 reabsorption that is associated with acidosis (76).

III.3 *The Collecting Duct*

This nephron segment conducts NH_4^+ excretion into the final urine and is associated with acidification of the lumen. In both rats and rabbits, an acid disequilibrium pH is generated as a result of absence of carbonic anhydrase in the lumen, ultimately enhancing luminal NH_3 secretion (76, 130). Further, metabolic acidosis leads to increased NH_4^+ secretion in the collecting duct system (119). There is evidence suggesting that basolateral NH_4^+ uptake into the collecting duct cells from the medullary interstitium occurs via NH_4^+ substitution for K^+ on NKCC1 and Na^+-K^+-ATPase (144, 145).

Rhesus-like glycoproteins have recently been identified as potential candidates for collecting duct NH_4^+ transport. The Rh B glycoprotein (Rhbg) and Rh C glycoprotein (Rhcg) isoforms have been localized to the basolateral and apical membranes of the collecting duct cells, respectively (39, 110, 142). The Rhcg protein has recently been studied in a mutant mouse model (13). Rhcg mutant mice fed a control diet showed a decrease in urinary NH_4^+ excretion and a more alkaline urinary pH. Acid-loading these mice revealed reduced NH_4^+ excretion despite normal ammoniagenesis, suggesting NH_4^+ transport into the final urine has been affected by deletion of Rhcg (13). Microperfusion experiments demonstrated reduced luminal NH_3 permeability suggesting that Rhcg is critical for NH_3 secretion. Therefore, Rhcg is crucial for ammonium excretion by the collecting duct in contrast to studies in an Rhbg mutant mouse model where no phenotype was observed (22).

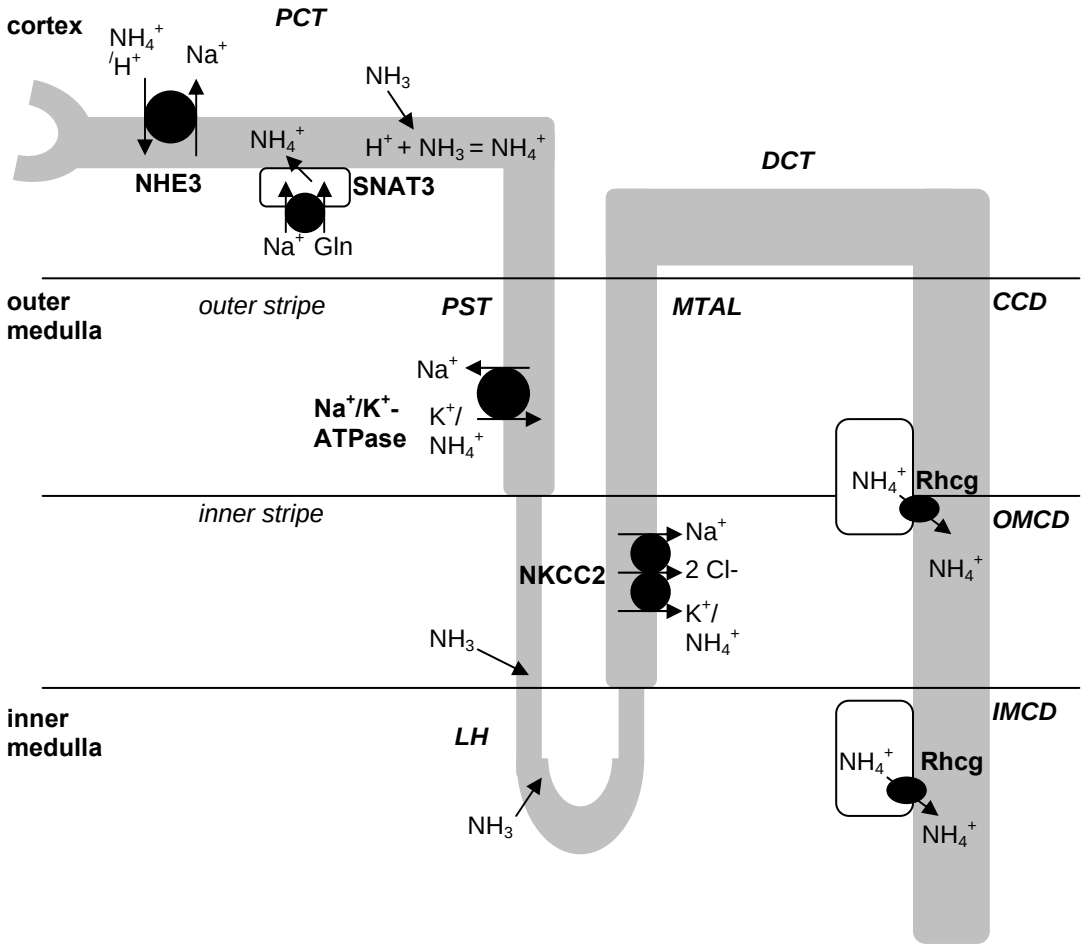

Figure 2. Renal ammonium transport in the nephron. SNAT3 localized to the basolateral aspect of the proximal tubule cell transports glutamine into the cytosol for ammoniagenesis. NH_4^+ is either transported via NHE3 into the lumen or as ammonia via diffusion through the apical membrane. After pooling in the medullary interstitium, NH_4^+ is absorbed via NKCC2 in the TAL. NH_4^+ is secreted into the final urine is a result of apical Rhcg activity. Proximal convoluted tubule (PCT); proximal straight tubule (PST); loop of Henle (LH); medullary thick ascending limb (MTAL); cortical collecting duct (CCD); outer and inner medullary collecting duct (OMCD, IMCD). Modified from Seldin and Giebisch's *The Kidney 2008.*

IV. Potassium restriction, high protein intake and metabolic acidosis increase expression of the glutamine transporter SNAT3 (Slc38a3) in mouse kidney

IV.1 Dietary effecters of acid-base homeostasis

Dietary potassium (K^+) restriction and high protein intake affect acid-base homeostasis. Studies in both animals and humans have observed enhanced renal ammoniagenesis, ammonium and acid excretion, and subsequently development of a mild alkalosis-like state during dietary K^+ depletion (61, 88, 123, 135, 136). In isolated mouse and rat renal proximal tubules, K^+ restriction stimulates gluconeogenesis and ammonium production (94, 101).

Potassium depletion leads to metabolic alkalosis and acidification of the urine, while causing a concomitant intracellular acidification (2). Using ^{31}Phosphorus-nuclear magnetic resonance imaging spectroscopy, Adam et al. determined that potassium restriction caused a substantial drop in intracellular pH without eliciting an extracellular acidosis (2). The reduction in intracellular pH associated with K^+ restriction emulates an acidosis-like state due to changes in a variety of proximal tubule acid-base regulatory mechanisms. HCO_3 absorption in the proximal tubules of K^+ restricted rats increases substantially in comparison to controls (23). This increase in HCO_3 absorption is proposed to be secondary to increased basolateral $Na^+/3HCO_3$ cotransporter and the apical Na^+/H^+ Exchanger activity induced by dietary K^+ depletion (128). Further, OKP cells incubated in low K^+ media showed a reduction in intracellular pH and a concomitant increase in NHE3 activity, similar to increases in NHE3 activity observed during metabolic acidosis (5). Interestingly, changes in both NHE3 mRNA and protein abundances did not follow a time-specific pattern and therefore suggest that variable regulation of this protein in the kidney, possibly via a tyrosine-kinase related mechanism (5) .

K^+ depletion is also associated with increases in bicarbonate reabsorption in the distal tubule, which appears to involve regulation of H^+/K^+-ATPases (6, 20, 21, 49, 151). Alternatively, H^+-ATPase membrane insertion and activity in the collecting duct was also

found to be enhanced during K^+ restriction, suggesting enhanced H^+ secretion in the collection duct system (10, 131, 132).

High dietary protein intake in the form of casein causes increased net renal acid and NH_4^+ excretion, suggesting that metabolism of sulfur-containing amino acids elicits the observed effects on acid-base handling (115, 150). These alterations in acid–base homeostasis were also observed in studies using *in vivo* microperfusion techniques; a diet containing 50% casein resulted in increased net renal acid and NH_4^+ excretion, due in part to enhanced Na^+/H^+ exchanger, H^+-ATPase, and endothelin-1 activities (69). Excess dietary protein given as casein showed remarkable increases in distal nephron acidification in an endothelin-stimulated mechanism. Endothelin stimulation increases both Na^+/H^+ Exchanger and aldosterone-induced H^+-ATPase activity (70). High protein intake is associated with increased salt reabsorption in the TAL via increased Na^+/K^+-ATPase activity; the effect may be related to increased blood levels of aldosterone observed after high protein intake (126).

IV.2 Amino acid transporters involved in acid-base balance

In order for cells to utilize glutamine, specialized molecular transport mechanisms must be in place to allow for glutamine influx and efflux. Much work in the area of amino acid transport proteins has led to the identification of a number of highly specialized transport systems in non-epithelial and epithelial cells (29, 30, 155). The sodium-coupled neutral amino acid transporters of the SLC38 family are a group of system A and N transporters. Members that are associated with System A transport include SNAT1, SNAT2 and SNAT4, while members exhibiting System N transport activities include SNAT3 and SNAT5. These System N transporters also exhibit H^+ countertransport and can operate in a multi-directional fashion.

The SLC38 family was initially discovered by cloning of SNAT3 and SNAT1, secondary to their similar sequence identity with the vesicular inhibitory amino acid transporter (VIAAT, vesicular GABA transporter) (25, 45, 141). VIAAT has been identified as an important transporter involved in synaptic vesicular exocytosis of the neurotransmitters glycine and GABA in central inhibitory neurons (86, 118). Chaudhry

was the first to functionally identify SNAT3 (formerly SN1), and showed that it involved Na^+ cotransport and proton exchange, and can mediate glutamine influx or efflux.

The SLC38 family members fall into two categories; having either System A or N functional characteristics. Both systems exhibit Na^+-dependent transport of zwitterionic neutral amino acids, with System N having fewer amino acid substrates than System A. The members of the SLC38 family belonging to the System A subfamily include SNAT1, SNAT2, and SNAT4. Members of System N include SNAT3 and SNAT5, and prefer glutamine, histidine and asparagine as transport substrates. Interestingly, System A subtypes exhibit cotransport with Na^+, while System N participates in Na^+ cotransport with H^+ antiport.

SNAT3 is highly expressed in brain astrocytes and retina, and has also been detected in liver, kidney, heart, skeletal muscle and in adipose tissue in varying degrees of mRNA and protein abundances (25, 45, 141). SNAT3 performs electroneutral amino acid transport with a stoichiometry of 1 Na^+ : 1 glutamine with antiport of 1 H^+ (17, 24, 25). Studies of System N transport properties show that SNAT3 preferentially chooses glutamine as a substrate for transport (73). Previous data has detected inwardly-directed currents in the presence of glutamine, asparagine or histidine in *Xenopus* oocytes expressing SNAT3 (41). These currents show Na^+ dependence and are also Li^+ sensitive, a key characteristic of System N transport. Interestingly, SNAT1 and 2 (System A), mediate electrogenic and not electroneutral transport, but lack an H^+ antiport mechanism that is observed with SNAT3, suggesting a glutamine uptake rather than efflux mechanism associated with System A transport (24, 114, 133). Interestingly, the H^+ antiport mechanism appears to be a competitive inhibition of activation by Na^+, similar to SNAT1 and SNAT2. However with SNAT3, Na^+ binding elicits amino acid uptake, while H^+ binding elicits efflux. Thus the transport mechanism involves a built in regulatory mechanism as H^+ antiport, so that when amino acid flux is high, which increases intracellular pH through coupled H^+ efflux, the uncoupled H^+ transport acts as a buffer (24). The uncoupled H^+ transport then serves to drive amino acid transport through coupled H^+ movement when the amino acid is readily available or initiate efflux when concentrations of amino acid are reduced (24).

This was, however, a much disputed mechanistic view. Schneider et al. observed in addition to the findings above, that SNAT3 expressed in *Xenopus* oocytes exhibited a substrate-independent cation conductance active at alkaline pH (124). When Na^+ binds, this cation conductance is effectively inhibited. Additionally, with glutamine available as a substrate, SNAT3 exhibits Na^+/H^+ exchange activity; this was originally described above as a blunting of intracellular pH, but is now shown to be due to a Na^+/H^+ exchange-related mechanism. In sum, Schneider et al. found that this uncoupled Na^+/H^+ exchange activity results in significantly increased Na^+ influx when glutamine is the substrate (124).

SNAT3 expression varies among different organs. It has been originally localized in brain astrocytes but not neurons, and is also expressed in adipose tissue, heart, kidney, liver and muscle (15, 16, 25, 46, 141). A recent paper by Sundberg et al. describes the tissue mapping of SLC38 family in various species and performed a complete quantitative real-time RT-PCR analysis in rat. Their work revealed that SLC38 family members are in fact ancient transporters, with expression in mammals, *C.elegans, D. melanogaster and A. thaliana* (134).

In the brain, astrocytes play a role in the glutamate-glutamine cycle, producing glutamate and γ-aminobutyric acid (GABA) from glutamine in the presence of glutamine synthetase. The glutamine produced is then shuttled into neurons where it is converted to glutamate and used for neurotransmission. SNAT3 has been localized to astrocyte processes surrounding glutamatergic, GABAergic and glycinergic synapses throughout the CNS, and it is suggested that SNAT3 plays a role in recycling of neurotransmitters during synaptic transmission in these areas (15, 25). In mouse primary astrocytes cultures, both Na^+-independent and Na^+-dependent amino acid transport systems have been identified (100), with SNAT3-like activity being the most pronounced.

The liver is crucial in detoxifying ammonia from the portal blood(53). In the liver acinus, SNAT3 appears to be the likely candidate for periportal uptake of glutamine. SNAT3 expressed on periportal hepatocytes participates in glutamine influx and in the presence of glutaminase, convert it to glutamate and NH_4^+ which enters the urea cycle and is excreted as urea. Meanwhile, glutamate is exported from the periportal site and

metabolized in the perivenous hepatocyte by glutamine synthetase where ultimately glutamine is synthesized and possibly exported via SNAT3 (25, 141).

Increases in SNAT3 activity in the kidney have been observed during metabolic acidosis. This is primarily due to increased ammoniagenesis associated with increased glutamine transport via SNAT3 on the basolateral aspect of the proximal tubule cell. Increases in SNAT3 gene expression have been observed during metabolic acidosis using microarray analysis (102). Since plasma glutamine levels increase substantially during metabolic acidosis and are thus redirected from the splanchnic pool to the kidney, it has been proposed that SNAT3 could be the transport mechanism involved in glutamine influx necessary for ammoniagenesis. SNAT3 has been detected in the kidney (25), and has been shown in many studies to increase on both mRNA and protein level during acidosis (68, 91, 102, 127).

Articles in PresS. Am J Physiol Renal Physiol (May 20, 2009). doi:10.1152/ajprenal.90318.2008

Potassium restriction, high protein intake, and metabolic acidosis increase expression of the glutamine transporter SNAT3 (Slc38a3) in mouse kidney

Stephanie M. Busque[1], Carsten A. Wagner[1]
Institute of Physiology, Zurich Center for Integrative Human Physiology ZIHP,
University of Zurich, Zurich, Switzerland

Running head: Regulation of SNAT3 expression in kidney

Address correspondence to:
Carsten A. Wagner
Institute of Physiology
University of Zurich
Winterthurerstrasse 190
CH-8057 Zurich
Switzerland
Phone: +41-44-63 50659
Fax: +41-44-63 56814
Wagnerca@access.uzh.ch

ABSTRACT

Kidneys produce ammonium to buffer and excrete acids through metabolism of glutamine. Expression of the glutamine transporter Slc38a3 (SNAT3) increases in kidney during metabolic acidosis (MA) suggesting a role during ammoniagenesis. Potassium depletion and high dietary protein intake are known to elevate renal ammonium excretion. Here, we examined SNAT3, phosphate-dependent glutaminase (PDG), and phosphoenolpyruvate carboxykinase (PEPCK) regulation during a control (0.36%) or low K^+ (0.02%) diet for 7 or 14 days; or a control (20%) or high protein (50%) diet for 7 days. MA was induced in control and low K^+ groups by addition of NH_4Cl. Urinary ammonium excretion increased during MA, K^+ restriction alone after 14 days, and during high protein intake. SNAT3, PDG and PEPCK mRNA abundance was elevated in MA and 14 day K^+ restriction but not during high protein intake. SNAT3 protein abundance was enhanced during MA (both control and low K^+) , 14 day low K^+ treatment alone, and during high protein intake. Seven day dietary K^+ depletion alone had no effect. Immunohistochemistry showed SNAT3 staining in earlier parts of the proximal tubule during 14 day K^+ restriction with and without NH_4Cl treatment and during high protein intake. In sum, SNAT3, PDG and PEPCK mRNA expression was congruent with urinary ammonium excretion during MA. Chronic dietary K^+ restriction, high protein intake and MA enhance ammoniagenesis, an effect that may involve enhanced SNAT3 mRNA and protein expression. Our data suggest that SNAT3 plays an important role as the glutamine uptake mechanism in ammoniagenesis under these conditions.

Keywords: glutamine transporters, renal ammoniagenesis, SNAT3, PDG, PEPCK

INTRODUCTION

The production of nonvolatile acids in the body, occurring during various disease states or alterations in dietary intake, can affect physiological pH manifesting as metabolic acidosis. Nonvolatile acids cannot be removed from the body via the lungs; therefore another regulatory mechanism must be in place to reestablish homeostasis. The kidney is responsible for regulating acid-base homeostasis through the synthesis and excretion of ammonium (NH_4^+) in the urine and the regeneration of bicarbonate. During metabolic acidosis, ammonium is produced in the proximal tubule cell by way of metabolism of glutamine to glutamate. Phosphate-dependent glutaminase (PDG) catalyzes this reaction in the mitochondria, converting glutamine to glutamate, and liberating one molecule of ammonium. Glutamate is then further metabolized either through transamination or via glutamate dehydrogenase to yield α-ketoglutarate (11, 27). This metabolic substrate can be shuttled into the tricarboxylic acid cycle or the gluconeogenic pathway whereby phosphoenolpyruvate carboxykinase (PEPCK), a key enzyme of gluconeogenesis, converts α-ketoglutarate to glucose and two bicarbonate molecules (11, 27). Thus, PDG and PEPCK are important regulators of ammoniagenesis during metabolic acidosis (2, 12, 14). The bicarbonate molecules generated from these processes help to partially alleviate acidosis after release into the blood, while the ammonium is excreted into the urine, ultimately restoring systemic pH.

Dietary potassium (K^+) restriction and high protein intake affect acid-base homeostasis. Studies in both animals and humans have observed enhanced renal ammoniagenesis, ammonium and acid excretion, and subsequently development of a mild alkalosis-like state during dietary K^+ depletion (18, 24, 34, 42, 43). In isolated mouse and rat renal proximal tubules, K^+ restriction stimulates gluconeogenesis and ammonium production (26, 28). Moreover, high dietary protein intake causes increased net renal acid and ammonium excretion, suggesting that metabolism of sulfur-containing amino acids elicits the observed effects on acid-base handling (33, 49). These alterations in acid–base homeostasis were also observed in other studies using *in vivo* microperfusion techniques; a diet containing 50% casein resulted in increased net renal acid and

ammonium excretion, due in part to enhanced Na^+/H^+ exchanger, H^+-ATPase, and endothelin-1 activities (22).

SNAT3, formerly named SN1, (Slc38a3), belongs to the SLC38 family of sodium-coupled neutral amino acid transporters, comprised of both system A and N transport systems (23). This transport system is purported to function in the presence of sodium with proton countertransport, with the main driving force for glutamine transport being both the Na^+ and the glutamine gradient (7, 8). SNAT3 is highly expressed in the liver and brain astrocytes, with modest expression in the kidney, heart and muscle (8, 23). Its expression is enhanced on the mRNA and protein level in the kidney during metabolic acidosis induced by addition of NH_4Cl to the drinking water (20, 21, 25, 29, 37). We and others have previously localized SNAT3 to the basolateral portion of the late proximal tubule S3 segment, with expression expanding to the S1 and S2 segments during acidosis. Its preference for glutamine and regulation during metabolic acidosis suggest a pivotal role in providing substrate for renal ammoniagenesis (21, 25, 37). Using microarray gene expression profiling, we have shown that SNAT3, PDG and PEPCK gene expression are concomitantly upregulated in mouse kidney after generating an acid load with NH_4Cl (29).

Based on the data described above, we hypothesized that dietary K^+ restriction and high protein dietary intake could regulate SNAT3, ultimately providing further evidence for a role in ammoniagenesis.

MATERIAL AND METHODS

Animal experiments and metabolic cage studies

Twelve week old male NMRI mice (Charles River Laboratories, Sulzfeld, Germany) were housed in light-cycled and climate controlled rooms. Experimental dietary treatment consisted of placing mice on a control (0.36%) or low K^+ (0.02%) diet for 7 or 14 days. The animals were subdivided into either NH_4Cl or low K^+/NH_4Cl treated groups (n=8 animals per group); 0.28M NH_4Cl and 2% sucrose were added to the drinking water for the final 2 days of dietary treatment (3, 39). Likewise, control and low K^+ groups were given 2% sucrose in the drinking water. In a separate series, animals were given either a control (20 %) or high (50 %) protein diet for 7 days (n = 8 animals per group), where casein was the primary constituent of the high protein diet. All diets were obtained from Kliba (Kaiseraugst, Switzerland). For all groups, during the final 3 days of experimental dietary treatment, animals were housed in metabolic cages where intake and output were monitored. Urine was collected under mineral oil for the final two consecutive 24 h intervals, and urinary pH was measured immediately using a pH microelectrode (691 pH meter, Metroholm). Urinary NH_3/NH_4^+ and creatinine were assessed using the Berthelot and Jaffe methods, respectively (6, 36). Mice were anesthetized by intraperitoneal injection of ketamine and xylazine, and mixed arterial-venous blood was collected from the abdominal aorta into heparinized tubes and immediately analyzed with a Radiometer ABL 505 blood gas analyzer (Radiometer; Copenhagen, Denmark). Mice were not perfused prior to harvesting kidneys. Since SNAT3 is not expressed in whole blood, nor is there evidence that erythrocytes express PDG or PEPCK, kidneys were not perfused prior to harvesting them (40). While there are some data suggesting white blood cells exhibit PDG activity, the likelihood of contamination by these cells and subsequent false-positive results in our study is minimal due to exsanguination resulting during blood collections (9, 10, 31). Kidneys were immediately flash-frozen under liquid nitrogen and placed at -80ºC until further processing. All animal experiments were conducted according to Swiss animal welfare laws and approved by the Swiss local Animal authority, Zurich, Switzerland.

Immunohistochemistry

For immunohistochemical studies on kidney slices, mice were perfused through the left ventricle with phosphate-buffered saline (PBS) followed by a paraformaldehyde-cacodylate fixative containing a mixture of three buffers: 1) a sodium-cacodylate-Sucrose buffer (100 mM sodium-cacodylate, 100 mM sucrose); 2) a sodium-cacodylate-HAES fixative containing (60% of final volume of buffer 1, 40% HAES-10%, 3.24 mM $MgCl_2$ x 6 H_2O, 4.36 mM picric acid) and a 3) 25% paraformaldehyde solution (final concentration 3%), pH 7.4). Kidneys were flushed with PBS, removed, cut into slices, washed three times with PBS, and frozen in liquid propane cooled with liquid nitrogen. The immunostaining procedure was carried out as previously described (39). Briefly, 5 μm cryosections were incubated with 0.5% SDS for 5 min, washed three times with PBS, and incubated with PBS containing 1% BSA for 15 min before application of the primary antibodies. The primary antibodies (rabbit anti-SNAT3 affinity purified 1:200 (25), goat anti 4F2hc 1:400, Santa Cruz Biotechnology, CA, USA) were diluted in PBS and applied either for 75 min at RT or overnight at 4°C. Sections were washed twice with PBS + 2.7% NaCl for 5 min, once with PBS, and incubated for 1 h at RT with their respective secondary antibodies (donkey anti-rabbit Alexa 594 and donkey anti-goat Alexa 488 diluted 1:1000, Invitrogen, Basel, Switzerland). Sections were then washed twice with PBS + 2.7% NaCl and once with PBS before mounting with Dako Glycergel Mounting Media (Dako North America Inc., Carpenteria, CA, USA). All sections were viewed using a confocal microscope (Leica CLSM). Pictures were processed (overlaid) using Adobe Photoshop software.

Quantitative Real-time RT-PCR

Total RNA was extracted from 30 mg of previously frozen, non-perfused kidney tissue. Kidneys were homogenized using a Rotor-stator homogenizer, and RNA immediately extracted using Qiagen RNeasy Mini Kit (Qiagen; Hilden, Germany) following the manufacturer's instructions. DNAse digestion was performed using the RNase-free DNAase Set (Qiagen; Hilden, Germany). Total RNA extractions were analyzed for quality, purity and concentration using the NanoDrop ND-1000 spectrophotometer (Wilmington, DE, USA). RNA samples were diluted to a final

concentration of 100 ng/µl, and cDNA was prepared using the TaqMan Reverse Transcriptase Reagent Kit containing 10X RT buffer, $MgCl_2$, random hexamers, dNTPs, RNase inhibitors and Multiscribe reverse transcription enzyme (Applied Biosystems/Roche; Forster City, CA, USA). Reverse transcription was performed with the Biometra TGradient thermocycler (Goettingen, Germany), with thermocycling conditions set at 25ºC for 10 min, 48ºC for 30 min, and 95ºC for 5 min. Relative mRNA expression was determined using quantitative Real-Time RT-PCR using the Applied Biosystems 7500 Fast Real-Time PCR system. Thermocycling conditions consisted of: 50ºC (2 min), 95ºC (10 min), 95ºC (15 sec; 40 cycles) and 60ºC (1 min). Forward and reverse primer and probe concentrations were 25 µM and 5 µM, respectively. TaqMan Universal PCR master mix 2X (Applied Biosystems/Roche) was used as the Taq polymerase. Primers and probes for SNAT3, phosphate-dependent glutaminase (PDG), cytosolic phosphoenolpyruvate carboxykinase (PEPCK) and Hypoxanthine-guanine phosphoribosyltransferase (HPRT) were generated using Primer Express software from Applied Biosystems and synthesized at Microsynth (Balgach, Switzerland) as described previously (29). Probes were generated with the reporter dye FAM at the 5' end and TAMRA at the 3' end. Reactions were run in a 96 well plate with each sample run in triplicate including a negative control (without Multiscribe reverse transcription enzyme). The cycle threshold (C_t) values obtained were ultimately compared to C_t values of the endogenous gene HPRT. Relative mRNA expression ratios were calculated as: $R = 2^{[Ct(HPRT/\beta\text{-actin})-Ct(\text{gene of interest})]}$.

Immunoblotting

Total membrane and cytosolic protein preparations from whole, non-perfused kidneys were prepared using a K-HEPES buffer composed of 200 mM mannitol, 80 mM HEPES, 41 mM KOH along with the protease inhibitors, PMSF, K-EDTA and leupeptin (pH 7.5). Kidneys were sonicated with 200 µl of K-HEPES buffer on ice using a tip sonicator and subsequently centrifuged for 20 min at 2000 rpm at 4ºC. The supernatant was aspirated and placed in an ultracentrifuge (Sorvall, Thermo Fischer Scientific) for 1 h at 41,000 rpm at 4ºC. The supernatant, containing cytosolic proteins, was removed while the pellet (membrane proteins) was resuspended in K-HEPES buffer and sonicated

briefly to evenly distribute proteins. Protein concentration was measured using the BioRad Dc Protein assay (Bio-Rad; Hercules, CA, USA). 75 μg of total membrane proteins or 50 μg of cytosolic fraction were mixed with Laemmli sample buffer and samples were loaded onto a 10% polyacrylamide gel and SDS-PAGE was performed. Proteins were transferred to PVDF membranes (polyvinylidene difluoride membranes; Immobilon-P, Millipore, Bedford MA, USA). Membranes were blocked with Tris-buffered saline/ 0.1% Tween and 5% non-fat dry milk for 1 h. Primary antibodies were subsequently applied, either for 2 h RT or overnight at 4ºC. The primary antibodies used were: phosphate-dependent glutaminase (PDG), which recognizes both the rat (KGA) and human (GAC) kidney-type isoforms of PDG forming the mature PDG protein (66 and 68 kDa; a kind gift from N. Curthoys, Colorado State University, USA; diluted 1:500) (13); anti-PEPCK polyclonal antibody (63 kDa; Cayman Chemical, Ann Arbor, MI, USA; diluted 1:1,000), and mouse monoclonal antibody against β-actin (42 kDa; Sigma, St. Louis, MO, USA; diluted 1:5,000). The anti-Slc38a3 antibody was generated by immunizing rabbits with a KLH-linked C-terminal peptide for the mouse Slc38a3 sequence: MEAPLQTEMVEPVPNGKHSEGLLPVI-C (Pineda Antibody Service, Berlin, Germany). The antibody recognized one major band of approximately 55 kDa which was completely blocked by preincubation of the serum with the immunizing peptide. Furthermore, this band was not detected in mutant mice lacking the SNAT3 (Slc38a3) transporter (unpublished observations, S.M. Busque, C.A. Wagner; diluted 1:10,000). The secondary antibodies used were donkey anti-rabbit horseradish peroxidase conjugated diluted 1:12,000, anti-rabbit alkaline phosphatase conjugated diluted 1:5,000, and anti-mouse IgG alkaline phosphatase conjugated diluted 1:5,000. Following a series of washing steps and blocking, membranes were treated with alkaline phosphatase or horseradish peroxidase conjugated developing solution and exposed to the Diana III chemiluminescence detection system (Raytest). Specific bands on PVDF membranes were later quantified using AIDA Image analyzer version 3.44. Membranes were stripped and reprobed for anti-β-actin and subsequent analysis of the protein of interest was determined relative to β-actin quantification and reported as relative protein abundance (ratio of β-actin/protein of interest).

Statistical analyses were performed using unpaired Student's *t*-test, and results with $p < 0.05$ were considered statistically significant. Data are presented as means ± SEM.

RESULTS

Dietary potassium restriction increases ammonium excretion and SNAT3 expression

To corroborate the effects of the experimental diets in both NH_4Cl treated control and low K^+ groups, arterial blood gases, plasma electrolytes, and urinary NH_4^+ and creatinine were evaluated (table 1 and figure 1, respectively). Blood Cl^- was markedly elevated in all NH_4Cl treated groups (control and low K^+ both 7 or 14 days), consistent with hyperchloremic metabolic acidosis. Blood pH and HCO_3^- levels were notably lower in the NH_4Cl treated and 14 day low K^+/NH_4Cl treated groups, however not during 7 day low K^+/NH_4Cl treatment. As expected, blood K^+ levels were found to be appreciably lower in the 14 days K^+ restricted groups (low K^+ alone and NH_4Cl treated), while 7 day restriction alone showed only a trend towards reduced blood K^+ levels. Urinary pH was significantly decreased in all NH_4Cl treated groups, but only slightly decreased after 14 day low K^+/NH_4Cl treatment, bearing no significance. Low K^+ treatment alone (7 or 14 days) did not alter urinary pH. 24 hr urinary NH_4^+ excretion was augmented in all NH_4Cl treated groups as well as during 14 day low K^+ treatment alone. Dietary K^+ restriction after 14 days, compounded by NH_4Cl treatment for 2 days, caused massive ammoniuria.

Kidneys from all groups: control, NH_4Cl treated, and 7 and 14 day low K^+ diet with and without NH_4Cl treatment, were assessed for mRNA expression of SNAT3, PDG and PEPCK using quantitative Real-time RT-PCR. SNAT3 mRNA abundance was found to be markedly enhanced in all NH_4Cl treated groups, with a significant further increase after 14 days of combined low K^+/NH_4Cl treatment (figure 2A). In parallel to SNAT3 mRNA expression, both PDG and PEPCK mRNA were found to be similarly regulated in that all NH_4Cl treated groups showed significantly increased expression of each enzyme (figure 2B, C), similar to previous findings (14). Dietary K^+-restriction for 7 days did not increase SNAT3, PDG, or PEPCK mRNA abundance appreciably in comparison to control mice, while 14 days of K^+ restriction resulted in a significant decrease in PDG expression, with SNAT3 and PEPCK remaining unchanged. In sum, mRNA expression of SNAT3, PDG and PEPCK paralleled urinary NH_4 excretion in these animals, suggesting that SNAT3 may play a role in providing glutamine for ammoniagenesis under these conditions.

To substantiate the results of our mRNA analyses using quantitative Real-time RT-PCR, we performed immunoblotting with both total membrane (for SNAT3) and cytosolic proteins (for PDG, PEPCK) from homogenized kidneys. Immunoblots were normalized to controls relative to β-actin protein quantification. We observed a significant increase in SNAT3 protein abundance in NH_4Cl (2 days), low dietary K^+ (14 days) treatment alone, and after 14 day low K^+/NH_4Cl treatment (figure 3A-F). Alternatively, enhanced PDG protein abundance was only observed after 14 day low K^+ treatment, (both low K^+ alone and low K^+/NH_4Cl treated; figure 4A-F) while PEPCK protein abundance was augmented only during NH_4Cl treatment in both control and 14 day low K^+ treatment (figure 5A-F). These data suggest that key enzymes involved in renal ammoniagenesis and gluconeogenesis are indeed regulated after K^+ restriction and acid loading. To determine whether it was solely K^+ restriction or the combination of K^+ restriction in addition to acid loading, we immunoblotted kidneys from 14 day treated mice with and without NH_4Cl treatment. We found significantly more SNAT3 and PEPCK protein abundance in K^+ restricted mice after administering an acid load relative to non-acid loaded mice (figure 6A-F). Therefore, in agreement with both SNAT3 mRNA expression levels and urinary ammonium excretion, compounding K^+ depletion and NH_4Cl treatment significantly increases SNAT3 and PEPCK protein in these mice.

High dietary protein intake stimulates ammonium excretion and SNAT3 abundance

High dietary protein intake has been shown to provide a substantial acid load to the body. Mice were assigned to a control (20 %) or high (50 %) dietary protein (purely casein) diet for 7 days. Arterial blood gases and urinary ammonium were measured to determine the effectiveness of the diet. Blood parameters were unremarkable and similar between the normal and high protein groups (table 2). The only disparities in renal acid-base handling were observed in the urine. Urinary pH was significantly decreased in the high protein group compared to controls (pH = 6.90 ± 0.20 vs 7.49 ± 0.01, respectively), suggesting excretion of acid equivalents by the kidneys. Moreover, urine volume, 24 hr NH_4 excretion and NH_4/creatinine ratio were substantially increased in comparison to controls (table 2, figure 7), in agreement with previous observations (22).

Relative mRNA expression was determined in both the normal and high protein groups. SNAT3, PDG and PEPCK mRNA did not significantly change in comparison to the normal protein intake group (figure 8A-C). In fact, the only discernable difference between groups was observed on the protein level. SNAT3 protein abundance was significantly upregulated in the high protein group, in accordance with a trend towards higher protein abundances of PDG and PEPCK, however no statistical significance was observed (figure 9A-F). Thus, high dietary protein intake resulted in reduced urinary pH and elevated urinary ammonium excretion paralleled by increased SNAT3 protein abundance.

SNAT3 localization spreads to the convoluted segments of the proximal tubule after K^+ restriction and high protein intake

We and others have previously shown that SNAT3 is localized to the basolateral membrane of late proximal tubule segments under basal conditions and that its expression spreads to earlier parts of the proximal tubule during NH_4Cl-induced acidosis (25, 29, 37). Here, we tested whether 14 day K^+ restriction, 14 day K^+ restriction with additional NH_4Cl-treatment, or a high protein diet had a similar effect by using immunohistochemistry. Early proximal tubules were identified by staining with antibodies against the 4F2hc (CD98) subunit of heteromeric amino acid transporters (5, 25). Under basal conditions, SNAT3 related staining was observed mostly in the late proximal tubule (straight or S3 segment). In kidneys from animals with 14 day K^+ restriction, 14 day K^+ restriction and NH_4Cl, or high protein dietary treatment, a distinct and more intensive SNAT3 related signal was observed in the S2 segment with some additional staining of the S1 segment (figure 10). Thus, SNAT3 expression expanded to earlier segments of the proximal tubule in response to treatments that stimulate renal proximal tubular ammoniagenesis and ammonium excretion.

DISCUSSION

The aim of this study was to test for regulation of the renal glutamine transporter SNAT3 during conditions associated with increased ammoniagenesis. We also measured induction of two major enzymes involved in renal ammoniagenesis, namely, mitochondrial phosphate-dependent glutaminase (PDG) and cytosolic phosphoenolpyruvate carboxykinase (PEPCK). Our data demonstrate that K^+ restriction, high dietary protein intake, and metabolic acidosis induced by NH_4Cl feeding, increased urinary ammonium excretion, paralleled by a concomitant elevation in abundance of the glutamine transporter SNAT3.

We used three distinct dietary animal models to stimulate renal ammoniagenesis and ammonium excretion; classic NH_4Cl-loading which, after metabolism in the liver, produces a metabolic acid load; dietary K^+ restriction, which is thought to induce an intracellular acidosis due to the shift of intracellular potassium in exchange for extracellular protons (1); and a high protein diet rich in sulfur-containing amino acids which also constitutes as a metabolic acid load. In all three animal models, renal ammonium excretion was stimulated and SNAT3 protein expression increased, however, with distinct differences.

NH_4Cl-loading has been previously reported to increase SNAT3 mRNA and protein abundance (21, 25, 29, 37). During NH_4Cl-induced metabolic acidosis, SNAT3 expression spreads from the late to the early proximal tubule (25, 29, 37). Similarly, we found increased SNAT3 related staining in the earlier portions of the proximal tubule (S2 and weakly in S1) during 14 day K^+ depletion, 14 day K^+ depletion with NH_4Cl treatment, and during high protein intake. Increased SNAT3 expression is paralleled by enhanced mRNA expression of two key ammoniagenic enzymes, PDG and PEPCK, as previously reported (11, 17, 29). Protein abundance of PEPCK was also increased, whereas enhancement of PDG protein is known to occur with slightly more delay (11). Of note, we did not directly measure transport or enzyme activity, and therefore, additional conclusions regarding regulation on the functional level cannot be inferred from our data. The effect of K^+ restriction on renal acid-base transport and ammoniagenesis has been well documented in animals and humans (15, 16, 19, 30, 41,

43, 44). In the proximal tubule, enhanced expression and activity of the apical Na^+/H^+ exchanger, NHE3, contributes to enhanced NH_4^+ excretion into the lumen (38). Moreover, K^+ restriction increases H^+-ATPase and H^+/K^+-ATPase transport activities in the distal nephron and reduces expression of the collecting duct bicarbonate exchanger, pendrin, promoting the development of metabolic alkalosis (4, 35, 45). Importantly, renal ammoniagenesis in the proximal tubule is stimulated during K^+ depletion (15, 16, 30, 34, 44). In our experiments, we observed hypokalemia in both 14 day K^+ restricted groups, with and without NH_4Cl treatment. Interestingly, 14 days of low K^+ treatment alone resulted in a small but significant increase in urinary ammonium excretion, while compounding K^+ restriction with NH_4Cl resulted in excessive ammonium excretion. Despite having observed the development of mild hypokalemia in 7 day dietary K^+ restricted mice, there was no significant increase in urinary ammonium excretion. In addition, mRNA expression of SNAT3, PDG and PEPCK did not considerably change after 7 days of K^+ restriction in comparison to controls, while the 14 day K^+ restricted group showed only decreased PDG mRNA expression. No differences in SNAT3 or PEPCK mRNA levels could be detected in the 14 day low K^+ treatment group alone despite a slight increase in urinary ammonium excretion. Whether this minor increase in ammonium excretion is due to ammoniagenesis per se or enhanced collecting duct ammonium excretion remains to be examined, however it has been shown that hypokalemia can enhance ammonium uptake in collecting duct cells via Na^+,K^+-ATPases (46).

Acid loading mice with NH_4Cl in both 7 and 14 day low K^+ treated mice showed massive increases in ammonium excretion. In contrast to mRNA expression, 14 day low K^+ treatment alone showed enhanced SNAT3 and PDG, but not PEPCK protein abundance. NH_4Cl-loading these mice showed increased protein levels of all three proteins; SNAT3, PDG and PEPCK in congruence with mRNA expression. These data suggest that regulation of ammonium excretion differs during hypokalemia stimulated ammoniagenesis and NH_4Cl-induced metabolic acidosis. This interpretation is supported by the fact that urinary ammonium excretion, SNAT3, PDG, and PEPCK mRNA, and protein increased even more when dietary K^+ restriction and NH_4Cl-loading were combined, suggesting an additive effect of the two treatments.

Increased protein intake is associated with higher consumption of sulfur-containing amino acids, generating a physiological acid load. High protein intake decreases urinary pH and increases net acid excretion (22, 32, 33, 47, 49). Additionally, increases in luminal Na^+/H^+ exchange activity in the proximal tubule as a result of enhanced endothelin production are associated with high dietary protein consumption, which may contribute to higher renal ammonium excretion (48). In agreement, we found a significant decrease in urinary pH in high protein treated animals in comparison to controls. Further, these animals had substantially elevated 24 hr urinary ammonium excretion and NH_4^+/creatinine ratios suggesting enhanced ammoniagenesis. Interestingly, despite higher urinary ammonium excretion, no differences in mRNA expression of SNAT3, PEPCK, and PDG could be detected. Moreover, only SNAT3 protein abundance was significantly enhanced, whereas the mildly elevated protein abundance of PDG and PEPCK did not reach significance. Thus, as in the case of dietary K^+ restriction, regulatory mechanisms appear to differ between NH_4Cl-induced metabolic acidosis and dietary protein loading.

The mechanism by which SNAT3 expression is regulated in response to these distinct stimuli may vary. In the case of NH_4Cl-loading, Solbu et al. suggested that binding of an unidentified protein to SNAT3 mRNA via a pH-responsive AU-rich domain in the 3'UTR may lead to its stabilization and thereby contribute to elevated SNAT3 mRNA expression (37). A similar mechanism has been identified for PDG and PEPCK (11, 17). It remains to be investigated if such mechanisms also contribute to SNAT3 regulation during K^+ restriction or dietary protein loading. Several hormones have been implicated in stimulating ammoniagenesis, such as glucocorticoids, angiotensin II, insulin and aldosterone (11). The increased expression of SNAT3 during NH_4Cl-induced metabolic acidosis may, at least in part, be mediated by cortisol; cortisol could potentially stimulate SNAT3 expression, independent of metabolic acidosis (20).

In sum, we have demonstrated that diets and conditions that stimulate renal ammoniagenesis and urinary ammonium excretion lead to higher expression of the SNAT3 glutamine transporter. This positive correlation and the localization of SNAT3 to the basolateral membrane of the late proximal tubule strongly suggest that SNAT3 plays a pivotal role in supplying the proximal tubule with glutamine for ammoniagenesis.

Notably, not all conditions that increased SNAT3 protein abundance resulted in a concomitant increase in mRNA expression, suggesting that variations in underlying regulatory mechanisms may be responsible. Further studies are needed in order to address these points in more detail. SNAT3 expression and activity may be rate-limiting and key for fueling ammoniagenesis and renal acid excretion.

Acknowledgements

This study was supported by a grant from the Swiss National Science Foundation to C.A. Wagner (3100A0-122217/1) and the 6th EU Frame work project EUGINDAT.

FIGURE LEGENDS

Table 1

Summary of results from arterial blood gas and urine analyses for mice treated for 7 or 14 days with a low K^+ diet with or without NH_4Cl supplementation in the drinking water for the final 2 days. Control animals received standard rodent chow (n = 8 mice per group). *$p \leq 0.05$, **,§§$p \leq 0.01$, ***,§§§$p \leq 0.001$. Comparisons between control and treatment groups are designated by *, while comparisons between K^+ restricted groups are designated by §.

Table 2

Summary of results from arterial blood gas and urine analyses for mice receiving 20 % or 50 % protein diet for 7 days (n = 8 animals). *$p \leq 0.05$, **$p \leq 0.01$, ***$p \leq 0.001$ between control and treatment groups.

Figure 1

Urinary NH_4 excretion is elevated in K^+ restricted animals with and without NH_4Cl treatment. Mice were placed on either a control or low K^+ diet for 7 or 14 days, further subdivided, and treated with NH_4Cl in the drinking water for the final 2 days of dietary treatment. Mice were subsequently placed in metabolic cages for 24 hr urine collections. Urinary NH_4^+ excretion was elevated in all groups receiving NH_4Cl. Mice on 7 day K^+ restriction had normal ammonium excretion, whereas mice on 14 day K^+-restriction had notably higher ammonium excretion. *$p \leq 0.05$, **$p \leq 0.01$, ***$p \leq 0.001$.

Figure 2

mRNA expression of renal SNAT3, PDG, and PEPCK is enhanced in potassium restricted mice and after NH_4Cl supplementation. mRNA abundance of the SNAT3 glutamine transporter, **(A)**, phosphate-dependent glutaminase (PDG), **(B)**, and phosphoenolpyruvate carboxykinase (PEPCK), **(C)** was determined by quantitative real-time RT-PCR in total kidneys. Significant increases in SNAT3, PDG, and PEPCK mRNA was observed in all NH_4Cl-treated groups (both 7 and 14 day treatment). Relative mRNA expression was normalized to HPRT mRNA expression. *$p \leq 0.05$, **$p \leq 0.01$, ***$p \leq 0.001$.

Figure 3

SNAT3 protein abundance is enhanced during K^+ restriction and NH_4Cl loading. Total membranes were extracted from whole, non-perfused kidneys from mice on K^+ restriction with or without NH_4Cl supplementation. Membranes were probed with antibodies against SNAT3 and reprobed after stripping for β-actin to control for equal loading. Original blots are depicted with bar graphs summarizing normalized data. **(A, B)** Enhanced SNAT3 protein abundance was observed after 2 days of NH_4Cl treatment. **(C,D)** SNAT3 protein abundance is upregulated after 14 days of K^+ restriction. **(E,F)** Combined K^+ restriction for 14 days and 2 days of NH_4Cl treatment markedly enhanced SNAT3 protein abundance. $^{**}p \leq 0.01$ between control and treatment groups.

Figure 4

PDG protein levels are enhanced during K^+ restriction. Cytosolic proteins were extracted from whole, non-perfused kidney samples from mice on a low K^+ diet with or without NH_4Cl supplementation. Membranes were probed with antibodies against the mitochondrial phosphate-dependent glutaminase and reprobed after stripping for β-actin to control for equal loading. Original blots are depicted along with bar graphs summarizing normalized data. **(A, B)** NH_4Cl treatment for 2 days did not alter PDG protein abundance. **(C,D)** After 14 days of dietary K^+ restriction, PDG abundance is significantly increased. **(E,F)** Combined K^+ restriction for 14 days with 2 days of NH_4Cl treatment also enhanced PDG protein expression. $^{*}p \leq 0.05$, $^{***}p \leq 0.001$ between control and treatment groups.

Figure 5

Phosphoenolpyruvate carboxykinase (PEPCK) protein abundance is augmented only by NH_4Cl loading but not K^+ restriction. The expression of PEPCK was assessed in cytosolic protein preparations by immunoblotting, Membranes were probed with antibodies against PEPCK and reprobed after stripping for β-actin to control for equal loading. Original blots are depicted along with bar graph summarizing normalized data. **(A, B)** 2 day NH_4Cl treatment strongly enhanced PEPCK protein abundance. **(C,D)** After 14 days of dietary K^+ restriction, PEPCK abundance was not significantly altered. **(E,F)**

Combined dietary K^+ restriction for 14 days with 2 days of NH_4Cl supplementation enhanced PEPCK protein expression. *p ≤ 0.05, **p ≤ 0.01 between control and treatment groups.

Figure 6

NH_4Cl loading in 14 day K^+ restricted mice showed augmented SNAT3 and PEPCK protein abundance. Plasma membrane and cytosolic proteins were extracted from whole, non-perfused kidneys and probed for SNAT3, PDG, PEPCK, and β-actin. Original blots and bar graphs summarizing normalized data are shown. **(A,B)** SNAT3 abundance is markedly enhanced after NH_4Cl administration. **(B, C)** No changes in PDG abundance were noted among K^+ restricted groups with or without NH_4Cl treatment. **(E,F)** Acid-loading K^+ restricted mice showed augmented PEPCK protein in comparison to non-acid loaded controls. **p ≤ 0.01, ***p ≤ 0.001 between groups.

Figure 7

Urinary NH_4 excretion was substantially elevated in high protein diet fed animals. Mice were given either a normal (20%) or high (50%) protein diet for 7 days. The final 3 days of dietary treatment animals were placed in metabolic cages and urine was collected every 24 hrs. Ammonium excretion was significantly elevated in the high protein treated group (n = 8 mice per group). **p ≤ 0.01.

Figure 8

SNAT3, PDG, and PEPCK are not regulated on mRNA level during high dietary protein intake. Total kidney homogenates were prepared from mice either on a 20 % or 50 % protein diet. mRNA expression of SNAT3, PDG, and PEPCK was assessed by quantitative real-time RT-PCR and normalized against HPRT mRNA expression. No significant differences were found between the two groups.

Figure 9

SNAT3 protein abundance is markedly upregulated during high dietary protein intake. Plasma membrane and cytosolic proteins were extracted from whole, non-perfused

kidneys and probed for SNAT3, PDG, PEPCK, and β-actin. Origianl blots and bar graphs summarizing normalized data are shown. **(A,B)** SNAT3 abundance is increased during 50 % protein intake. **(C-F)** PDG and PEPCK protein abundance showed mildly, but not significantly, elevated expression after 7 days of high protein diet. ***$p \leq 0.001$ between groups.

Figure 10

SNAT3 related staining expands to earlier segments of the proximal tubule in response to treatments stimulating ammoniagenesis. Kidneys were stained with antibodies against the 4F2hc (CD98) amino acid transporter subunit (green) to mark the early convoluted proximal tubule (S1 segment) and against SNAT3 (red). The dashed line marks the transition from the outer stripe of the outer medulla to the inner stripe of the outer medulla. (A) Control conditions, (B) 2 day NH_4Cl treatment, (C) 14 day K^+ restriction, (D) 14 day K^+ restriction and 2 day NH_4Cl treatment, and (F) high dietary protein (50 %) intake. Original magnification 40 x.

Table 1
Arterial blood gas and urine analysis

	7 days				14 days		
Groups	Control	NH_4Cl 2 days	Low K^+	Low K^+ NH_4Cl 2 days	Control	Low K^+	Low K^+ NH_4Cl 2 days
Blood							
pH	7.28 ± 0.01	7.15 ± 0.03**	7.32 ± 0.03	7.26 ± 0.03	7.28 ± 0.01	7.29 ± 0.01	7.10 ± 0.04**§§§
pCO_2	40.1 ± 1.2	35.8 ± 1.7	37.9 ± 3.3	35.9 ± 3.6	48.6 ± 1.1	48.8 ± 1.7	54.8 ± 5.7
HCO_3^- (mM)	17.8 ± 0.7	12.6 ± 1.2**	18.1 ± 2.7	16.1 ± 1.3	19.5 ± 0.6	20.2 ± 0.4	13.04 ± 1.2***§§§
Na^+ (mM)	145.6 ± 0.8	148.4 ± 1.5	145.9 ± 1.5	148.7 ± 0.7**	145.6 ± 0.6	146.0 ± 1.3	148.4 ± 0.8*
Cl^- (mM)	107.8 ± 0.6	120.9 ± 1.5***	105.8 ± 2.4	119.7 ± 1.0***§§§	108.5 ± 0.8	106.7 ± 1.2	117.6 ± 1.3***§§§
K^+ (mM)	3.9 ± 0.3	4.6 ± 0.9	3.1 ± 0.4	4.3 ± 0.4	3.5 ± 0.1	3.1 ± 0.1*	3.6 ± 0.2§
Body wt (g)	36.2 ± 0.7	36.1 ± 0.6	34.7 ± 0.8	33.8 ± 0.5**	39.2 ± 1.2	36.9 ± 1.0	34.4 ± 1.8*
Urine							
pH	6.59 ± 0.1	5.68 ± 0.1***	6.81 ± 0.2	5.94 ± 0.2**§§	6.77 ± 0.1	6.89 ± 0.3	6.31 ± 0.2
urine vol (µl/g body wt/24h)	46.8 ± 8.0	23.0 ± 7.0*	85.9 ± 24.1	29.6 ± 6.2	47.0 ± 20.2	79.2 ± 22	73.4 ± 27.0
NH_4(mmol)/creatinine (mg/dl)	1.9 ± 0.6	10.3 ± 1.1***	1.8 ± 0.5	7.9 ± 1.2	1.3 ± 0.2	2.6 ± 0.9	26.0 ± 10.7**
NH_4(mmol)/24h	0.14 ± 0.05	0.46 ± 0.17*	0.11 ± 0.04	0.47 ± 0.12*§§	0.07 ± 0.01	0.21 ± 0.07*	1.12 ± 0.1*** §§§

Table 2
Arterial blood gas and urine analysis

Groups	20 % protein	50 % protein
Blood		
pH	7.30 ± 0.01	7.31 ± 0.02
pCO_2	42.7 ± 3.7	41.1 ± 1.2
HCO_3^- (mM)	20 ± 1.3	19.8 ± 1.04
Na^+ (mM)	148.0 ± 2.0	147.0 ± 1.0
Cl^- (mM)	111.0 ± 1.1	109.0 ± 1.0
K^+ (mM)	7.01 ± 0.4	6.6 ± 0.3
Body wt (g)	36.5 ± 2.0	35.3 ± 1.0
Urine		
pH	7.49 ± 0.10	6.90 ± 0.20**
urine vol (µl/g body wt/24h)	63.2 ± 25.0	190.9 ± 16.1***
NH_4(mmol)/creatinine (mg/dl)	0.7 ± 0.35	5.1 ± 1.6*
NH_4(mmol)/24h	0.03 ± 0.01	0.37 ± 0.09**

Figure 1

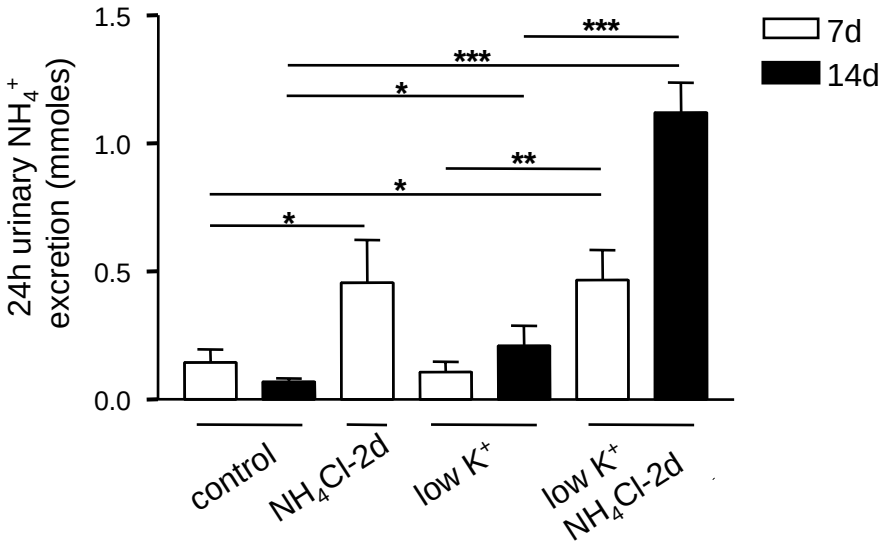
1.5
1.0
0.5
0.0
24h urinary NH_4^+ excretion (mmoles)
7d
14d
***
***
*
**
*
*
control
NH_4Cl-2d
low K^+
low K^+ NH_4Cl-2d

Figure 2

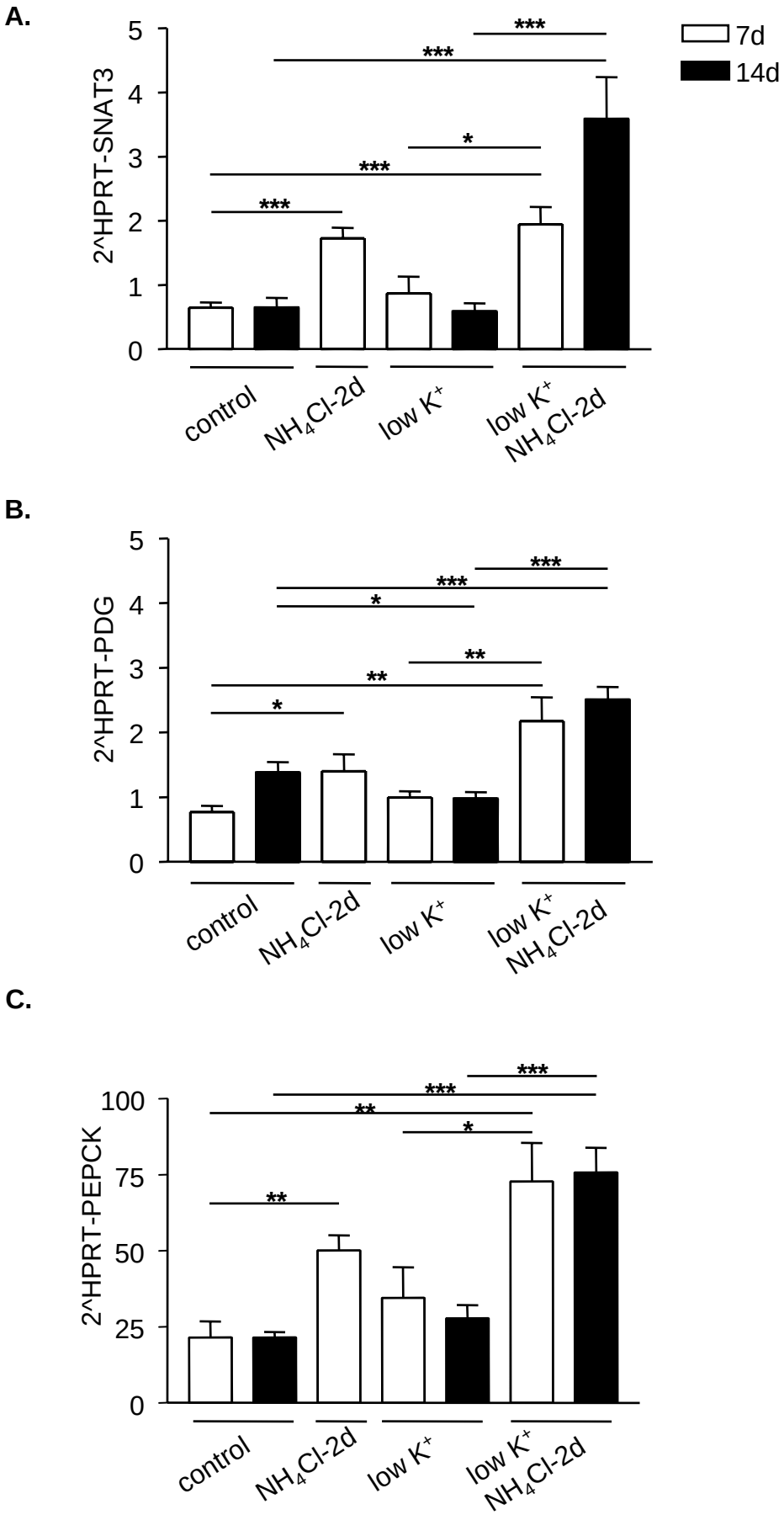
A.
2^HPRT-SNAT3
7d
14d
control
NH4Cl-2d
low K+
low K+ NH4Cl-2d
B.
2^HPRT-PDG
C.
2^HPRT-PEPCK

Figure 3

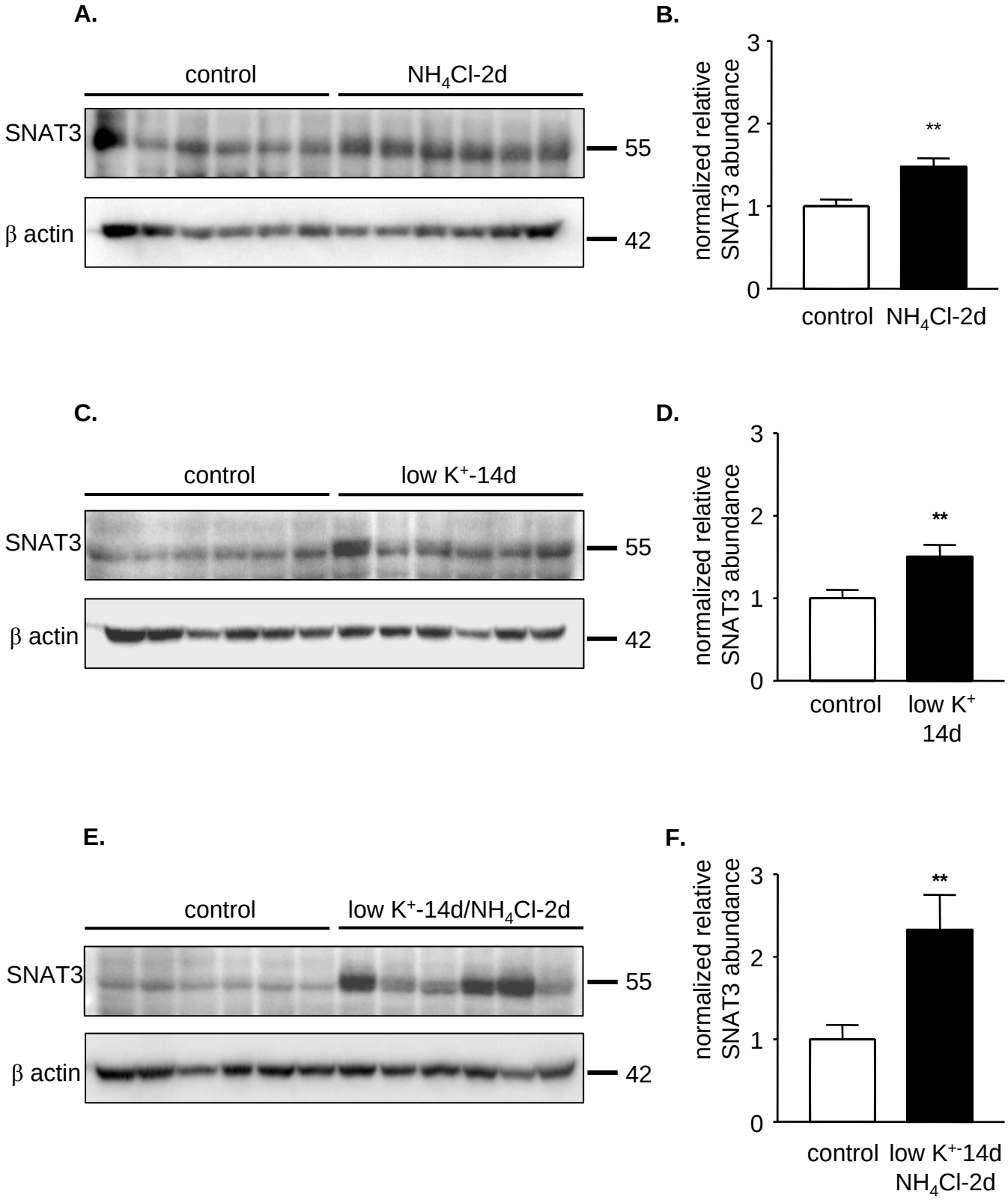
A.
control
NH4Cl-2d
SNAT3
β actin
55
42
B.
normalized relative SNAT3 abundance
3
2
1
0
**
control
NH4Cl-2d
C.
control
low K+-14d
SNAT3
β actin
55
42
D.
normalized relative SNAT3 abundance
3
2
1
0
**
control
low K+ 14d
E.
control
low K+-14d/NH4Cl-2d
SNAT3
β actin
55
42
F.
normalized relative SNAT3 abundance
3
2
1
0
**
control
low K+-14d NH4Cl-2d

Figure 4

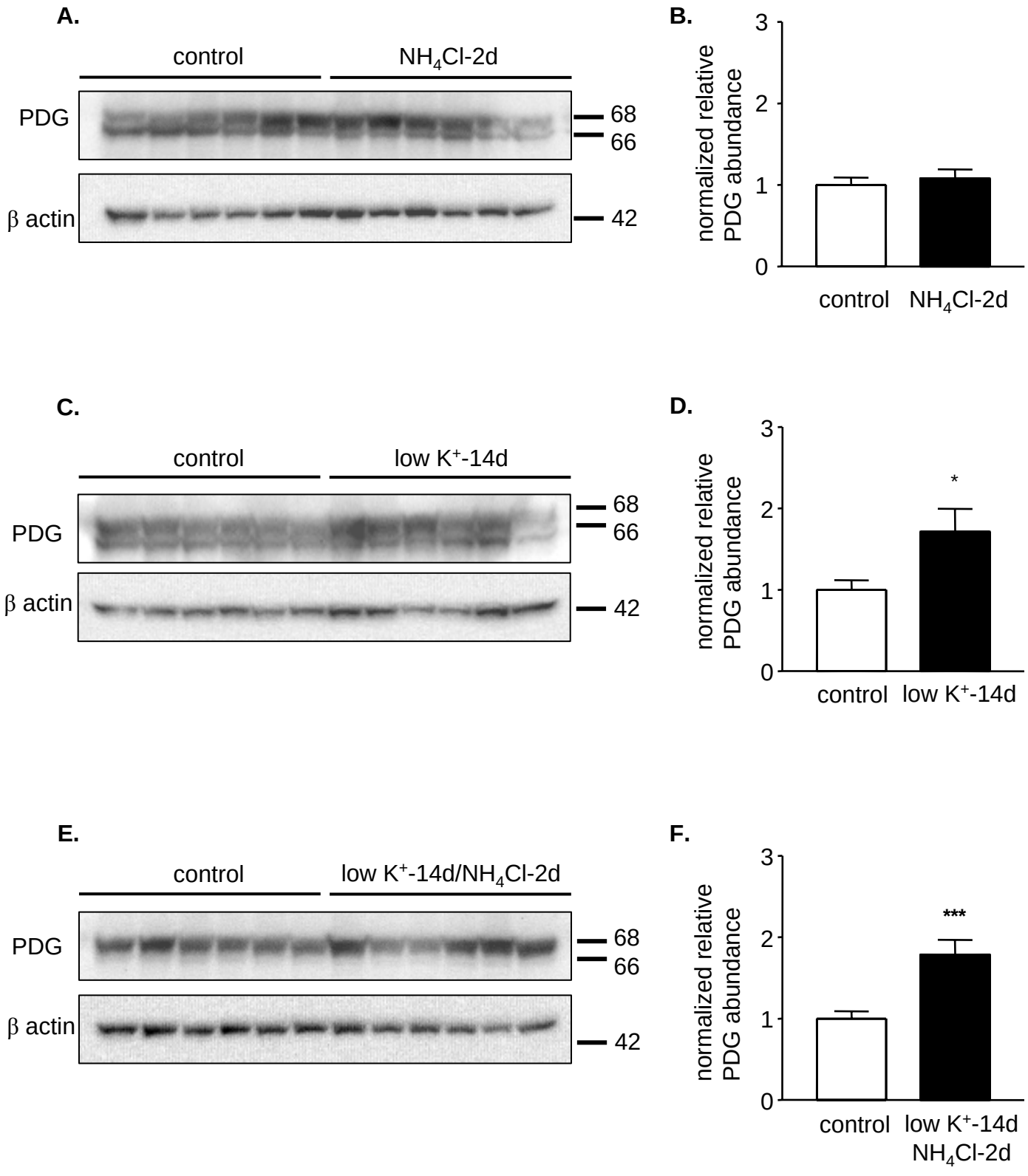
A.
control
NH4Cl-2d
PDG
β actin
68
66
42
B.
normalized relative PDG abundance
3
2
1
0
control
NH4Cl-2d
C.
control
low K+-14d
PDG
β actin
68
66
42
D.
normalized relative PDG abundance
3
2
1
0
*
control
low K+-14d
E.
control
low K+-14d/NH4Cl-2d
PDG
β actin
68
66
42
F.
normalized relative PDG abundance
3
2
1
0
***
control
low K+-14d
NH4Cl-2d

Figure 5

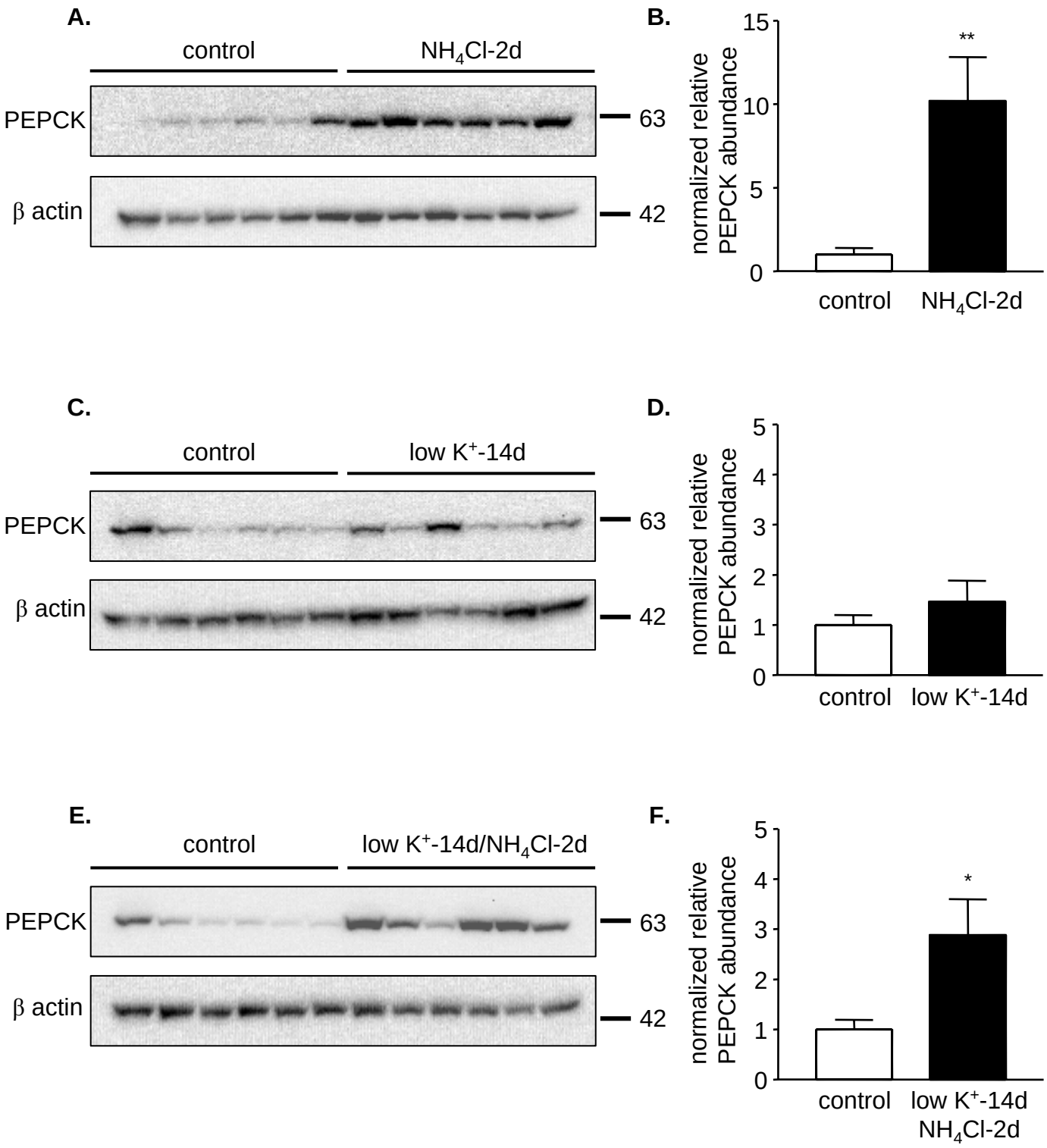
A.
control
NH4Cl-2d
PEPCK
β actin
63
42
B.
normalized relative PEPCK abundance
15
10
5
0
**
control
NH4Cl-2d
C.
control
low K+-14d
PEPCK
β actin
63
42
D.
normalized relative PEPCK abundance
5
4
3
2
1
0
control
low K+-14d
E.
control
low K+-14d/NH4Cl-2d
PEPCK
β actin
63
42
F.
normalized relative PEPCK abundance
5
4
3
2
1
0
*
control
low K+-14d
NH4Cl-2d

Figure 6

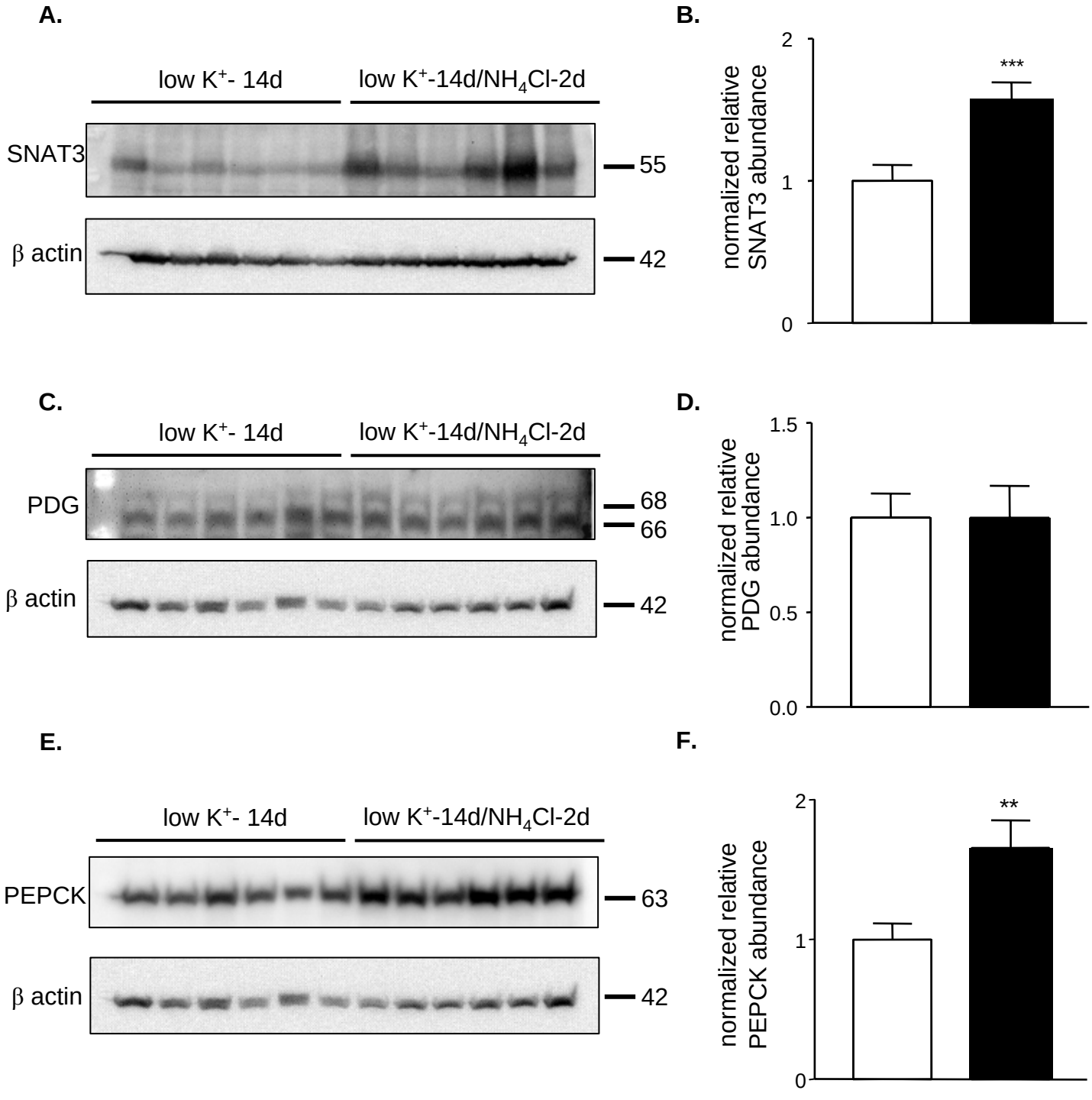
A.
low K+- 14d
low K+-14d/NH4Cl-2d
SNAT3
55
β actin
42
B.
normalized relative SNAT3 abundance
2
1
0
***
C.
low K+- 14d
low K+-14d/NH4Cl-2d
PDG
68
66
β actin
42
D.
normalized relative PDG abundance
1.5
1.0
0.5
0.0
E.
low K+- 14d
low K+-14d/NH4Cl-2d
PEPCK
63
β actin
42
F.
normalized relative PEPCK abundance
2
1
0
**

Figure 7

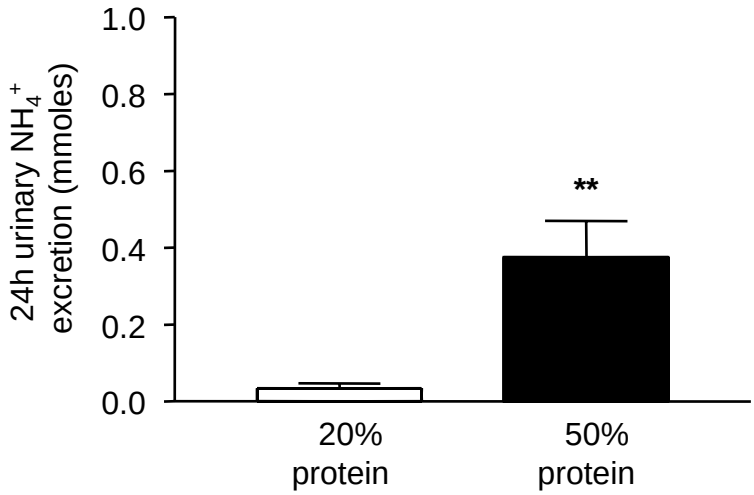
1.0
0.8
0.6
0.4
0.2
0.0
24h urinary NH_4^+ excretion (mmoles)
**
20% protein
50% protein

Figure 8

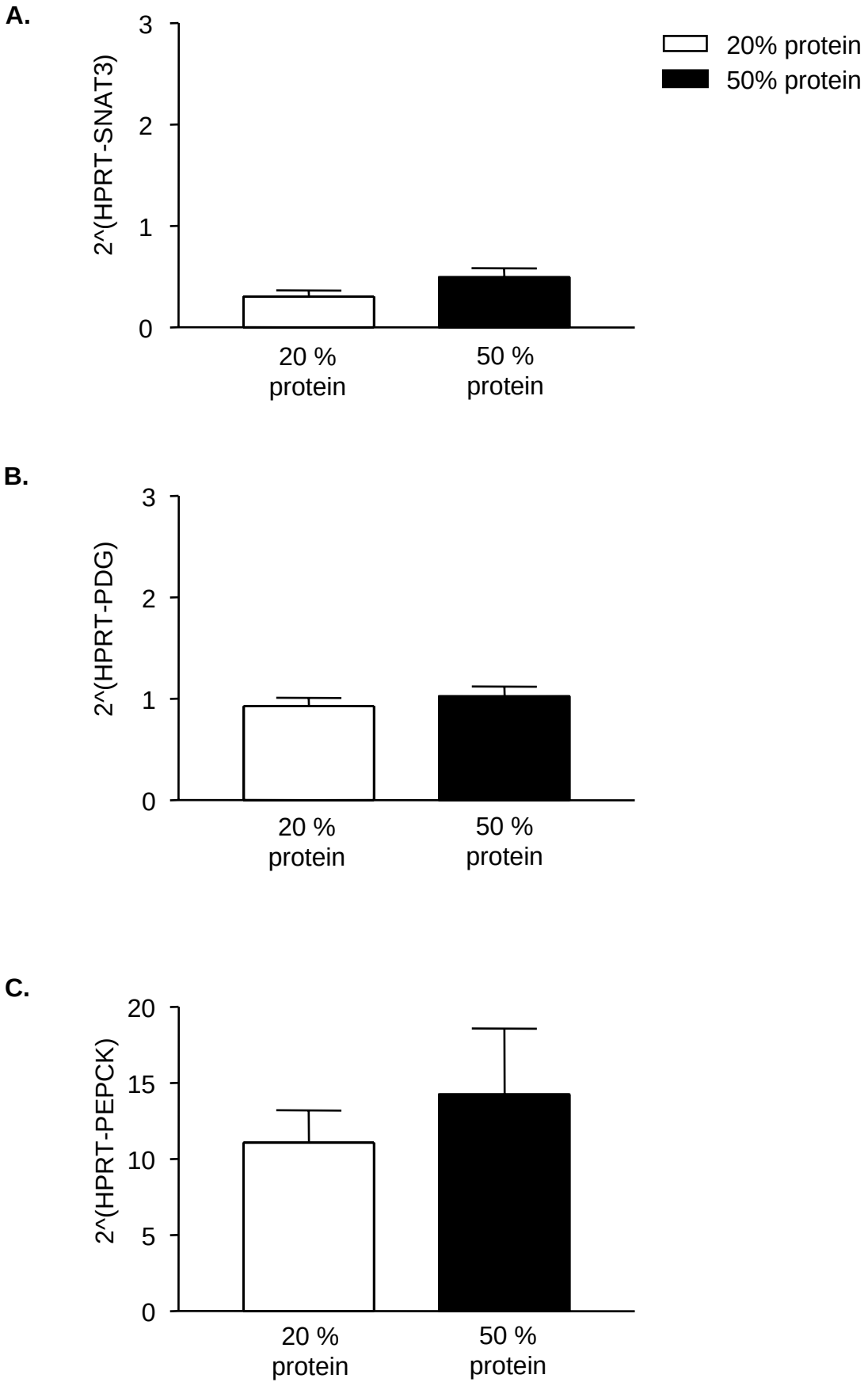
A.
2^(HPRT-SNAT3)
3
2
1
0
20% protein
50% protein
20 % protein
50 % protein
B.
2^(HPRT-PDG)
3
2
1
0
20 % protein
50 % protein
C.
2^(HPRT-PEPCK)
20
15
10
5
0
20 % protein
50 % protein

Figure 9

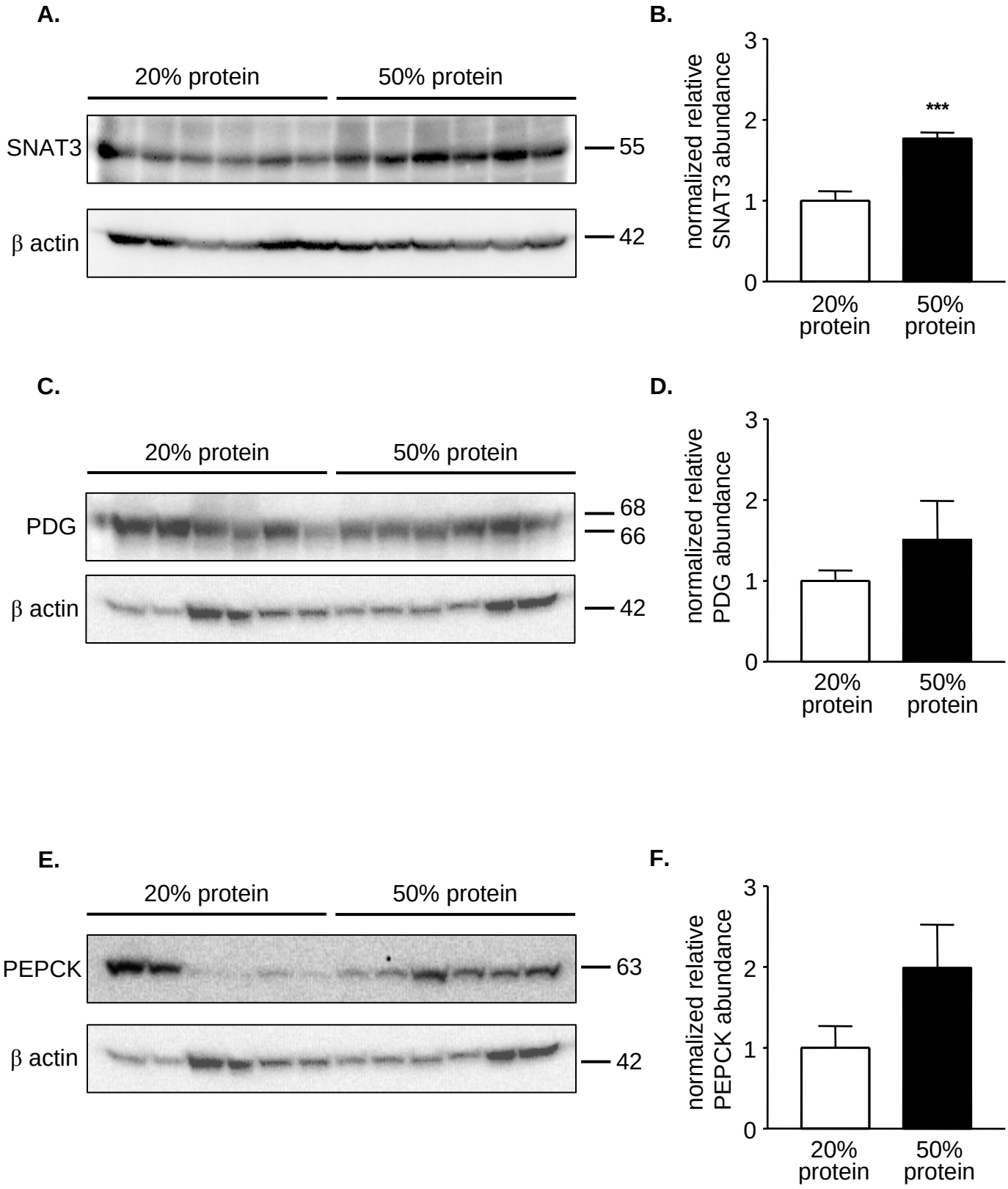
A.
20% protein
50% protein
SNAT3
55
β actin
42
B.
normalized relative SNAT3 abundance
***
20% protein
50% protein
C.
20% protein
50% protein
PDG
68
66
β actin
42
D.
normalized relative PDG abundance
20% protein
50% protein
E.
20% protein
50% protein
PEPCK
63
β actin
42
F.
normalized relative PEPCK abundance
20% protein
50% protein

Figure 10

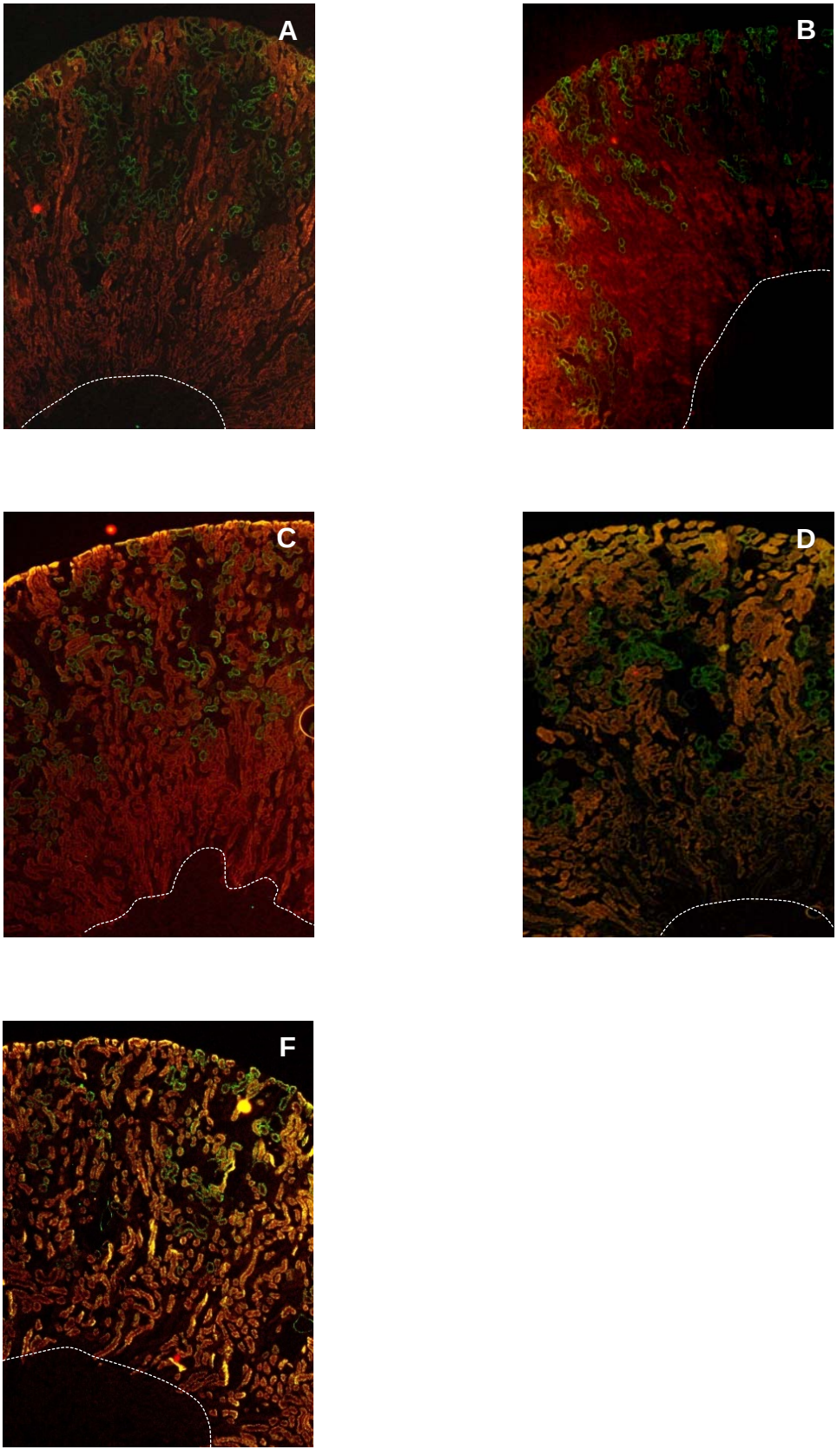

References

1. **Adam WR, Koretsky AP, and Weiner MW**. 31P-NMR in vivo measurement of renal intracellular pH: effects of acidosis and K+ depletion in rats. *Am J Physiol* 251: F904-910, 1986.

2. **Alleyne GA, and Scullard GH**. Renal metabolic response to acid base changes. I. Enzymatic control of ammoniagenesis in the rat. *J Clin Invest* 48: 364-370, 1969.

3. **Aruga S, Wehrli S, Kaissling B, Moe OW, Preisig PA, Pajor AM, and Alpern RJ**. Chronic metabolic acidosis increases NaDC-1 mRNA and protein abundance in rat kidney. *Kidney Int* 58: 206-215, 2000.

4. **Bailey MA, Fletcher, R M, Woodrow, D F, Unwin, R J, Walter, S J**. Upregulation of H^+-ATPase in the distal nephron during potassium depletion: structural and functional evidence. *Am J Physiol* 275: F878-884, 1998.

5. **Bauch C, Forster N, Loffing-Cueni D, Summa V, and Verrey F**. Functional cooperation of epithelial heteromeric amino acid transporters expressed in madin-darby canine kidney cells. *J Biol Chemy* 278: 1316-1322, 2003.

6. **Berthelot M**. Violet d'aniline. *Rep Chim App* 1: 284, 1859.

7. **Broer A, Albers A, Setiawan I, Edwards RH, Chaudhry FA, Lang F, Wagner CA, and Broer S**. Regulation of the glutamine transporter SN1 by extracellular pH and intracellular sodium ions. *J Physiol* 539: 3-14, 2002.

8. **Chaudhry FA, Reimer RJ, Krizaj D, Barber D, Storm-Mathisen J, Copenhagen DR, and Edwards RH**. Molecular analysis of system N suggests novel physiological roles in nitrogen metabolism and synaptic transmission. *Cell* 99: 769-780, 1999.

9. **Costa Rosa LF, Curi R, Murphy C, and Newsholme P**. Effect of adrenaline and phorbol myristate acetate or bacterial lipopolysaccharide on stimulation of pathways of macrophage glucose, glutamine and O2 metabolism. Evidence for cyclic AMP-

dependent protein kinase mediated inhibition of glucose-6-phosphate dehydrogenase and activation of NADP+-dependent 'malic' enzyme. *Biochem J* 310 (Pt 2): 709-714, 1995.

10. **Curi TC, De Melo MP, De Azevedo RB, Zorn TM, and Curi R**. Glutamine utilization by rat neutrophils: presence of phosphate-dependent glutaminase. *Am J Physiol* 273: C1124-1129, 1997.

11. **Curthoys NP**. Renal ammonium ion production and excretion. In: *Seldin and Giebisch's The Kidney Physiology and Pathophysiology*, edited by Alpern RJ, and Hebert SC, Elsevier, 2008, p. 1601-1619.

12. **Curthoys NP, and Gstraunthaler G**. Mechanism of increased renal gene expression during metabolic acidosis. *Am J Physiol Renal Physiol* 281: F381-390, 2001.

13. **Curthoys NP, Kuhlenschmidt T, Godfrey SS, and Weiss RF**. Phosphate-dependent glutaminase from rat kidney. Cause of increased activity in response to acidosis and identity with glutaminase from other tissues. *Arc Biochem Biophys* 172: 162-167, 1976.

14. **Drewnowsk KD, Craig MR, Digiovanni SR, McCarty JM, Moorman AF, Lamers WH, and Schoolwerth AC**. PEPCK mRNA localization in proximal tubule and gene regulation during metabolic acidosis. *J Physiol Pharmacol* 53: 3-20, 2002.

15. **Iacobellis M, Muntwyler E, and Griffin GE**. Enzyme concentration changes in the kidneys of protein- and/or potassium-deficient rats. *Am J Physiol* 178: 477-482, 1954.

16. **Iacobellis M, Muntwyler E, and Griffin GE**. Kidney glutaminase and carbonic anhydrase activity and tissue electrolyte composition in potassium-deficient dogs. *Am J Physiol* 183: 395-400, 1955.

17. **Ibrahim H, Lee YJ, and Curthoys NP**. Renal response to metabolic acidosis: Role of mRNA stabilization. *Kidney Int* 73: 11-18, 2007.

18. **Jaeger P, Karlmark B, and Giebisch G**. Ammonium transport in rat cortical tubule: relationship to potassium metabolism. *The Am J Physiol* 245: F593-600, 1983.

19. **Kamm DE, and Strope GL**. Glutamine and glutamate metabolism in renal cortex from potassium-depleted rats. *Am J Physiol* 224: 1241-1248, 1973.

20. **Karinch AM, Lin CM, Meng Q, Pan M, and Souba WW**. Glucocorticoids have a role in renal cortical expression of the SNAT3 glutamine transporter during chronic metabolic acidosis. *Am J Physiol Renal Physiol* 292: F448-455, 2007.

21. **Karinch AM, Lin, C M, Wolfgang, C L, Pan, M, Souba, W W**. Regulation of expression of the SN1 transporter during renal adaptation to chronic metabolic acidosis in rats. *Am J Physiol Renal Physiol* 283: F1011-1019, 2002.

22. **Khanna A, Simoni J, Hacker C, Duran MJ, and Wesson DE**. Increased endothelin activity mediates augmented distal nephron acidification induced by dietary protein. *J Am Soc Nephrol* 15: 2266-2275, 2004.

23. **Mackenzie B, and Erickson JD**. Sodium-coupled neutral amino acid (System N/A) transporters of the SLC38 gene family. *Pflugers Arch* 447: 784-795, 2004.

24. **McKinney TD, and Davidson KK**. Effect of potassium depletion and protein intake in vivo on renal tubular bicarbonate transport in vitro. *Am J Physio* 252: F509-516, 1987.

25. **Moret C, Dave MH, Schulz N, Jiang JX, Verrey F, and Wagner CA**. Regulation of renal amino acid transporters during metabolic acidosis. *Am J PhysiolRenal Physiol* 292: F555-566, 2007.

26. **Nagami GT**. Effect of bath and luminal potassium concentration on ammonia production and secretion by mouse proximal tubules perfused in vitro. *J Clin Invest* 86: 32-39, 1990.

27. **Nagami GT**. Renal ammonia production and excretion. In: *The Kidney Physiology and Pathophysiology*, edited by Seldin D, Giebisch, G., Lippincott Williams & Wilkins, 2000, p. 1995-2013.

28. **Nonoguchi H, Takehara Y, and Endou H**. Intra- and inter-nephron heterogeneity of ammoniagenesis in rats: effects of chronic metabolic acidosis and potassium depletion. *Pflugers Arch* 407: 245-251, 1986.

29. **Nowik M, Lecca MR, Velic A, Rehrauer H, Brandli AW, and Wagner CA**. Genome-wide gene expression profiling reveals renal genes regulated during metabolic acidosis. *Physiol Genom* 32: 322-334, 2008.

30. **Pagliara AS, and Goodman AD**. Relation of renal cortical gluconeogenesis, glutamate content, and production of ammonia. *J Clin Invest* 49: 1967-1974, 1970.

31. **Pithon-Curi TC, De Melo MP, and Curi R**. Glucose and glutamine utilization by rat lymphocytes, monocytes and neutrophils in culture: a comparative study. *Cell Biochem funct* 22: 321-326, 2004.

32. **Remer T, Dimitriou T, and Manz F**. Dietary potential renal acid load and renal net acid excretion in healthy, free-living children and adolescents. *Am J Clin Nutr* 77: 1255-1260, 2003.

33. **Remer T, and Manz F**. Estimation of the renal net acid excretion by adults consuming diets containing variable amounts of protein. *Am J Clinl Nut* 59: 1356-1361, 1994.

34. **Sastrasinh S, and Sastrasinh M**. Renal mitochondrial glutamine metabolism during K^+ depletion. *Am J Physiol* 250: F667-673, 1986.

35. **Silver RB, and Soleimani M**. H^+-K^+-ATPases: regulation and role in pathophysiological states. *Am J Physiol* 276: F799-811, 1999.

36. **Slot C**. Plasma creatinine determination. A new and specific Jaffe reaction method. *Scand J Clin Lab Invest* 17: 381-387, 1965.

37. **Solbu TT, Boulland JL, Zahid W, Lyamouri Bredahl MK, Amiry-Moghaddam M, Storm-Mathisen J, Roberg BA, and Chaudhry FA**. Induction and targeting of the glutamine transporter SN1 to the basolateral membranes of cortical

kidney tubule cells during chronic metabolic acidosis suggest a role in pH regulation. *J Am Soc Nephrol* 16: 869-877, 2005.

38. **Soleimani M, Bergman JA, Hosford MA, and McKinney TD**. Potassium depletion increases luminal Na^+/H^+ exchange and basolateral $Na^+:CO_3^=:HCO_3^-$ cotransport in rat renal cortex. *J Clin Invest* 86: 1076-1083, 1990.

39. **Stehberger PA, Schulz N, Finberg KE, Karet FE, Giebisch G, Lifton RP, Geibel JP, and Wagner CA**. Localization and regulation of the ATP6V0A4 (a4) vacuolar H^+-ATPase subunit defective in an inherited form of distal renal tubular acidosis. *J Am Soc Nephrol* 14: 3027-3038, 2003.

40. **Sundberg BE, Waag E, Jacobsson JA, Stephansson O, Rumaks J, Svirskis S, Alsio J, Roman E, Ebendal T, Klusa V, and Fredriksson R**. The evolutionary history and tissue mapping of amino acid transporters belonging to solute carrier families SLC32, SLC36, and SLC38. *J Mol Neurosci* 35: 179-193, 2008.

41. **Tannen RL**. The effect of uncomplicated potassium depletion on urine acidification. *J Clin Invest* 49: 813-827, 1970.

42. **Tannen RL**. Relationship of renal ammonia production and potassium homeostasis. *Kidney Int* 11: 453-465, 1977.

43. **Tannen RL, and McGill J**. Influence of potassium on renal ammonia production. *Am J Physiol* 231: 1178-1184, 1976.

44. **Tizianello A, Garibotto G, Robaudo C, Saffioti S, Pontremoli R, Bruzzone M, and Deferrari G**. Renal ammoniagenesis in humans with chronic potassium depletion. *Kidney Int* 40: 772-778, 1991.

45. **Wagner CA, Finberg, K E, Stehberger, P A, Lifton, R P, Giebisch, G H, Aronson, P S, Geibel, J P**. Regulation of the expression of the Cl^-/anion exchanger pendrin in mouse kidney by acid-base status. *Kidney Int* 62: 2109-2117, 2002.

46. **Wall SM**. Mechanisms of NH_4^+ and NH_3 transport during hypokalemia. *Acta physiologica Scandinavica* 179: 325-330, 2003.

47. **Wesson DE**. Dietary acid increases blood and renal cortical acid content in rats. *Am J Physiol* 274: F97-103, 1998.

48. **Wesson DE**. Endogenous endothelins mediate increased distal tubule acidification induced by dietary acid in rats. *J Clin Invest* 99: 2203-2211, 1997.

49. **Wesson DE, Nathan T, Rose T, Simoni J, and Tran RM**. Dietary protein induces endothelin-mediated kidney injury through enhanced intrinsic acid production. *Kidney Int* 71: 210-217, 2007.

V. Dysregulation of the glutamine transporter SNAT3 (Slc38a3) and ammoniagenic enzymes in obese, glucose-intolerant mice

V.1 Diabetes mellitus and uric acid nephrolithiasis

The prevalence of diabetes and metabolic syndrome in industrialized countries has reached epidemic proportions. Type II diabetes in particular is a condition associated with insulin resistance; the body is incapable of effectively transporting glucose into insulin-dependent cells in response to a carbohydrate-containing meal. Metabolic syndrome, on the other hand, is characterized as having a variety of medical disorders including hyperlipidemia, hypertension, insulin resistance, and increased abdominal adiposity. The combination of these disorders increases the risk of developing cardiovascular disease and diabetes (8, 82). In recent years, the incidence of nephrolithiasis has increased in parallel to that of type II diabetes and metabolic syndrome, and it has been suggested that a relationship may exist between these metabolic disorders and renal stone formation (89, 129, 137, 139). A large cross-sectional analysis comparing three large epidemiological studies over a 44 year period found that diabetes appeared to be a significant risk factor for developing uric acid nephrolithiasis, and had suggested that insulin resistance could be the effecter (137). Uric acid nephrolithiasis (UAN) is highly associated with low urinary pH and urine volume, hyper- or normouricosuria, an increased incidence of diabetes or insulin resistance (7, 36, 37, 84, 120). Pharmacological treatment with potassium or sodium citrate has been proven to increase urinary pH and inhibit UA stone formation, providing further evidence that UAN is linked to low urinary pH (65, 71, 104, 105, 121). Diabetic patients with UAN also have reduced urinary NH_4^+ excretion which may explain the occurrence of low urinary pH values and thus may increase the risk of developing UAN. This may indicate a defect in renal ammoniagenesis or excretion, since a low urinary pH usually results in enhanced NH_4^+ excretion in the urine (1, 50, 54, 65, 111, 120). Moreover, giving these subjects an acid challenge results in a reduced capacity to acidify their urine in comparison to healthy controls (120).

V.2 Insulin action in the kidney

In addition to NH_3 production, the renal proximal tubule is also an important site of insulin action. At steady state the liver is the predominate gluconeogenic organ, however the kidney can supply the body with relatively low levels of *de novo* glucose, which can increase substantially during a prolonged fast, starvation or hepatic injury (40, 72, 103). Induction of diabetes in rats *in vivo* or in renal cortex slices results in increased gluconeogenesis, while insulin administration results in a substantial decrease in gluconeogenic activity (62, 72, 83, 116). Furthermore, gluconeogenic enzyme activity and stimulation of gluconeogenesis via various precursors is enhanced and has been localized to the renal proximal tubule (19, 47, 48, 116, 143).

Insulin resistance is a condition whereby physiological amounts of insulin are not sufficient enough to induce a typical insulin response, such as mobilizing glucose into muscle after a meal. There is evidence suggesting that insulin resistance can reduce renal ammoniagenesis, resulting in a lower urine pH and the potent formation of uric acid stones (1, 120). Increases in renal PDG production and glutamine utilization have been observed upon insulin administration, suggesting enhanced renal ammoniagenesis (26, 77).

Taken the above observations into consideration, our aim was to determine if renal SNAT3, PDG and PEPCK are altered using a model of diet-induced-obesity and insulin-resistance, which could explain the observed effects on renal ammoniagenesis and low urinary pH in patients with type II diabetes.

V.3 Manuscript under submission

Dysregulation of the glutamine transporter Slc38a3 (SNAT3) and ammoniagenic enzymes in obese, glucose-intolerant mice

Stephanie M. Busque[1], Gerti Stange[1] and Carsten A. Wagner[1]
Institute of Physiology, Zurich Center for Integrative Human Physiology ZIHP,
University of Zurich, Zurich, Switzerland

Running head: Obesity and dysregulation of SNAT3

Address correspondence to:
Carsten A. Wagner
Institute of Physiology
University of Zurich
Winterthurerstrasse 190
CH-8057 Zurich
Switzerland
Phone: +41-44-63 50659
Fax: +41-44-63 56814
Wagnerca@access.uzh.ch

ABSTRACT

Uric acid nephrolithiasis is prevalent among patients with type 2 diabetes and metabolic syndrome; it is correlated with an acidic urine and lower urinary ammonium excretion and is likely associated with insulin resistance. Insulin stimulates ammoniagenesis in renal cell lines, possibly via increased phosphate-dependent glutaminase (PDG) activity and glutamine metabolism. Ammonium excretion is mediated at least in part by the proximal tubule Na^+/H^+-exchanger NHE3 and in the collecting duct involving the Rhesus protein Rhcg. Here we tested, whether obesity and insulin resistance in a diet-induced model could contribute to deranged ammonium excretion. Diet-induced obesity was produced and confirmed by pathological intraperitoneal glucose tolerance tests (IPGTT). Three groups of mice were compared: control; **o**bese, **g**lucose-**i**ntolerant with abnormal IPGTT (O-GI); or moderate weight with normal IPGTT mice (**n**on-**r**esponders, NR). Basal urinary ammonium excretion did not differ among groups. However, acid loading increased urinary ammonium excretion in all groups, but to a lesser extent in the O-GI group. SNAT3 mRNA expression was enhanced in both obese groups. PDG expression was elevated only in acid-loaded O-GI mice, whereas PEPCK was enhanced in both O-GI and NR groups given NH_4Cl. NHE activity in the brush border membrane of the proximal tubule was strongly reduced in the O-GI group whereas Rhcg expression was similar. In sum, obesity and glucose intolerance impairs renal ammonium excretion in response to NH_4Cl feeding most likely through reduced NHE activity. The stimulation of SNAT3 and ammoniagenic enzyme expression may be compensatory but futile.

INTRODUCTION

The prevalence of diabetes from a global perspective has reached approximately 170 million and is expected to rise (86). In the United States alone, approximately 23.6 million people have diabetes, while 76 million have metabolic syndrome, a combination of disorders including hyperlipidemia, hypertension, insulin resistance and increased abdominal adiposity, increasing the risk of developing cardiovascular disease and diabetes (4, 51). Interestingly, the incidence of nephrolithiasis in this population has increased in parallel, and it has been suggested that a relationship may exist between these metabolic disorders and renal stone formation (56, 76, 79, 81). A recent cross-sectional analysis comparing three large epidemiological studies over a 44 year period found that diabetes appeared to be a significant risk factor for developing uric acid nephrolithiasis (UAN), and had suggested that insulin resistance could be the effecter (79). UAN is highly associated with low urinary pH and urine volume, hyper- or normouricosuria, and the increased incidence of diabetes or insulin resistance (3, 19, 20, 53, 69). Pharmacological treatment with potassium or sodium citrate has been proven to increase urinary pH and inhibit UA stone formation, providing further evidence that UAN is linked to low urinary pH (36, 40, 63, 64, 70). Patients with diabetes and UAN not only have low urinary pH values, but also exhibit decreased renal ammonium (NH_4^+) excretion. The mechanism likely involves defective renal ammoniagenesis or excretion since a low urinary pH usually is associated with enhanced NH_4^+ excretion in the urine (1, 27, 30, 36, 66, 69). Furthermore, functional acid-loading tests in these patients resulted in a reduced capacity to acidify their urine in comparison to healthy controls (69).

Renal ammoniagenesis and gluconeogenesis increase substantially in the proximal tubule (PT) in response to acute or chronic metabolic acidosis. This is a direct result of the shunting of glutamine from the visceral or splanchnic pool to the kidney, with concomitant increases in glutamine extraction from arterial blood (61, 84). We and others have shown that glutamine influx is likely due to the basolateral proximal tubule glutamine transporter Slc38a3 (SNAT3), since increased SNAT3 expression has been observed during MA (38, 39, 57, 60, 75). Recent work by our group has also shown

enhanced SNAT3 mRNA and protein in response to potassium restriction or a high protein diet,, conditions that create an acidosis-like state and stimulate renal ammoniagenesis (12, 34, 55, 58, 59, 67, 71, 78, 85). Glutamine is then transported into the mitochondrial matrix of the PT cell and metabolized. One NH_4^+ ion is liberated through the deamidation of glutamine to glutamate via phosphate-dependent glutaminase (PDG), while another NH_4^+ ion is produced upon conversion of glutamate to α-ketoglutarate. In the PT cell cytosol, α-ketoglutarate has two metabolic fates; as a substrate in the tricarboxylic acid cycle, or as a precursor of *de novo* glucose synthesis in the presence of phosphoenolpyruvate carboxykinase (PEPCK), resulting in the production of two bicarbonate molecules. Increases in PDG and PEPCK enzyme activity during MA have been associated with a concomitant increase in mRNA levels and protein abundance and are thus important regulators of ammoniagenesis (11, 13, 16, 18, 32, 33, 80). These two enzymes are, however, differentially regulated. PDG is augmented during MA as a result of increased stabilization of its mRNA secondary to the binding of ξ-crystallin/NADPH:quinone reductase to a pH responsive AU-rich region in the 3' untranslated region of its mRNA, while increases in PEPCK are mostly the result of augmented transcription of the PEPCK gene (16, 28, 29, 44, 45).

Once NH_4^+ is produced in the PT, it is transported into the tubular lumen. This is accomplished either via diffusion as NH_3 where it can trap protons, or it can be transported as NH_4^+. A key protein involved in the luminal transport of NH_4^+ as well as providing protons for bicarbonate reabsorption is the Na^+/H^+ exchanger, NHE3. It has been localized to the brush borer membrane of the PT and has been shown to increase during NH_4Cl-induced MA (2, 43, 87). Reabsorption of NH_4^+ produced by the PT occurs in the medullary thick ascending limb largely by the activation of a luminal $Na^+/K^+/2Cl^-$ cotransporter (NKCC2) (5). After accumulation in the medullary interstitium, NH_4^+ is ultimately excreted in the final urine, via the Rhesus factor Rhcg protein (37). In response to an acid load, Rhcg mutant mice reveal defective urinary NH_4^+ excretion (9)

In addition to ammoniagenesis, the renal proximal tubule is also an important gluconeogenic site and is responsive to insulin action (11, 25, 26, 68, 83). Induction of diabetes in rats *in vivo* or in renal cortex slices results in increased gluconeogenesis, while supplying insulin results in a substantial decrease in gluconeogenic activity (35, 41,

52). Further, insulin can also stimulate NHE3 activity in the proximal tubule (21, 24, 42, 73). A recent study has shown that Zucker diabetic fatty rats exhibit reduced urinary NH_4^+ and pH, with a concomitant reduction in renal brush border membrane NHE3 activity, suggesting that renal NH_4^+ excretion is reduced in part by a reduction in NHE3 activity (10).

Given that both ammoniagenesis and gluconeogenesis are closely linked in the renal proximal tubule cell, we hypothesized that a diet-induced, glucose-intolerant state could alter renal ammoniagenesis through dysregulation of the glutamine transporter SNAT3, renal ammoniagenic and gluconeogenic enzymes, PDG and PEPCK, or transport proteins involved in renal NH_4^+ excretion. Modifications in the regulation of these proteins could ultimately result in perturbations in ammoniagenesis and excretion, and could help to explain the pathogenesis of UAN in subjects with diabetes and metabolic syndrome.

RESULTS

"Cafeteria-diet" feeding induces obesity and pathological glucose intolerance in mice

After 10 weeks of a high fat, high energy "cafeteria-style diet", or a standard control diet, all mice (n=72) were subjected to intraperitoneal glucose tolerance testing (IPGTT). Distinct differences were observed among the cohort of cafeteria-diet fed mice. Weights were taken weekly throughout the experimental dietary treatment; immediately before the IPGTT and on the final 2 days in the metabolic cages (supplemental figure 1, figure 1 B, and table 1, respectively). We observed that the cafeteria-fed mice were significantly more obese than control mice. Further, IPGTT revealed two distinct tiers of glucose intolerance among the cafeteria-fed mice (figure 1 A) paralleling the weight differential. Approximately half of the cafeteria-fed mice were significantly obese and did not reach euglycemia at the end of the IPGTT (**o**bese, **g**lucose-**i**ntolerant; O-GI group), while the other half of cafeteria-fed mice were moderately obese and clearly less glucose intolerant (**n**on-**r**esponders; NR group). A similar phenomenon has been described in rats showing that chronic consumption of a high fat, high calorie diet led to a weight differential in roughly half of the study population tested, resulting in obesity and insulin resistance (46, 47, 49). Furthermore, these observations were noted without a further increase in food intake in these animals, which has been suggested to be associated with irreversible changes in body weight and adiposity set-points. In our study, both O-GI and NR mice gained weight rapidly during the last 7 weeks of cafeteria diet-feeding, despite reduced food intake in the metabolic cages during the final days of the experimental period (table 1).

Abnormal urinary acid excretion in obese, glucose-intolerant mice

Mice (n = 48) were placed in metabolic cages after one week of recovery from IPGTT and maintained on their respective diets. The O-GI, NR and control groups were subdivided and challenged with an acid load consisting of NH_4Cl powdered into the food for 48 h (2 g/100 g food; 40 mM NH_4Cl). At baseline, there were no differences in urinary pH or NH_4^+ excretion between groups. Differences were noted after the acid load was provided. Acid-loading resulted in significantly lower urinary pH in all groups in

comparison to respective controls (Figure 2 A, table 1). Although most clinical data show an acidic urine pH in patients with metabolic syndrome (3, 20, 69), we observed a more alkaline urinary pH in O-GI/NH_4Cl treated mice than acid-loaded control mice fed a standard diet. Further, there was a small but significant difference in urine volumes between cafeteria-fed (both O-GI and NR) and control mice on Day 1 in the metabolic cages; however this discrepancy disappeared on Day 2 (table 1). Low urine volumes have also been observed in subjects with UAN (53). Urinary electrolytes were analyzed (table 2). Treatment with NH_4Cl resulted in elevated urinary Cl^- levels; while at baseline, both O-GI and NR groups showed elevated urinary Cl^- in comparison to controls. Urinary K^+ levels were lower in the O-GI group in comparison to controls and further decreased after an NH_4Cl load. NR mice also showed reduced urinary K^+ during NH_4Cl administration when compared to NR mice alone and NH_4Cl-loaded controls. Urinary phosphate levels were unremarkable between groups, however 24 h phosphate excretion relative to urine volume showed reduced phosphate excretion in the O-GI group compared to controls (table 2, figure 2 C). All acid-challenged mice had increased urinary NH_4^+ excretion as expected, however, O-GI mice given NH_4Cl had less NH_4^+ excretion relative to urine volume (figure 2 B, table 2 and supplemental figure 2.).

Dysregulation of SNAT3 and key ammoniagenic enzymes in obese, glucose-intolerant mice

We and others have previously shown that gene expression of SNAT3, and the key ammoniagenic enzymes PDG and PEPCK increases after inducing acidosis with NH_4Cl treatment (12, 16, 18, 32, 39, 57, 60, 75) . All acid-loaded groups showed enhanced SNAT3 mRNA and protein levels (figure 3 A-K), however each group showed varying expression. O-GI mice treated with NH_4Cl had considerably higher SNAT3 mRNA abundance in comparison to controls given NH_4Cl (6.7-fold vs 3-fold; table 4). SNAT3 protein abundance was exceptionally higher in O-GI/NH_4Cl treated mice in comparison to NR/NH_4Cl treated mice (6.7-fold vs 2.8-fold) despite lower total NH_4^+ excretion. Similarly, immunoblotting revealed elevated SNAT3 protein abundance in O-GI/NH_4Cl mice when compared to acid-loaded control mice (figure 3 H and I). PDG expression followed similar trends, with increased mRNA expression in all groups treated

with NH_4Cl (figure 4 A). Acid-challenged mice (both O-GI and NR) showed relatively more PDG protein abundance than respective controls, similar to mRNA expression (figure 4 A-E). O-GI/NH_4Cl mice showed markedly elevated PDG mRNA abundance in comparison to NR/NH_4Cl mice; however no differences were detected on protein level (figure 4 A, F-G). In parallel, PEPCK mRNA expression was markedly enhanced after an acid-load (2.5-fold) and in both cafeteria-fed groups; O-GI mice given NH_4Cl showed the greatest fold change in mRNA expression (4.4-fold vs 2.2—fold; O-GI and NR groups, respectively) (table 4). Protein abundance for PEPCK was also increased after an acid load, but similar to PDG, showed no differences among the two acid-loaded cafeteria fed groups (figure 5 B-F).

Daily NH_4Cl acid load concentrations were calculated to determine if mice received similar acid loads. Acid-loaded control mice received significantly more NH_4Cl in the diet in metabolic cages than both cafeteria-fed groups (table 3, supplemental figure 3 A and B), when calculated based on per gram food/g body weight. Despite this discrepancy, there was no major difference in the daily NH_4Cl-load between the two obese groups despite differences in urinary NH_4^+ excretion. Thus, the reduced NH_4^+ excretion in O-GI mice is not due to a reduced dietary acid load.

Dysregulated renal gluconeogenesis likely contributes to reduced NH_4^+ excretion in obese, glucose-intolerant mice

Renal ammoniagenesis and gluconeogenesis are closely linked in the proximal tubule cell. The series of enzymatic reactions that occur in the conversion of phosphoenolpyruvate carboxykinase (PEPCK) to glucose in the proximal tubule cell cytosol involve several rate-limiting enzymes, such as fructose 1,6-bisphosphatase and fructose 2,6-bisphosphatase (FBP1 and FBP2, respectively). FBP1 catalyzes the conversion of fructose 1,6-bisphosphate to fructose 6-phosphate and inorganic phosphate, and has been recently immunolocalized to PT cells in human kidney (88). Mutation of the FBP1 gene results in a rare gluconeogenic disorder exhibiting symptoms such as metabolic acidosis (6). On mRNA level, we observed a substantial increase in FBP1 expression in O-GI/NH_4Cl treated mice in comparison to O-GI mice without NH_4Cl treatment (figure 6, A). We have previously shown that after 2 days of NH_4Cl-induced

acidosis, FBP2 is down-regulated (60). Further, we found that FBP2 mRNA was significantly down-regulated after 10 weeks of cafeteria style feeding, but only in the obese fraction of the group (figure 6 B). NR mice showed a trend towards decreased mRNA expression levels, but no significance could be determined in comparison to control mice fed standard chow. Furthermore, we observed that acid-loading O-GI mice produced even greater reductions in FBP2 mRNA in comparison to O-GI in the absence of acid-loading. Thus, these data strongly suggest dysregulation of renal gluconeogenesis in glucose-intolerant, obese mice.

In addition to a potential defect in renal gluconeogenesis, we sought to determine if there were any distal defects in NH_4^+ transport in the kidney, in particular of the Rhesus glycoprotein, Rhcg, in our mice. Rhcg is largely expressed in the connecting tubule and the collecting duct, and plays an important role in apical NH_4^+ extrusion into the final urine (9, 22, 50, 82). Rhcg mRNA expression was unremarkable between groups, however O-GI mice given an acute acid load showed increased Rhcg mRNA expression levels in comparison to O-GI treated without NH_4Cl treatment (figure 8).

Brush border membrane sodium-proton exchanger activity is reduced in acid loaded obese, glucose-intolerant mice

To further identify mechanisms that could contribute to a reduction in urinary NH_4^+ excretion, we examined the activity and protein abundance of NHE3 in brush border membrane vesicles using an acridine orange quenching method and immunoblotting. Reduced NHE3 activity was observed in acid-loaded O-GI mice (figure 7A). In contrast, immunoblotting revealed no significant differences among groups (figure 7 B-G).

DISCUSSION

We created a mouse model of diet-induced obesity and glucose-intolerance to examine if changes in the regulation of the glutamine transporter, SNAT3, and enzymes involved in renal ammoniagenesis and gluconeogenesis, PDG and PEPCK could explain the urinary acidification and NH_4^+ excretory defects seen in subjects with UAN and diabetes. After 10 weeks of dietary treatment, cafeteria-diet fed mice fell into two distinct cohorts based on body weight and response to IPGTT. O-GI mice were significantly obese and had severely elevated blood glucose, while NR mice were moderately obese with more normal blood glucose levels. Similar observations have been previously reported in rats (46-49). Since we used a highly inbred mouse strain (C57BL6) with very little genetic variance in our study, the underlying reason for this difference remains unknown at present. We show that challenging these obese, diabetic mice with an oral acid load leads to defective urinary NH_4^+ excretion despite enhanced expression of key ammoniagenic proteins. O-GI mice exhibited strong upregulation of SNAT3, PDG and PEPCK mRNA and protein abundance suggesting enhanced ammoniagenesis. This was paralleled by dysregulation of key enzymes of gluconeogenesis. Moreover, the proximal tubular brush border membrane sodium-proton exchanger activity was rather reduced in obese and glucose-intolerant mice whereas Rhcg mRNA expression appeared normal.

Studies by Abate et al. and Sakhaee et al. assessed whether or not insulin resistance is associated with UAN. Most patients with UAN had symptoms of metabolic syndrome and a low urinary pH, but were without changes in urinary NH_4^+ excretion. The NH_4^+ concentration as a major component of net acid excretion, however, was significantly reduced in these subjects (1, 69). Many other clinical studies have observed consistently low urinary pH values in patients with UAN and insulin resistance (3, 19, 20, 53). Our results show a slightly higher urinary pH and reduced urinary NH_4^+ excretion in O-GI but not NR mice after an acid challenge, despite reduced NH_4Cl intake in O-GI mice. Importantly, these differences were not observed at baseline and cannot be explained by differences in NH_4Cl intake.

A possible explanation for the higher urinary pH could be attributed to increased rates of NH_3 diffusion and buffering of H^+ in the urine secondary to increased ammoniagenesis as we have observed indirectly via increased SNAT3, PDG and PEPCK (54). Further, these observations could be a species specific response to obesity and/or insulin resistance. It should also be noted that previous studies reporting decreased urinary pH in patients with metabolic syndrome, sampled urine only over a 4 to 12 hour period (36, 69). In contrast, our samples were collected over 24 hrs and the differences may due to changes in circadian rhythm urine and acid excretion.

To date, the renal manifestation of insulin resistance is not fully understood. Work by Bobulescu et al. found that Zucker diabetic fatty rats exhibit reduced urinary NH_4^+ excretion and pH, as well as reduced NHE3 activity in the renal brush border membrane (10). Interestingly, these rats showed an increase in renal triglyceride content, suggesting that there could be a lipotoxic effect of fatty acids in the kidney. In opossum kidney cell lines (OKP), administration of long-chain fatty acids produced a similar reduction in NHE3 activity, NHE3 membrane surface expression and NH_4^+ excretion. This led to the hypothesis that the accumulation of lipids, particularly free fatty acids (FFA) in the kidney could result in alterations in normal, physiological cellular processes, such as ammoniagenesis or gluconeogenesis. The etiological relationship between insulin resistance and low urinary pH has not been identified yet, but it most likely involves the proximal tubule. O-GI mice showed strong upregulation of SNAT3, PDG and PEPCK on both protein and mRNA level, which would imply that ammoniagenesis and likely gluconeogenesis is being maximally fueled by the influx of glutamine into the PT cells. The increased levels of FBP1 in obese mice are consistent with this interpretation. Under normal physiological conditions, the liver is the predominate gluconeogenic organ, however the kidney can supply the body with relatively additional *de novo* glucose, which can increase substantially during a prolonged fast, starvation or hepatic injury (23, 41, 62). The reason for FBP1 upregulation in obese mice is unclear but could be related to relative insulin-resistance of the proximal tubule.

A defect in the more distal parts of the nephron may also be involved, such as reduced excretion of NH_4^+ and H^+ along the collecting duct. mRNA expression levels of

Rhcg, critical for renal ammonium excretion (9), however, did not show significant differences between groups.

In summary, a diet-induced mouse model of obesity and glucose-intolerance demonstrates major changes in the regulation of enzymes and transporters involved in proximal tubular ammoniagenesis, gluconeogenesis, and NH_4^+ excretion, and may help to explain the urinary defects observed in patients with UAN and diabetes.

MATERIAL AND METHODS

Animals

Male C57BL6 mice (n=72) were randomly assigned to two different dietary treatment groups and placed on either a standard diet (control, n = 24) or "cafeteria" style diet (n = 48) for 10 weeks. A cafeteria style diet consists of various combinations of energy dense foodstuffs, and is widely used as a model for diet-induced obesity (72). Our experimental cafeteria diet consisted of unsalted ground peanuts (40%), cookies (25%) and chocolate (15%) mixed with standard rodent chow (20%) to ensure adequate macro- and micronutrient composition. The nutrient composition of the cafeteria diet was as follows: 460 kcal, 15 g of protein, 25 g of carbohydrate and 34 g of fat per 100 g of ground food. Mice had *ad libitum* access to food and water during the 10 week dietary treatment period, and were housed in climate controlled and 12 h light-cycled rooms. All mice were weighed weekly. Animal experiments were conducted according to the Swiss animal welfare laws and approved by the Swiss local animal authority, Zurich, Switzerland.

Intraperitoneal glucose tolerance tests (IPGTT)

After 10 weeks of dietary treatment, each mouse was subjected to IPGTT. The test was performed over a 2 h period. Mice were fasted overnight with free access to water. A single dose of glucose (2 mg/g body weight) was given upon initiation of testing, followed by blood collections from the tail vein every 30 minutes. Glucose monitoring was performed using the Accu-chek blood glucose meter (Roche). After the IPGTT, mice were divided into various groups depending on the test outcome: control with normal IPGTT; **O**bese, glucose-intolerant mice with abnormal IPGTT (subsequently named: O-GI); or moderately obese with relatively normal IPGTT (**N**on-**R**esponders, NR). All mice were allowed to recover from the IPGTT for one week, and were subsequently housed in metabolic cages for the next series of experiments.

Metabolic cage studies

Mice were individually placed in metabolic cages for a total of 4 days, and continued on the experimental diets. Control, O-GI and NR mice were subdivided into NH_4Cl treated groups; NH_4Cl was powdered into the food (2 g/100 g chow) for the final 48 h. Food and water intake, body weight and urinary output were monitored daily. During the final 48 h of dietary treatment, urine was collected every 24 hours under mineral oil and urinary pH was immediately assessed using a pH microelectrode (691 pH meter, Metroholm). The Berthelot and Jaffe methods were used to assess urinary NH_3/NH_4^+ and creatinine concentration (7, 74). At the end of the experimental treatment, mice were anesthetized by intraperitoneal injection of ketamine and xylazine, and blood was collected in heparinized tubes, immediately centrifuged to extract serum, and frozen at -80ºC. Mice were not perfused prior to harvesting kidneys given that neither SNAT3, nor PDG and PEPCK are expressed in whole blood or erythrocytes, respectively (77). Although there is some evidence suggesting white blood cells exhibit PDG activity, exsanguination caused by the blood collections minimized the likelihood of blood cell contamination in our preparations (14, 15, 65). Kidneys were harvested, flash-frozen in liquid nitrogen, and transferred to a -80ºC freezer until further use.

Quantitative Real-time RT PCR

Previously frozen kidneys were homogenized using a Rotor-stator homogenizer, and RNA was immediately extracted using Qiagen RNeasy Mini Kit (Qiagen; Hilden, Germany). DNase digestion was performed using the RNase-free DNase Set (Qiagen; Hilden, Germany). Total RNA extractions were analyzed using the NanoDrop ND-1000 spectophotometer (Wilmington, DE, USA). cDNA was prepared from diluted RNA samples (100 ng/µl) using the TaqMan Reverse Transcriptase Reagent Kit containing 10X RT buffer, $MgCl_2$, random hexamers, dNTPs, RNase inhibitors and Multiscribe reverse transcription enzyme (Applied Biosystems/Roche; Forster City, CA, USA). Thermocycling conditions for reverse transcription were set at 25ºC for 10 min, 48ºC for 30 min, and 95ºC for 5 min (Biometra TGradient thermocycler, Goettingen, Germany). Quantitative Real-time RT-PCR was used to determine relative mRNA expression (7500 Fast Real-Time PCR system, Applied Biosystems). Thermocycling conditions were set at: 50 ºC (2 min), 95ºC (10 min), 95 ºC (15 sec; 40 cycles) and 60 ºC (1 min). Forward

and reverse primer concentration was 25 μM; probe concentration was 5 μM. TaqMan Universal PCR master mix 2X (Applied Biosystems/Roche) was used as the Taq polymerase. Primers and probes for SNAT3, phosphate dependent glutaminease (PDG), phosphoenolpyruvate carboxykinase (PEPCK), fructose 2,6-bisphosphatase (FBP2), rhesus glycoprotein (Rhcg) and Hypoxanthine-guanine phosphoribosyltransferase (HPRT) were generated using the Primer Express software from Applied Biosystems and synthesized at Microsynth (Balgach, Switzerland) as described previously (60). The primer and probe sequences for fructose 2,6-bisphosphatase (FBP1) are as follows: 5'-CAA TGA GTA TCT CCA GAG GAA AA A GTT-3', forward primer; 5'-CCA CAT ACC GGG CAC CAT-3', reverse primer; CCT CCG GAT GGT TCA GCC CCC-3', probe. For Rhcg: 5'-GTT GGA GAA GAA GCG CAA GAA-3', forward; 5'-CGA AGA CCA TGG CGT GTA CA-3', reverse; 5'-TTA CTA TCG CTA CCC GAG CTT CCA G-3', probe. Probes were generated with the reporter dye FAM at the 5' end and TAMRA at the 3' end. Each sample was run in triplicate including a negative control (without Multiscribe reverse transcription enzyme). The cycle threshold (C_t) values obtained were ultimately compared to C_t values of the endogenous gene HPRT. Relative mRNA expression ratios were calculated as $R=2^{[Ct(HPRT)-Ct(gene\ of\ interest)]}$.

Immunoblotting

Total membrane and cytosolic protein preparations were prepared from whole, non-perfused kidneys using a K-HEPES buffer composed of 200 mM mannitol, 80 mM HEPES, 41 mM KOH, along with the protease inhibitors, PMSF, K-EDTA, and leupeptin (pH 7.5). Kidneys were homogenized in 200 μl of ice-cold K-HEPES buffer using a tip sonicator and immediately centrifuged at 2000 rpm for 20 min (4ºC). The supernatant was aspirated and placed in an ultracentrifuge (Sorvall, Thermo Fischer Scientific) for 1 h at 41,000 rpm 4ºC. The supernatant containing cytosolic protein from this second centrifugation step was removed and the pellet containing membrane protein was resuspended in K-HEPES buffer and sonicated to evenly distribute proteins. The BioRad Dc Protein assay was used to measure protein concentration (Bio-Rad; Hercules, CA, USA). Total membrane (75 μg) or cytosolic (50 μg) protein containing Laemmli sample buffer and loaded onto a 10% polyacrylamide gel and SDS-PAGE was performed.

Proteins were transferred to polyvinylidene difluoride membranes (PVDF; Immobilon-P, Millipore, Bedford, MA, USA). Membranes were blocked with Tris-buffered saline / 0.1% Tween and 5% non-fat dry milk for 1 h. Primary antibodies were applied for 2 h at RT or overnight at 4ºC. The primary antibodies used for this study were: phosphate-dependent glutaminase (PDG), which recognizes both the rat (KGA) and human (GAC) kidney-type isoforms of PDG forming the mature PDG protein (66 and 68 kDa; a kind gift from N. Curthoys, Colorado State University, USA; diluted 1:500) (17); anti-PEPCK polyclonal antibody (63 kDa; Cayman Chemical, Ann Arbor, MI, USA; diluted 1:1,000), and mouse monoclonal antibody against β-actin (42 kDa; Sigma, St. Louis, MO, USA; diluted 1:5,000). The anti-NHE3 antibody (90 kDa; a kind gift from O. Moe) diluted 1:5000). The anti-Slc38a3 antibody (1:500) was generated as previously described (57). The secondary antibodies used were anti-rabbit alkaline phosphatase conjugated diluted 1:5,000, and anti-mouse IgG alkaline phosphatase conjugated diluted 1:5,000 or anti-mouse IgG horseradish peroxidase-conjugated 1:10,000, and donkey anti-rabbit HRP 1:12,000. After a series of washing steps and blocking, membranes were treated with alkaline phosphatase- or horseradish peroxidase-conjugated developing solution (Imobilion, location) and exposed to the Diana III chemiluminescence detection system (Raytest). Specific bands on PVDF membranes were later quantified using AIDA Image analyzer version 3.44. Membranes were stripped and reprobed for anti-β-actin and subsequent analysis of the protein of interest was determined relative to β-actin quantification and reported as relative protein abundance (ratio of β-actin/protein of interest).

Brush border membrane acridine orange quenching experiments

Renal brush border membrane vesicle preparations (BBMV) were prepared as previously described (8). Briefly, kidneys were cut into small sections and homogenized using a Polytron homogenizer with a fine rod for 2 minutes in a buffer containing: 300 mM mannitol, 5 mM EGTA and 12 mM Tris-HCl, pH 7.1. A fraction of the homogenates was stored at -20 ºC for immunoblotting, while 1 M $MgCl_2$ was added to the remaining homogenate and allowed to precipitate on ice for 15 minutes. The sample

was then centrifuged at 4500 rpm for 15 minutes. The supernatant was aspirated and centrifuged at 18000 rpm for 30 minutes. The pellet was resuspended in membrane buffer consisting of: 300 mM mannitol, 20 mM HEPES-Tris, pH 7.4. Samples were then centrifuged at 18500 rpm for 30 minutes. Vesicle buffer was added to samples, containing: 280 mM mannitol, 5 mM MES/N-methyl-D-glutamine and 2 mM $MgCl_2$, pH 5.5. Protein concentration was measured using the BioRad fast method.

Acridine orange quenching measurements were performed as previously described (31). Briefly, BBMV suspensions (30 µl) and 6 µM of acridine orange dye were added to a spectrofluometer cuvette held at 25ºC. Excitation occurred at 493 nm and emission at 530 nm. NHE activity was calculated as the as the Δ pH per minute over *Q*, where *Q* represents the quenching of acridine orange detected upon addition of sodium gluconate to the cuvette (2 M).

Statistical analyses were performed using unpaired Student's *t*-test, and results with $p < 0.05$ were considered statistically significant. Data are reported as means ± SEM.

Acknowledgements

This study was supported by the Swiss National Science Foundation Grant 3100A0-122217 (to C.A. Wagner).

Statement of competing financial interests

The authors have no competing financial interests invested in this study.

FIGURE LEGENDS

Table 1

Intake and output was measured in control and cafeteria-fed mice for the final consecutive 24 hours of experimental dietary treatment, with or without NH_4Cl supplementation in the food. Values are means ± SE of results (n = 8 mice per group). $^{a}P \leq 0.05$; $^{b}P \leq 0.01$; $^{c}P \leq 0.001$, comparisons between control and treated groups. $^{d}P \leq 0.05$; $^{e}P \leq 0.01$; $^{f}P \leq 0.001$, comparisons between cafeteria-fed groups. $^{g}P \leq 0.05$; $^{h}P \leq 0.01$; $^{i}P \leq 0.001$, comparisons between acid-loaded groups.

Table 2

Urine analyses were performed to determine the effect of cafeteria style feeding and NH_4Cl treatment on urinary parameters. Values are means ± SE of results from analyses for urinary electrolytes, PO_4^{3-} and NH_4^{+} relative to creatinine in mice (n = 8 mice per group) treated with a standard or cafeteria diet for 10 weeks, with or without NH_4Cl supplementation in the food for the final 2 days. $^{a}P \leq 0.05$; $^{b}P \leq 0.01$; $^{c}P \leq 0.001$, comparisons between control and treated groups. $^{d}P \leq 0.05$; $^{e}P \leq 0.01$; $^{f}P \leq 0.001$, comparisons between cafeteria-fed groups. $^{g}P \leq 0.05$; $^{h}P \leq 0.01$; $^{i}P \leq 0.001$, comparisons between acid-loaded groups.

Table 3

Mean calculated 24 h dietary NH_4Cl load per g food/g body weight in acid-loaded mice fed either a control or cafeteria diet for 10 weeks. Values are means ± SE of results from individual mice given an NH_4Cl acid load for the final 48 h in metabolic cages (0.4 mM/g food). The average concentration of NH_4Cl ingested is calculated relative to daily food intake in grams per gram of body weight. $^{a}P \leq 0.05$; comparisons between cafeteria-fed mice on Day 2. $^{b}P \leq 0.01$; $^{c}P \leq 0.001$; comparisons between control and cafeteria-fed groups on Day 1 or 2.

Table 4

Fold change in mRNA expression in mice in response to NH_4Cl treatment. Mice were placed on either a control or cafeteria diet for 10 weeks. mRNA abundances were determined using quantitative real-time RT PCR in total kidneys. Values represent fold changes in mean C_t values for each gene of interest relative to the reference gene HPRT, and comparisons made between respective controls.

Figure 1

Two tiers of glucose intolerance are unmasked in cafeteria-fed mice after intraperitoneal glucose tolerance testing. Intraperitoneal glucose tolerance tests were performed on all mice (n = 72) after 10 weeks of a standard or cafeteria diet. Mice were fasted overnight and blood glucose monitoring was performed every 30 minutes for 2 h after an initial glucose injection (2mg/g body weight), **(A)**. The most severely glucose-intolerant mice were subsequently named obese, glucose-intolerant (O-GI), while the second tier of mice had moderately elevated blood glucose levels and were called the non-responders (NR). A weight differential was determined between O-GI and NR mice **(B)**. O-GI mice were significantly more obese than control or NR mice.

Figure 2

Acid challenging cafeteria-fed mice with NH_4Cl reveals a defect in ammonium excretion and urinary acidification in O-GI mice.

Mice were placed in metabolic cages and urine was collected for the final two consecutive 24 h intervals under mineral oil. All acid-loaded groups exhibited low urinary pH values in comparison to respective controls, however O-GI mice showed a slightly more alkaline urine than NH_4Cl-loaded mice fed a standard diet **(A)**. 24 h urinary ammonium **(B)** and phosphate **(C)** excretion relative to creatinine was significantly reduced in O-GI, but not NR mice.

Figure 3

O-GI mice show strong upregulation of SNAT3 mRNA and protein abundance after an acid challenge with NH_4Cl.

mRNA expression of SNAT3 was determined in kidneys using quantitative real-time RT PCR in mice fed a standard or cafeteria diet for 10 weeks with or without NH_4Cl supplementation in food, and normalized against HPRT mRNA expression. All acid-loaded groups showed enhanced SNAT3 mRNA expression, with the O-GI group showing a strong upregulation of SNAT3 **(A)**. Total membranes were extracted from whole, non-perfused kidney, and membranes were probed with an N-terminal antibody against SNAT3 and reprobed after stripping for β-actin to control for equal loading. Original blots are depicted with bar graphs summarizing normalized data. Enhanced SNAT3 protein abundance was observed after 2 days of NH_4Cl treatment, **(B, C)**. SNAT3 protein abundance is upregulated after 10 weeks of cafeteria feeding and 2 days of NH_4Cl supplementation in O-GI **(D,E)** and NR **(F,G)** mice. O-GI mice given NH_4Cl showed the most SNAT3 protein abundance in comparison to acid-loaded controls **(H,I)** or acid-loaded NR mice **(J,K)**. $*P \leq 0.05$, $**P \leq 0.01$, and $***P \leq 0.001$ between groups.

Figure 4

Phosphate-dependent glutaminase is strongly enhanced in O-GI mice after an acid-load.

mRNA expression of PDG was determined using quantitative real-time RT PCR. PDG mRNA was enhanced in all groups after an acid load, and most strongly in the O-GI group given NH_4Cl when compared to acid-loaded control and NR mice **(A)**. Cytosolic proteins were extracted from whole, non-perfused kidneys and probed for PDG. O-GI (B,C) and NR (D,E) mice given NH_4Cl had increased PDG protein abundance in comparison to respective controls, however no differences were observed between acid-loaded O-GI and NR groups when immunoblotted together (F,G). $*P \leq 0.05$, $**P \leq 0.01$

Figure 5

Phosphoenolpyruvate carboxykinase mRNA expression and protein abundance parallel PDG in cafeteria-fed mice.

RNA was extracted from total kidney homogenates and mRNA expression was determined by quantitative real-time RT PCR. PEPCK mRNA expression was elevated in all acid-loaded groups, however both cafeteria fed groups showed the greatest increase in mRNA expression **(A)**. Cytosolic protein fractions were prepared from whole, non-perfused kidneys. Similarly, both O-GI **(B,C)** and NR **(D,E)** mice given an acid-load had the greatest increases in PEPCK protein abundance in comparison to O-GI and NR mice without NH_4Cl supplementation. No differences were detected when both acid-loaded cafeteria groups were immunoblotted together **(E,F)**. $*P \leq 0.05$, $**P \leq 0.01$, and $***P \leq 0.001$ between groups.

Figure 6

Gluconeogeneogenic enzyme activity is regulated by cafeteria diet feeding

RNA was extracted from whole, non-perfused kidneys from mice on a standard or cafeteria diet for 10 weeks, with and without NH_4Cl supplementation. Quantitative real-time RT PCR was used to determine mRNA expression. Fructose 1,6-bisphosphatase (FBP1) was significantly increased in all cafeteria-fed mice **(A)**. In contrast, fructose 2,6-bisphosphatase (FBP2) was regulated only in the O-GI groups, showing reduced mRNA expression in the O-GI group compared to mice fed a standard diet **(B)**. Acid-loaded O-GI mice had significantly less FBP2 mRNA expression than O-GI mice alone. $*P \leq 0.05$, $**P \leq 0.01$ between groups.

Figure 7

Sodium/hydrogen exchanger 3 activity is reduced in BBMV from acid-loaded O-GI mice.

BBMV preparations were made and acridine orange quenching experiments were performed (A). O-GI mice given an NH_4Cl load had reduced NHE3 activity relative to respective controls. In contrast, acid-loaded NR mice showed enhanced NHE3 activity when compared with NR mice without NH_4Cl treatment. Total membrane preparations

were made from whole, non-perfused kidneys and immunoblotted for NHE3 protein. No changes were observed among the groups (HAVE TO ADD IN THE WB AND QUANTIFICATIONS) **(B-G)**. $*P \leq 0.05$, $**P \leq 0.01$, and $***P \leq 0.001$ between groups.

Figure 8

Reduced NH_4 excretion observed in O-GI mice is not likely due to alterations in distal NH_4 transport.

mRNA expression of Rhcg was determined in all groups. No significant changes were noted among groups, indicating the defect in NH_4 excretion is more proximal. $*P \leq 0.05$ between groups.

Supplemental figure 1

Cafeteria fed mice show rapid weight gain over the 10-week experimental period.

Body weights of all mice were measured weekly for 10 weeks. A weight differential was observed between cafeteria diet mice. O-GI mice gained the most weight, while NR mice had only modest weight gain.

Supplemental figure 2

All acid-loaded mice showed appropriate urinary responses to the acid challenge.

24 h urinary NH_4 excretion was determined in all mice. O-GI/NH_4Cl mice showed significantly less NH_4 excretion than NR/NH_4Cl treated mice. Urine volume was not included in the calculation. $*P \leq 0.05$, $**P \leq 0.01$, and $***P \leq 0.001$ between groups.

Supplemental figure 3

Cafeteria-fed mice received less NH_4Cl in the food due to reduced food intake at the end of the experimental period.

Mean NH_4Cl load was calculated based on individual food intakes and body weight. O-GI and NR mice ate less food and therefore ingested less NH_4Cl than controls. This was observed on both Day 1 **(A)** and Day 2 **(B)** in the metabolic cages. $*P \leq 0.05$, $**P \leq 0.01$, and $***P \leq 0.001$ between groups.

Table 1
Metabolic cage studies: differences in intake and output in control and cafeteria-fed mice
Final consecutive 24 h intervals

Groups	Control	NH_4Cl 2 days	O-GI	O-GI/NH_4Cl 2 days	NR	NR/NH_4Cl 2 days
Initial body weight (bw) after IPGTT	31.3 ± 0.6		43.5 ± 0.9[c]		37.8 ± 1.4[c,e]	
DAY 1						
Food intake g/g bw	0.11 ± 0.01	0.07 ± 0.01[c]	0.04 ± 0.002[c]	0.03 ± 0.004[e,i]	0.05 ± 0.004[c]	0.04 ± 0.01[i]
Water intake g/g bw	0.18 ± 0.01	0.14 ± 0.01[a]	0.13 ± 0.03	0.09 ± 0.01[h]	0.10 ± 0.01[c]	0.13 ± 0.02[d]
Urine output ml/g bw	0.04 ± 0.01	0.04 ± 0.01	0.03 ± 0.002[b]	0.03 ± 0.004	0.03 ± 0.004[a]	0.04 ± 0.01
Urine pH	6.17 ± 0.12	5.78 ± 0.04[b]	6.24 ± 0.07	6.09 ± 0.17[d]	6.07 ± 0.06	5.87 ± 0.07[d]
Body wt (g)	30.7 ± 0.61	30.05 ± 1.02	43.75 ± 1.45[c]	42.53 ± 0.66[i]	40.06 ± 1.49[c]	38.05 ± 2.51[g]
DAY 2						
Food intake g/g bw	0.12 ± 0.01	0.09 ± 0.01[a]	0.05 ± 0.003[c]	0.03 ± 0.003[e,i]	0.06 ± 0.004[c]	0.05 ± 0.01[e,i]
Water intake g/g bw	0.19 ± 0.01	0.19 ± 0.02	0.09 ± 0.01[c]	0.11 ± 0.01[h]	0.10 ± 0.01[c]	0.15 ± 0.02[d]
Urine output ml/g bw	0.05 ± 0.01	0.04 ± 0.01	0.02 ± 0.003[a]	0.03 ± 0.003[g]	0.03 ± 0.01	0.03 ± 0.003
Urine pH	6.28 ± 0.14	5.84 ± 0.04[b]	6.38 ± 0.05	6.01 ± 0.05[g]	6.42 ± 0.21	5.90 ± 0.06
Body wt (g)	30.63 ± 0.61	29.51 ± 1.01	42.98 ± 1.39[c]	41.62 ± 0.68[i]	39.59 ± 1.43[c]	37.04 ± 2.42[g]

Values are means ± SE of results from analyses from metabolic cage studies with mice (n = 8 mice per group) treated with a standard or cafeteria diet for 10 weeks, with or without NH_4Cl supplementation in the food for the final 2 days. [a]$P \leq 0.05$; [b]$P \leq 0.01$; [c]$P \leq 0.001$, comparisons between control and treated groups. [d]$P \leq 0.05$; [e]$P \leq 0.01$; [f]$P \leq 0.001$, comparisons between cafeteria-fed groups. [g]$P \leq 0.05$; [h]$P \leq 0.01$; [i]$P \leq 0.001$, comparisons between acid-loaded groups.

Table 2
Urinary analyses: effect of cafeteria-style feeding and NH_4Cl administration

Groups ***Electrolytes***	Control	NH_4Cl 2 days	O-GI	O-GI/NH_4Cl 2 days	NR	NR/NH_4Cl 2 days
Na^+, mM	1.07 ± 0.15	0.74 ± 0.09	0.71 ± 0.14	0.48 ± 0.08	0.93 ± 0.24	0.53 ± 0.09
K^+, mM	3.27 ± 0.44	2.38 ± 0.33	1.5 ± 0.24[b]	1.06 ± 0.22[h]	2.30 ± 0.43	1.24 ± 0.17[d,h]
Ca^{2+}, mM	0.036 ± 0.01	0.05 ± 0.01	0.04 ± 0.01	0.06 ± 0.01	0.06 ± 0.01	0.05 ± 0.01
Mg^{2+}, mM	0.25 ± 0.03	0.20 ± 0.03	0.17 ± 0.05	0.15 ± 0.04	0.19 ± 0.04	0.20 ± 0.04
Cl^-, mM	2.31 ± 0.42	5.12 ± 0.54[b]	0.91 ± 0.14[a]	3.25 ± 0.71[e]	1.07 ± 0.12[a]	4.1 ± 0.32[f]
PO_4^{3-}, mM	0.72 ± 0.11	0.63 ± 0.10	0.69 ± 0.12	0.63 ± 0.15	0.95 ± 0.06	0.95 ± 0.19
SO_4^{2-}, mM	0.48 ± 0.10	0.37 ± 0.04	0.24 ± 0.04[a]	0.21 ± 0.05[g]	0.30 ± 0.04	0.21 ± 0.02[h]
PO_4^{3-}/creatinine $mmol \cdot mg^{-1} \cdot dl$	0.782 ± 0.107	0.974 ± 0.13	0.957 ± 0.08	1.082 ± 0.154	1.103 ± 0.062	1.145 ± 0.189
PO_4^{3-}, mmol/ 24 h	0.094 ± 0.013	0.092 ± 0.015	0.057 ± 0.088[a]	0.067 ± 0.007	0.085 ± 0.014	0.065 ± 0.004
NH_4^+/creatinine $mmol \cdot mg^{-1} \cdot dl$	0.595 ± 0.238	6.21 ± 1.12[c]	0.691 ± 0.107	4.591 ± 0.722[f]	2.085 ± 0.755	6.886 ± 0.745[f,g]
NH_4^+, mmol/24 h	0.095 ± 0.045	0.577 ± 0.114[b]	0.041 ± 0.009	0.312 ± 0.03[f,g]	0.092 ± 0.026	0.481 ± 0.078[f]

Values are means ± SE of results from analyses for urinary electrolytes and PO_4^{3-} and NH_4^+ relative to creatinine in mice (n = 7-8 mice per group) treated with a standard or cafeteria diet for 10 weeks, with or without NH_4Cl supplementation in the food for the final 2 days. [a]$P \leq 0.05$; [b]$P \leq 0.01$; [c]$P \leq 0.001$, comparisons between control and treated groups. [d]$P \leq 0.05$; [e]$P \leq 0.01$; [f]$P \leq 0.001$, comparisons between cafeteria-fed groups. [g]$P \leq 0.05$; [h]$P \leq 0.01$; [i]$P \leq 0.001$, comparisons between acid-loaded groups.

Table 3
Mean calculated 24 h dietary NH_4Cl load per g food/g body weight in acid-loaded mice

Groups	Day 1	Day 2
NH_4Cl 2 days	0.029 mM ± 0.003	0.037 mM ± 0.003
O-GI/NH_4Cl 2 days	0.011 mM ± 0.002[c]	0.012 mM ± 0.001[c]
NR/NH_4Cl 2 days	0.016 mM ± 0.003[b]	0.018 mM ± 0.002[a,c]

Values are means ± SE of results from individual mice given an NH_4Cl acid load for the final 48 h in metabolic cages (0.4 mM/g food). The average concentration of NH_4Cl ingested is calculated relative to daily food intake in grams per gram of body weight. [a]$P \leq 0.05$; comparison among cafeteria-fed mice on Day 2. [b]$P \leq 0.01$; [c]$P \leq 0.001$; comparisons among control and cafeteria-fed groups on Day 1 or 2.

Table 4
Fold change in mRNA expression in mice in response to NH_4Cl treatment

Groups ***mRNA expression***	Control vs NH_4Cl 2 days	O-GI vs O-GI/NH_4Cl 2 days	NR vs NR/NH_4Cl 2 days
SNAT3	3.04	6.70	2.83
PDG	1.69	3.51	1.74
PEPCK	2.51	4.43	2.24
FBP1	0.76	1.46	1.09
FBP2	1.12	0.55	0.92
Rhcg	1.26	1.30	1.08

Values represent fold changes in mean C_t values for each gene of interest relative to the reference gene HPRT.

Figure 1

Busque et al.

A.

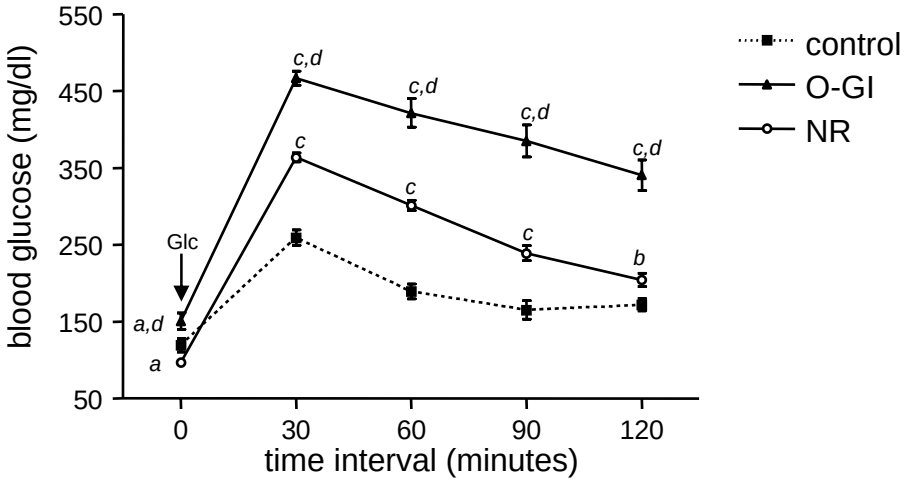

B.

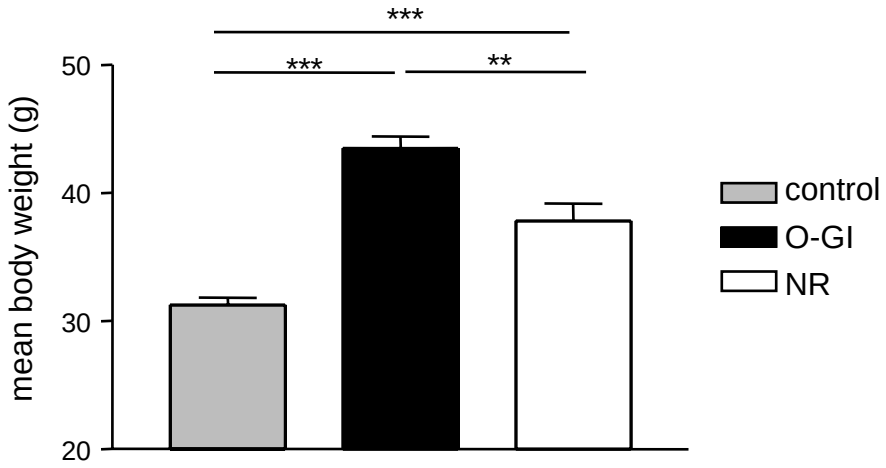

Figure 2

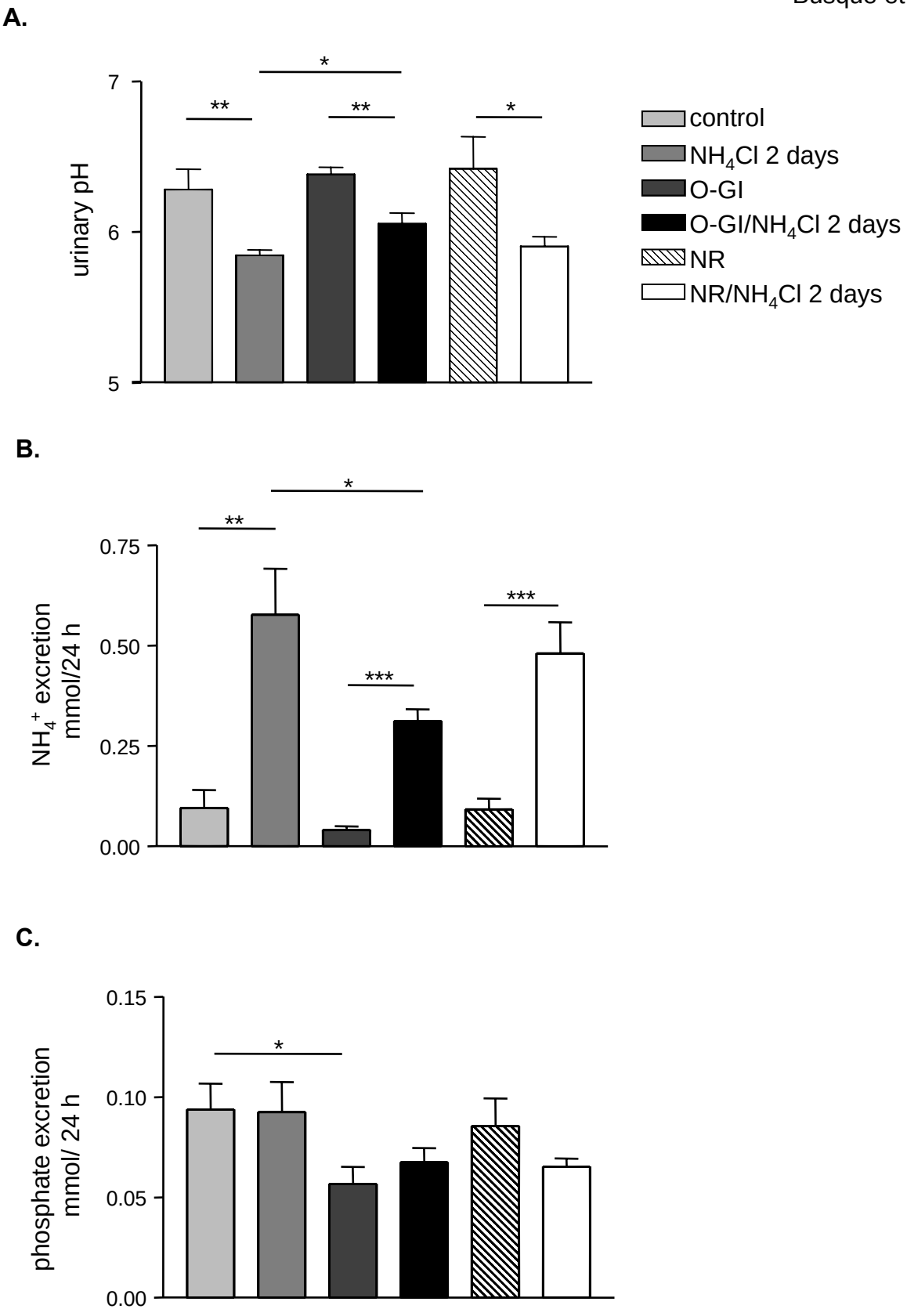
A.
urinary pH
7
6
5
*
**
**
*
control
NH4Cl 2 days
O-GI
O-GI/NH4Cl 2 days
NR
NR/NH4Cl 2 days
B.
NH4+ excretion
mmol/24 h
0.75
0.50
0.25
0.00
*
**
***
***
C.
phosphate excretion
mmol/ 24 h
0.15
0.10
0.05
0.00
*

Figure 3 Busque et al.

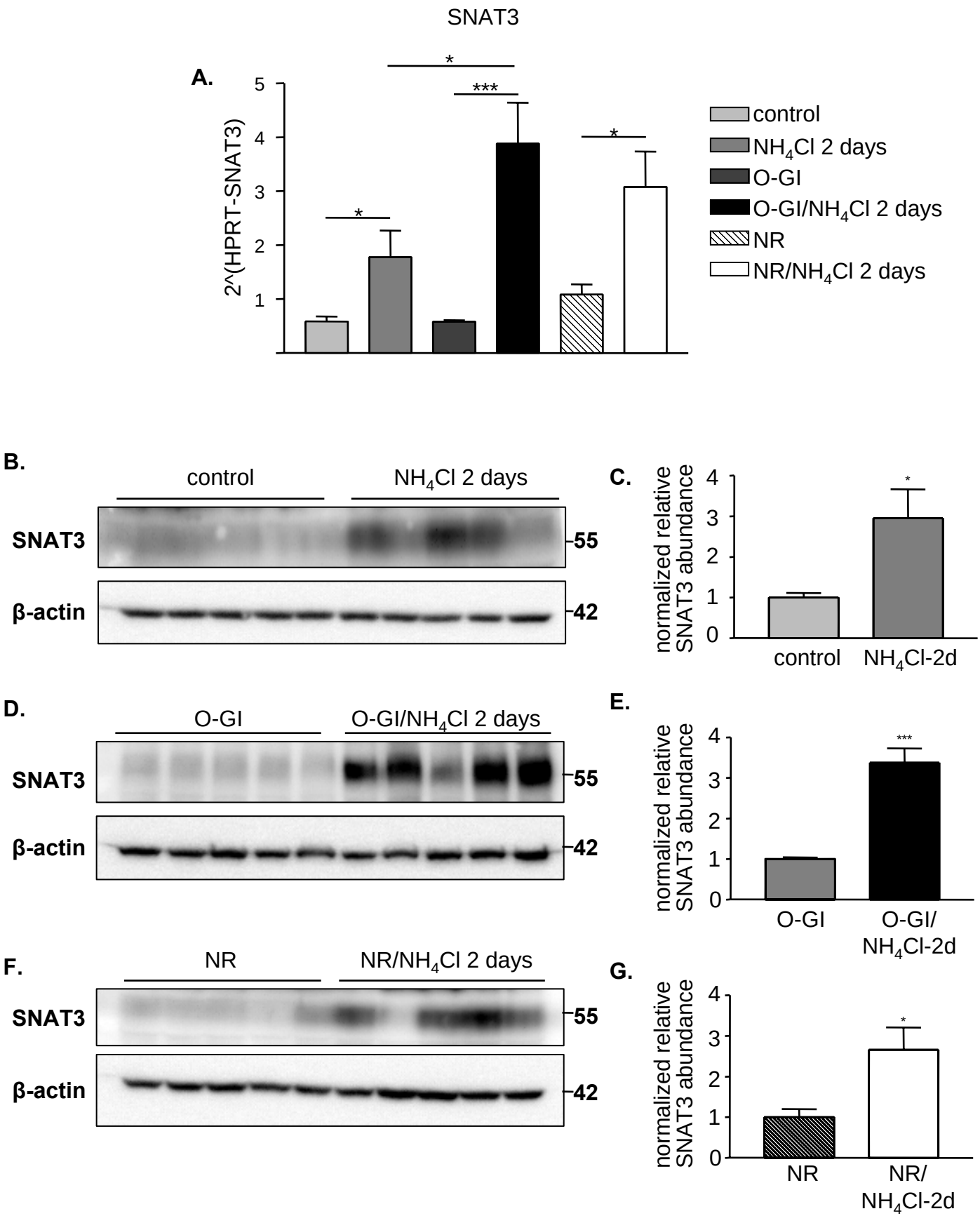

Figure 3

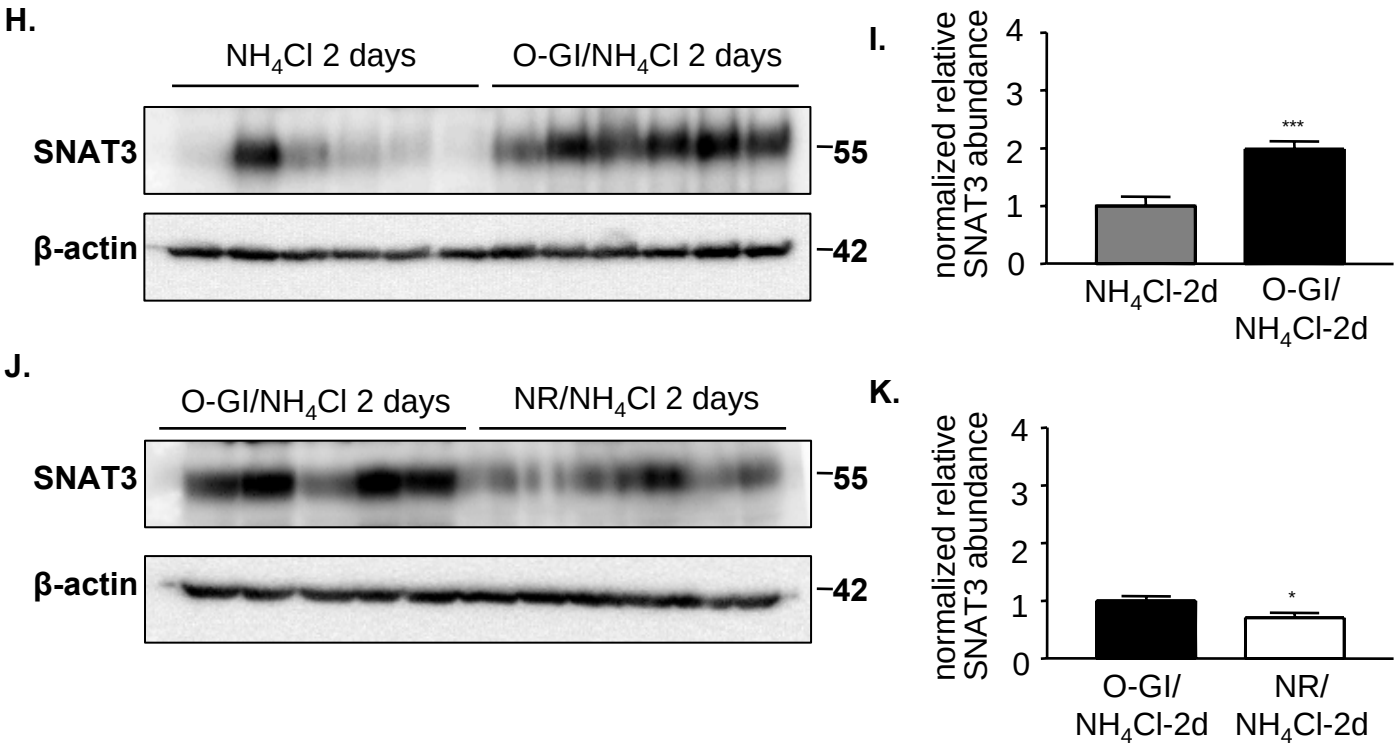
H.
NH4Cl 2 days
O-GI/NH4Cl 2 days
SNAT3
β-actin
55
42
I.
normalized relative SNAT3 abundance
0
1
2
3
4
***
NH4Cl-2d
O-GI/ NH4Cl-2d
J.
O-GI/NH4Cl 2 days
NR/NH4Cl 2 days
SNAT3
β-actin
55
42
K.
normalized relative SNAT3 abundance
0
1
2
3
4
*
O-GI/ NH4Cl-2d
NR/ NH4Cl-2d

Figure 4

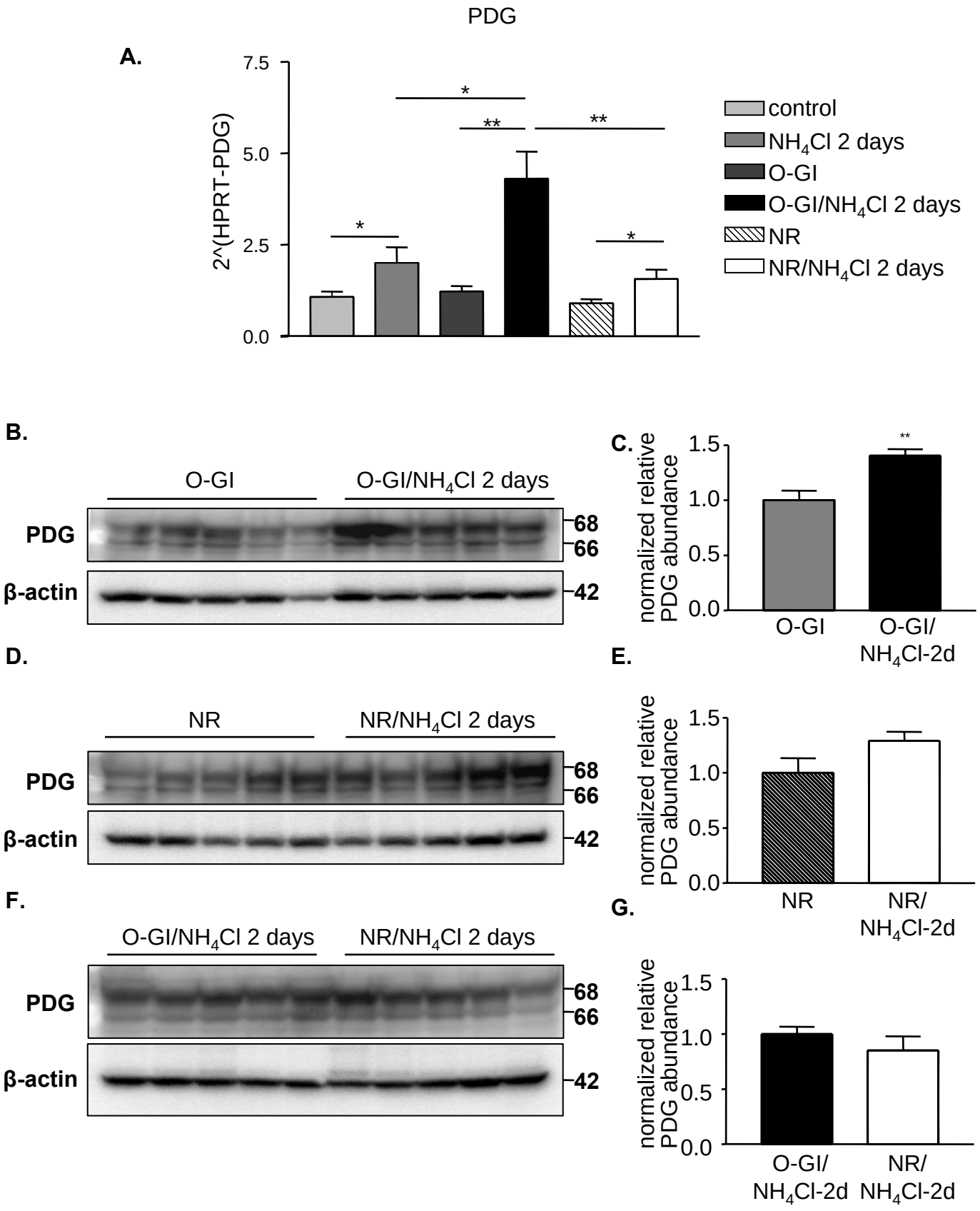
PDG
A.
2^(HPRT-PDG)
7.5
5.0
2.5
0.0
control
NH4Cl 2 days
O-GI
O-GI/NH4Cl 2 days
NR
NR/NH4Cl 2 days
B.
O-GI
O-GI/NH4Cl 2 days
PDG
β-actin
68
66
42
C.
normalized relative PDG abundance
1.5
1.0
0.5
0.0
O-GI
O-GI/ NH4Cl-2d
D.
NR
NR/NH4Cl 2 days
E.
NR
NR/ NH4Cl-2d
F.
O-GI/NH4Cl 2 days
NR/NH4Cl 2 days
G.
O-GI/ NH4Cl-2d
NR/ NH4Cl-2d

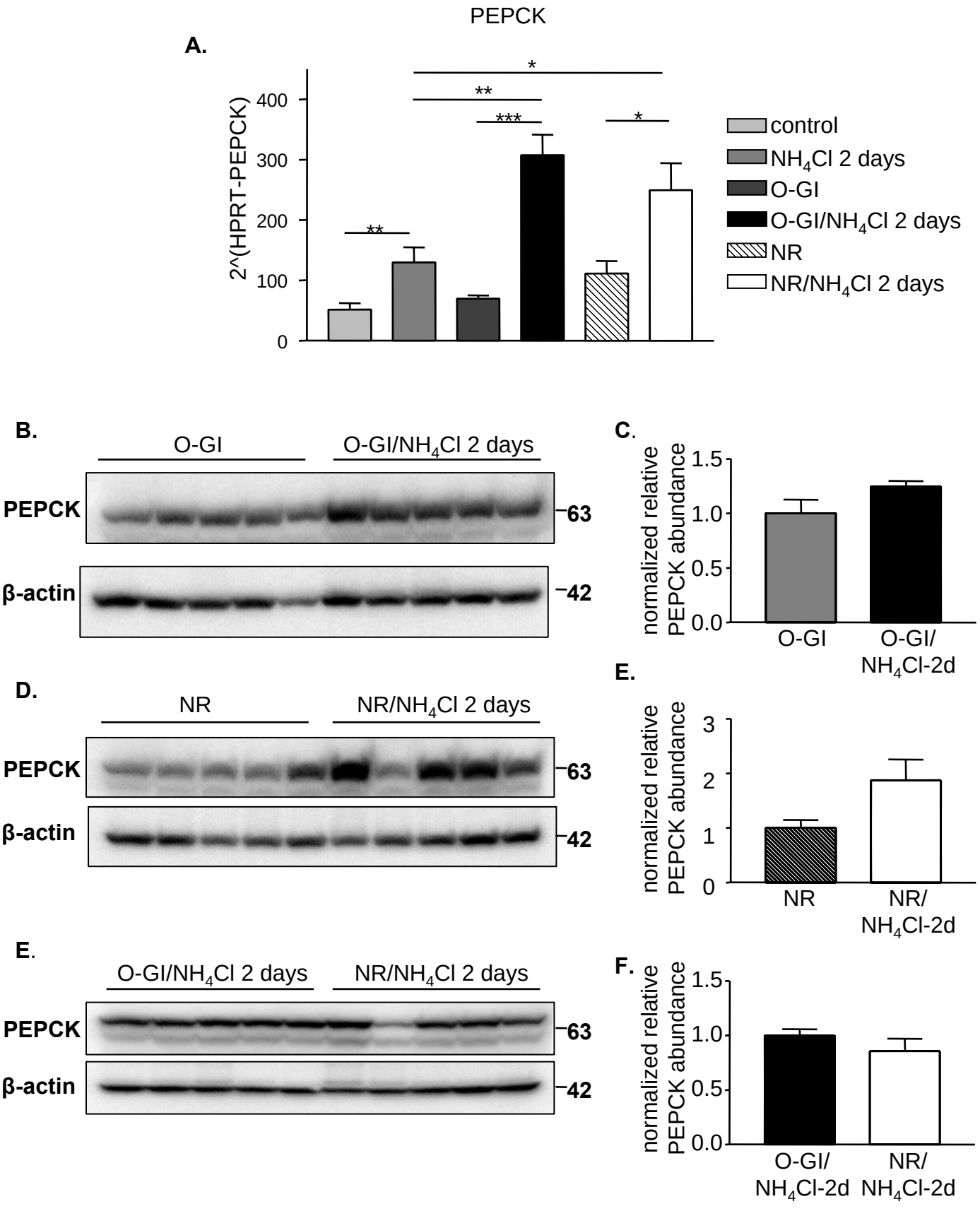
A.
PEPCK
2^(HPRT-PEPCK)
400
300
200
100
0
*
**
***
*
**
control
NH4Cl 2 days
O-GI
O-GI/NH4Cl 2 days
NR
NR/NH4Cl 2 days
B.
O-GI
O-GI/NH4Cl 2 days
PEPCK
β-actin
63
42
C.
normalized relative PEPCK abundance
1.5
1.0
0.5
0.0
O-GI
O-GI/ NH4Cl-2d
D.
NR
NR/NH4Cl 2 days
PEPCK
β-actin
63
42
E.
normalized relative PEPCK abundance
3
2
1
0
NR
NR/ NH4Cl-2d
E.
O-GI/NH4Cl 2 days
NR/NH4Cl 2 days
PEPCK
β-actin
63
42
F.
normalized relative PEPCK abundance
1.5
1.0
0.5
0.0
O-GI/ NH4Cl-2d
NR/ NH4Cl-2d

Figure 6

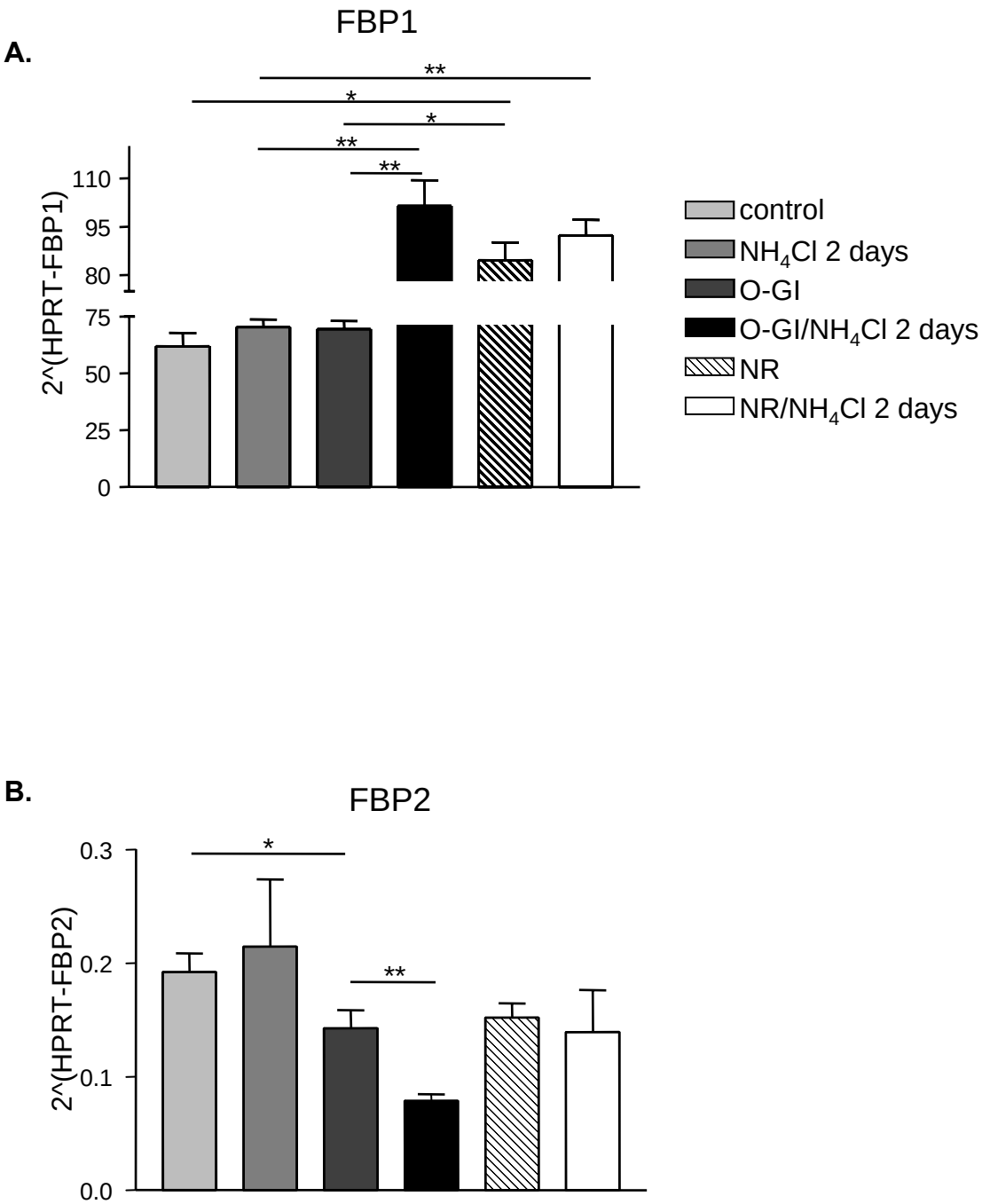
A.
FBP1
2^(HPRT-FBP1)
110
95
80
75
50
25
0
**
*
*
**
**
control
NH4Cl 2 days
O-GI
O-GI/NH4Cl 2 days
NR
NR/NH4Cl 2 days
B.
FBP2
2^(HPRT-FBP2)
0.3
0.2
0.1
0.0
*
**

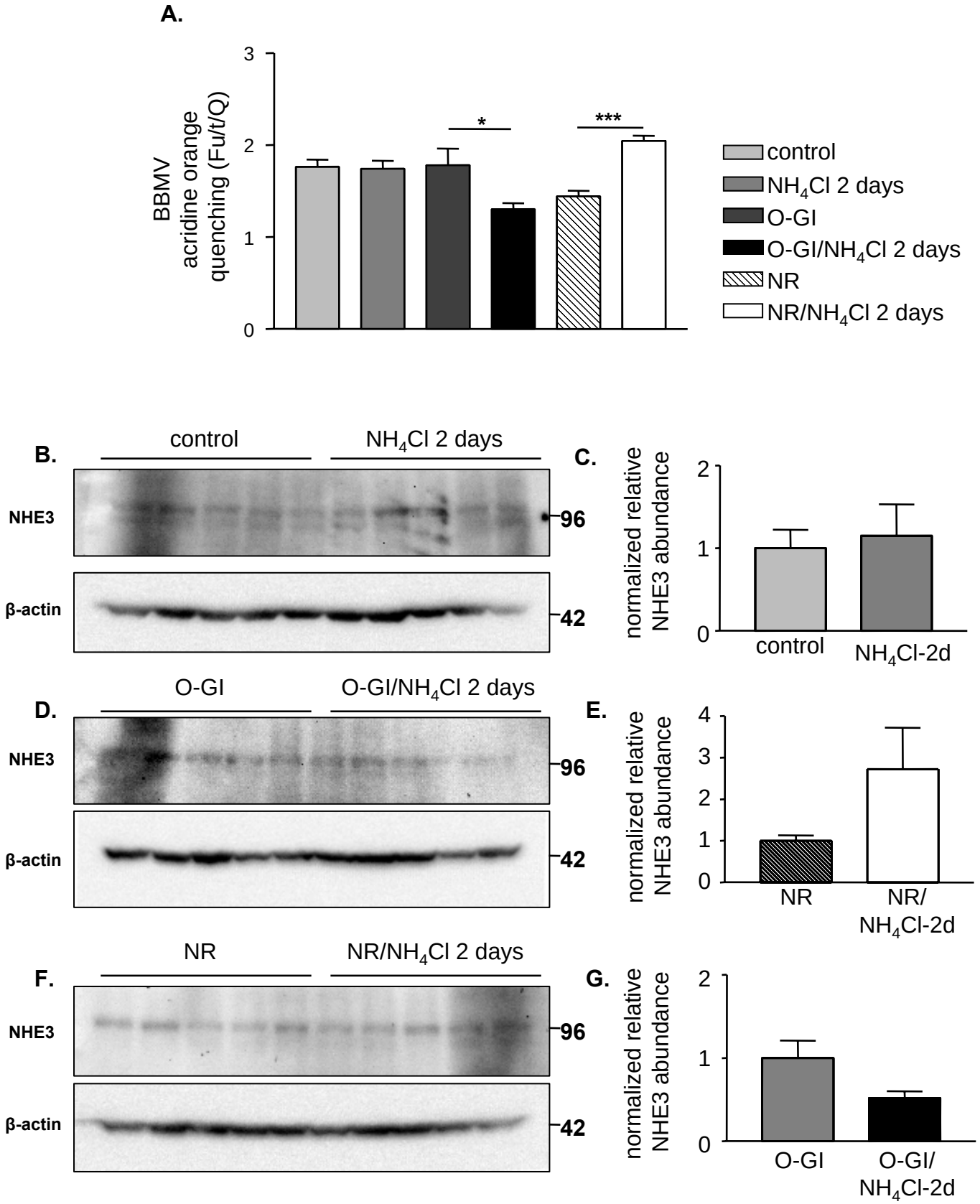
A.
BBMV acridine orange quenching (Fu/t/Q)
3
2
1
0
*
***
control
NH4Cl 2 days
O-GI
O-GI/NH4Cl 2 days
NR
NR/NH4Cl 2 days
B.
control
NH4Cl 2 days
NHE3
β-actin
96
42
C.
normalized relative NHE3 abundance
2
1
0
control
NH4Cl-2d
D.
O-GI
O-GI/NH4Cl 2 days
NHE3
β-actin
96
42
E.
normalized relative NHE3 abundance
4
3
2
1
0
NR
NR/ NH4Cl-2d
F.
NR
NR/NH4Cl 2 days
NHE3
β-actin
96
42
G.
normalized relative NHE3 abundance
2
1
0
O-GI
O-GI/ NH4Cl-2d

Figure 8

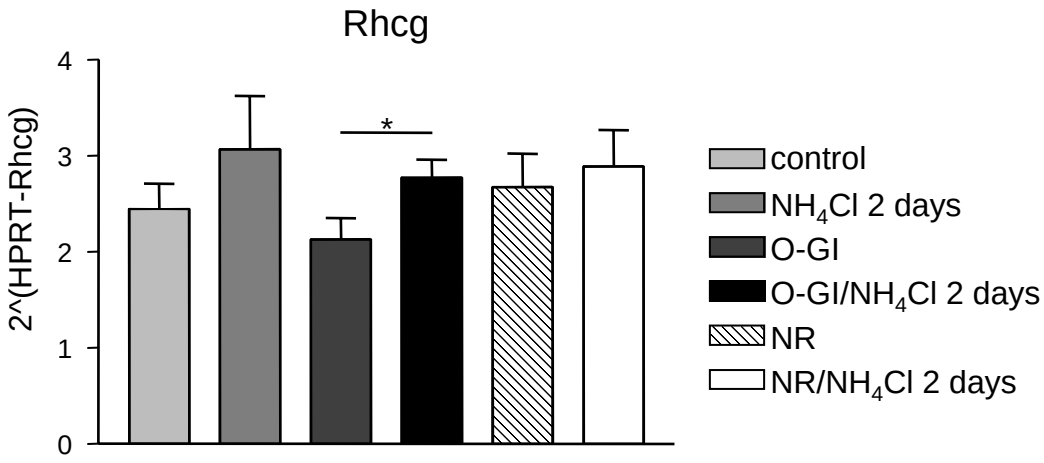
Rhcg
2^(HPRT-Rhcg)
4
3
2
1
0
*
control
NH4Cl 2 days
O-GI
O-GI/NH4Cl 2 days
NR
NR/NH4Cl 2 days

Supplemental Figure 1

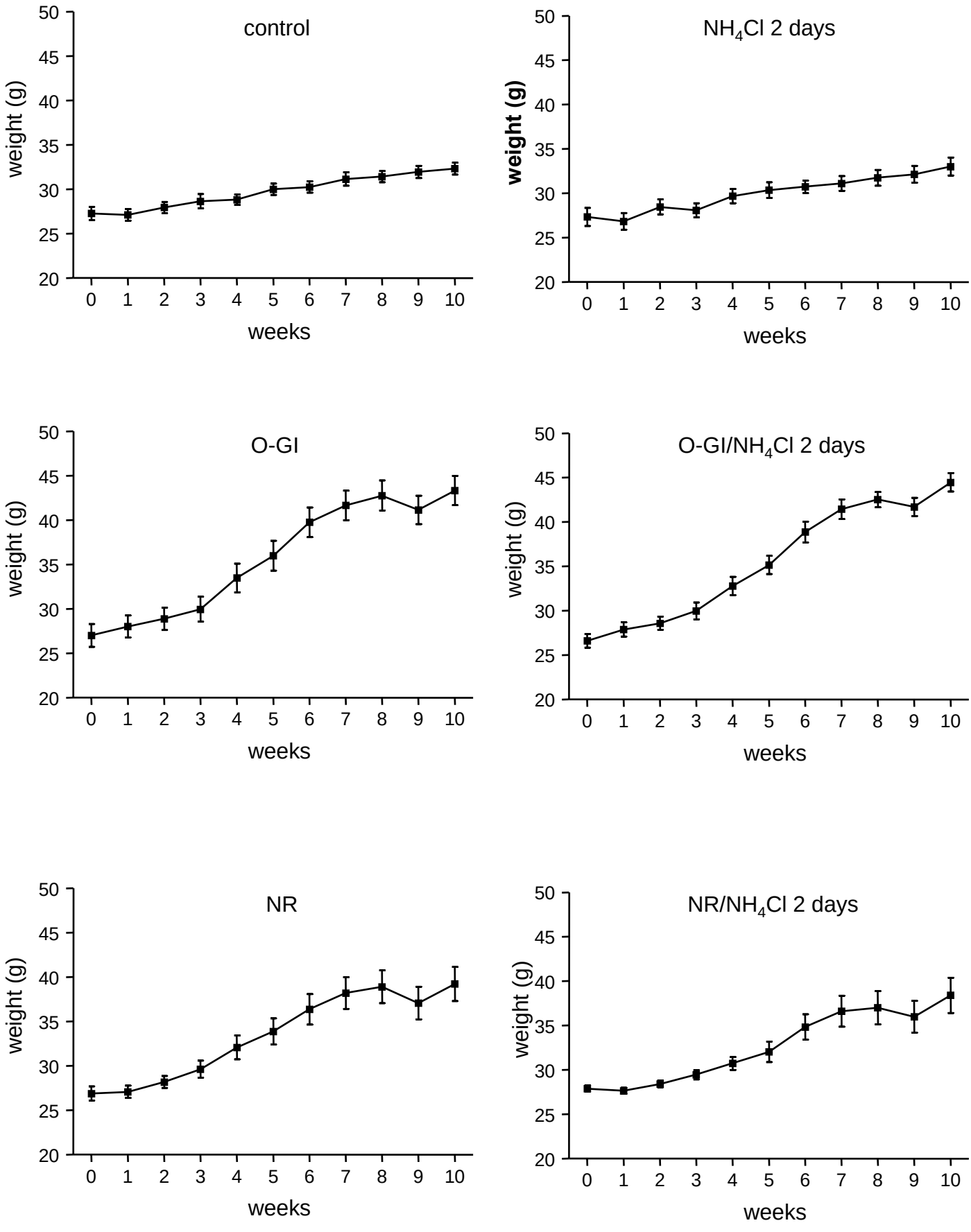

Supplemental Figure 2

Busque et al.

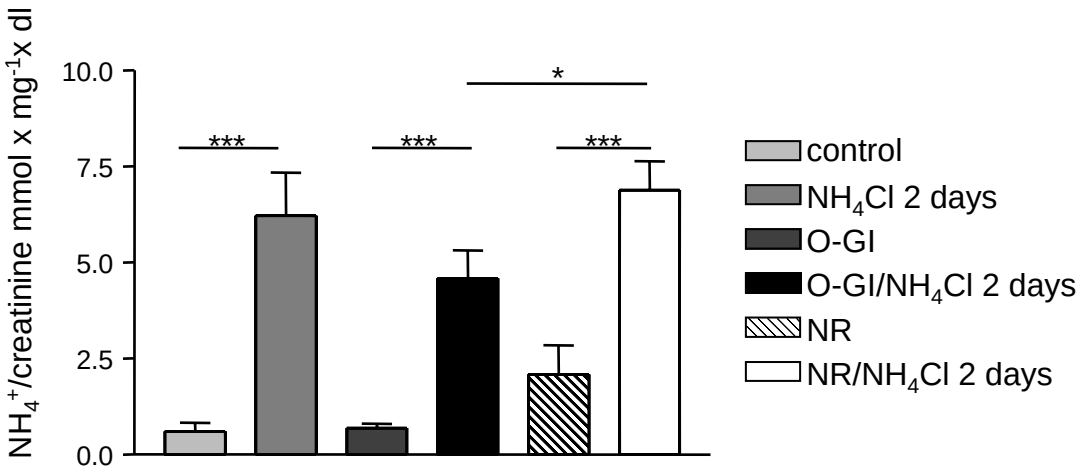

Supplemental Figure 3

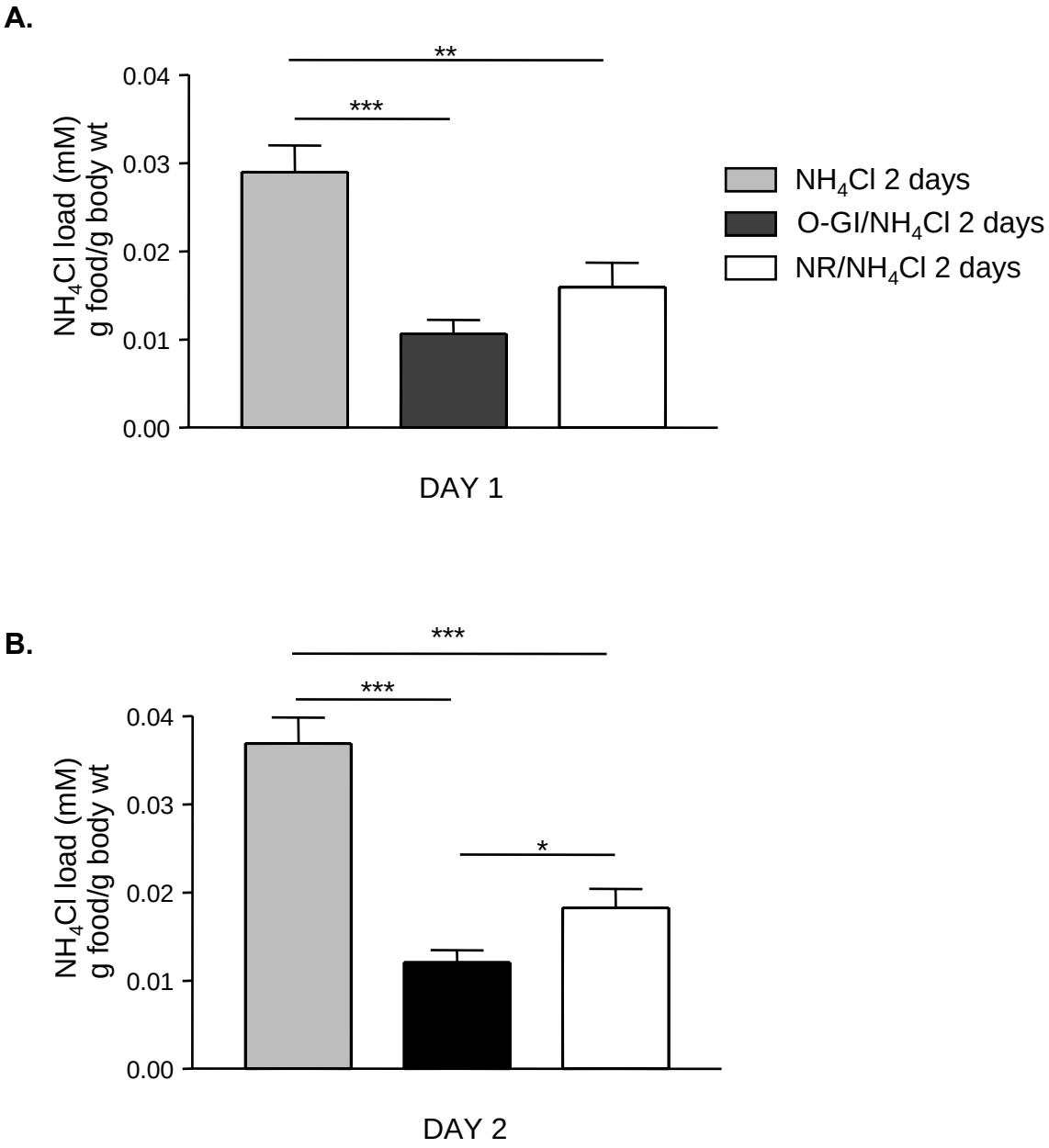

REFERENCES

1. **Abate N, Chandalia M, Cabo-Chan AV, Jr., Moe OW, and Sakhaee K**. The metabolic syndrome and uric acid nephrolithiasis: novel features of renal manifestation of insulin resistance. *Kidney international* 65: 386-392, 2004.

2. **Ambuhl PM, Amemiya M, Danczkay M, Lotscher M, Kaissling B, Moe OW, Preisig PA, and Alpern RJ**. Chronic metabolic acidosis increases NHE3 protein abundance in rat kidney. *The American journal of physiology* 271: F917-925, 1996.

3. **Asplin JR**. Uric acid stones. *Seminars in nephrology* 16: 412-424, 1996.

4. **Association AD**. http://www.diabetes.org/diabetes-statistics/prevalence.jsp. [March 31, 2009

5. **Attmane-Elakeb A, Mount DB, Sibella V, Vernimmen C, Hebert SC, and Bichara M**. Stimulation by in vivo and in vitro metabolic acidosis of expression of rBSC-1, the Na+-K+(NH4+)-2Cl- cotransporter of the rat medullary thick ascending limb. *The Journal of biological chemistry* 273: 33681-33691, 1998.

6. **Baker L, and Winegrad AI**. Fasting hypoglycaemia and metabolic acidosis associated with deficiency of hepatic fructose-1,6-diphosphatase activity. *Lancet* 2: 13-16, 1970.

7. **Berthelot M**. Violet d'aniline. *Rep Chim App* 1: 284, 1859.

8. **Biber J, Stieger B, Stange G, and Murer H**. Isolation of renal proximal tubular brush-border membranes. *Nature protocols* 2: 1356-1359, 2007.

9. **Biver S, Belge H, Bourgeois S, Van Vooren P, Nowik M, Scohy S, Houillier P, Szpirer J, Szpirer C, Wagner CA, Devuyst O, and Marini AM**. A role for Rhesus factor Rhcg in renal ammonium excretion and male fertility. *Nature* 456: 339-343, 2008.

10. **Bobulescu IA, Dubree M, Zhang J, McLeroy P, and Moe OW**. Effect of renal lipid accumulation on proximal tubule Na+/H+ exchange and ammonium secretion. *American journal of physiology* 294: F1315-1322, 2008.

11. **Burch HB, Narins RG, Chu C, Fagioli S, Choi S, McCarthy W, and Lowry OH**. Distribution along the rat nephron of three enzymes of gluconeogenesis in acidosis and starvation. *The American journal of physiology* 235: F246-253, 1978.

12. **Busque SM, and Wagner CA**. Potassium restriction, high protein intake, and metabolic acidosis increase expression of the glutamine transporter SNAT3 (Slc38a3) in mouse kidney. *American journal of physiology* 2009.

13. **Cimbala MA, Lamers WH, Nelson K, Monahan JE, Yoo-Warren H, and Hanson RW**. Rapid changes in the concentration of phosphoenolpyruvate carboxykinase mRNA in rat liver and kidney. Effects of insulin and cyclic AMP. *The Journal of biological chemistry* 257: 7629-7636, 1982.

14. **Costa Rosa LF, Curi R, Murphy C, and Newsholme P**. Effect of adrenaline and phorbol myristate acetate or bacterial lipopolysaccharide on stimulation of pathways of macrophage glucose, glutamine and O2 metabolism. Evidence for cyclic AMP-dependent protein kinase mediated inhibition of glucose-6-phosphate dehydrogenase and activation of NADP+-dependent 'malic' enzyme. *The Biochemical journal* 310 (Pt 2): 709-714, 1995.

15. **Curi TC, De Melo MP, De Azevedo RB, Zorn TM, and Curi R**. Glutamine utilization by rat neutrophils: presence of phosphate-dependent glutaminase. *The American journal of physiology* 273: C1124-1129, 1997.

16. **Curthoys NP, and Gstraunthaler G**. Mechanism of increased renal gene expression during metabolic acidosis. *American journal of physiology* 281: F381-390, 2001.

17. **Curthoys NP, Kuhlenschmidt T, Godfrey SS, and Weiss RF**. Phosphate-dependent glutaminase from rat kidney. Cause of increased activity in response to acidosis and identity with glutaminase from other tissues. *Archives of biochemistry and biophysics* 172: 162-167, 1976.

18. **Curthoys NP, and Lowry OH**. The distribution of glutaminase isoenzymes in the various structures of the nephron in normal, acidotic, and alkalotic rat kidney. *The Journal of biological chemistry* 248: 162-168, 1973.

19. **Daudon M, Lacour B, and Jungers P**. High prevalence of uric acid calculi in diabetic stone formers. *Nephrol Dial Transplant* 20: 468-469, 2005.

20. **Daudon M, Traxer O, Conort P, Lacour B, and Jungers P**. Type 2 diabetes increases the risk for uric acid stones. *J Am Soc Nephrol* 17: 2026-2033, 2006.

21. **DeFronzo RA, Cooke CR, Andres R, Faloona GR, and Davis PJ**. The effect of insulin on renal handling of sodium, potassium, calcium, and phosphate in man. *The Journal of clinical investigation* 55: 845-855, 1975.

22. **Eladari D, Cheval L, Quentin F, Bertrand O, Mouro I, Cherif-Zahar B, Cartron JP, Paillard M, Doucet A, and Chambrey R**. Expression of RhCG, a new putative NH(3)/NH(4)(+) transporter, along the rat nephron. *J Am Soc Nephrol* 13: 1999-2008, 2002.

23. **Faus MJ, Lupianez A, Vargas A, and Sanchez-Medina F**. Induction of rat kidney gluconeogenesis during acute liver intoxication by carbon tetrachloride. *The Biochemical journal* 174: 461-467, 1978.

24. **Gesek FA, and Schoolwerth AC**. Insulin increases Na(+)-H+ exchange activity in proximal tubules from normotensive and hypertensive rats. *The American journal of physiology* 260: F695-703, 1991.

25. **Guder WG, and Schmidt U**. The localization of gluconeogenesis in rat nephron. Determination of phosphoenolpyruvate carboxykinase in microdissected tubules. *Hoppe-Seyler's Zeitschrift fur physiologische Chemie* 355: 273-278, 1974.

26. **Gullans SR, Brazy PC, Dennis VW, and Mandel LJ**. Interactions between gluconeogenesis and sodium transport in rabbit proximal tubule. *The American journal of physiology* 246: F859-869, 1984.

27. **Gutman AB, and Yue TF**. Urinary Ammonium Excretion in Primary Gout. *The Journal of clinical investigation* 44: 1474-1481, 1965.

28. **Hansen WR, Barsic-Tress N, Taylor L, and Curthoys NP**. The 3'-nontranslated region of rat renal glutaminase mRNA contains a pH-responsive stability element. *The American journal of physiology* 271: F126-131, 1996.

29. **Hanson RW, and Reshef L**. Regulation of phosphoenolpyruvate carboxykinase (GTP) gene expression. *Annual review of biochemistry* 66: 581-611, 1997.

30. **Henneman PH, Wallach S, and Dempsey EF**. The metabolism defect responsible for uric acid stone formation. *The Journal of clinical investigation* 41: 537-542, 1962.

31. **Honegger KJ, Capuano P, Winter C, Bacic D, Stange G, Wagner CA, Biber J, Murer H, and Hernando N**. Regulation of sodium-proton exchanger isoform 3

(NHE3) by PKA and exchange protein directly activated by cAMP (EPAC). *Proceedings of the National Academy of Sciences of the United States of America* 103: 803-808, 2006.

32. **Hwang JJ, and Curthoys NP**. Effect of acute alterations in acid-base balance on rat renal glutaminase and phosphoenolpyruvate carboxykinase gene expression. *The Journal of biological chemistry* 266: 9392-9396, 1991.

33. **Iynedjian PB, Ballard FJ, and Hanson RW**. The regulation of phosphoenolpyruvate carboxykinase (GTP) synthesis in rat kidney cortex. The role of acid-base balance and glucocorticoids. *The Journal of biological chemistry* 250: 5596-5603, 1975.

34. **Jaeger P, Karlmark B, and Giebisch G**. Ammonium transport in rat cortical tubule: relationship to potassium metabolism. *The American journal of physiology* 245: F593-600, 1983.

35. **Joseph PK, and Subrahmanyam K**. Effect of growth hormone, insulin, thyroxine and cortisone on renal gluconeogenesis. *Archives of biochemistry and biophysics* 127: 288-291, 1968.

36. **Kamel KS, Cheema-Dhadli S, and Halperin ML**. Studies on the pathophysiology of the low urine pH in patients with uric acid stones. *Kidney international* 61: 988-994, 2002.

37. **Karim Z, Szutkowska M, Vernimmen C, and Bichara M**. Renal handling of NH3/NH4+: recent concepts. *Nephron* 101: p77-81, 2005.

38. **Karinch AM, Lin CM, Meng Q, Pan M, and Souba WW**. Glucocorticoids have a role in renal cortical expression of the SNAT3 glutamine transporter during chronic metabolic acidosis. *American journal of physiology* 292: F448-455, 2007.

39. **Karinch AM, Lin CM, Wolfgang CL, Pan M, and Souba WW**. Regulation of expression of the SN1 transporter during renal adaptation to chronic metabolic acidosis in rats. *American journal of physiology* 283: F1011-1019, 2002.

40. **Khatchadourian J, Preminger GM, Whitson PA, Adams-Huet B, and Pak CY**. Clinical and biochemical presentation of gouty diathesis: comparison of uric acid versus pure calcium stone formation. *The Journal of urology* 154: 1665-1669, 1995.

41. **Kida K, Nakajo S, Kamiya F, Toyama Y, Nishio T, and Nakagawa H**. Renal net glucose release in vivo and its contribution to blood glucose in rats. *The Journal of clinical investigation* 62: 721-726, 1978.

42. **Klisic J, Hu MC, Nief V, Reyes L, Fuster D, Moe OW, and Ambuhl PM**. Insulin activates Na(+)/H(+) exchanger 3: biphasic response and glucocorticoid dependence. *American journal of physiology* 283: F532-539, 2002.

43. **Laghmani K, Preisig PA, Moe OW, Yanagisawa M, and Alpern RJ**. Endothelin-1/endothelin-B receptor-mediated increases in NHE3 activity in chronic metabolic acidosis. *The Journal of clinical investigation* 107: 1563-1569, 2001.

44. **Laterza OF, and Curthoys NP**. Specificity and functional analysis of the pH-responsive element within renal glutaminase mRNA. *American journal of physiology* 278: F970-977, 2000.

45. **Laterza OF, Hansen WR, Taylor L, and Curthoys NP**. Identification of an mRNA-binding protein and the specific elements that may mediate the pH-responsive induction of renal glutaminase mRNA. *The Journal of biological chemistry* 272: 22481-22488, 1997.

46. **Levin BE, Finnegan M, Triscari J, and Sullivan AC**. Brown adipose and metabolic features of chronic diet-induced obesity. *The American journal of physiology* 248: R717-723, 1985.

47. **Levin BE, Hogan S, and Sullivan AC**. Initiation and perpetuation of obesity and obesity resistance in rats. *The American journal of physiology* 256: R766-771, 1989.

48. **Levin BE, and Keesey RE**. Defense of differing body weight set points in diet-induced obese and resistant rats. *The American journal of physiology* 274: R412-419, 1998.

49. **Levin BE, Triscari J, Hogan S, and Sullivan AC**. Resistance to diet-induced obesity: food intake, pancreatic sympathetic tone, and insulin. *The American journal of physiology* 252: R471-478, 1987.

50. **Liu Z, Chen Y, Mo R, Hui C, Cheng JF, Mohandas N, and Huang CH**. Characterization of human RhCG and mouse Rhcg as novel nonerythroid Rh glycoprotein homologues predominantly expressed in kidney and testis. *The Journal of biological chemistry* 275: 25641-25651, 2000.

51. **Lloyd-Jones D, Adams R, Carnethon M, De Simone G, Ferguson TB, Flegal K, Ford E, Furie K, Go A, Greenlund K, Haase N, Hailpern S, Ho M, Howard V, Kissela B, Kittner S, Lackland D, Lisabeth L, Marelli A, McDermott M, Meigs J, Mozaffarian D, Nichol G, O'Donnell C, Roger V, Rosamond W, Sacco R, Sorlie P, Stafford R, Steinberger J, Thom T, Wasserthiel-Smoller S, Wong N, Wylie-Rosett J, and Hong Y**. Heart disease and stroke statistics--2009 update: a report from the American Heart Association Statistics Committee and Stroke Statistics Subcommittee. *Circulation* 119: e21-181, 2009.

52. **Lupianez JA, Dileepan KN, and Wagle SR**. Interrelationship of somatostatin, insulin, and calcium in the control of gluconeogenesis in kidney cortex slices. *Biochemical and biophysical research communications* 90: 1153-1158, 1979.

53. **Maalouf NM, Cameron MA, Moe OW, and Sakhaee K**. Novel insights into the pathogenesis of uric acid nephrolithiasis. *Current opinion in nephrology and hypertension* 13: 181-189, 2004.

54. **Madison LL, and Seldin DW**. Ammonia excretion and renal enzymatic adaptation in human subjects, as disclosed by administration of precursor amino acids. *The Journal of clinical investigation* 37: 1615-1627, 1958.

55. **McKinney TD, and Davidson KK**. Effect of potassium depletion and protein intake in vivo on renal tubular bicarbonate transport in vitro. *The American journal of physiology* 252: F509-516, 1987.

56. **Meydan N, Barutca S, Caliskan S, and Camsari T**. Urinary stone disease in diabetes mellitus. *Scandinavian journal of urology and nephrology* 37: 64-70, 2003.

57. **Moret C, Dave MH, Schulz N, Jiang JX, Verrey F, and Wagner CA**. Regulation of renal amino acid transporters during metabolic acidosis. *American journal of physiology* 292: F555-566, 2007.

58. **Nagami GT**. Effect of bath and luminal potassium concentration on ammonia production and secretion by mouse proximal tubules perfused in vitro. *The Journal of clinical investigation* 86: 32-39, 1990.

59. **Nonoguchi H, Takehara Y, and Endou H**. Intra- and inter-nephron heterogeneity of ammoniagenesis in rats: effects of chronic metabolic acidosis and potassium depletion. *Pflugers Arch* 407: 245-251, 1986.

60. **Nowik M, Lecca MR, Velic A, Rehrauer H, Brandli AW, and Wagner CA**. Genome-wide gene expression profiling reveals renal genes regulated during metabolic acidosis. *Physiological genomics* 32: 322-334, 2008.

61. **Owen EE, and Robinson RR**. Amino acid extraction and ammonia metabolism by the human kidney during the prolonged administration of ammonium chloride. *The Journal of clinical investigation* 42: 263-276, 1963.

62. **Owen OE, Felig P, Morgan AP, Wahren J, and Cahill GF, Jr.** Liver and kidney metabolism during prolonged starvation. *The Journal of clinical investigation* 48: 574-583, 1969.

63. **Pak CY, Sakhaee K, and Fuller C**. Successful management of uric acid nephrolithiasis with potassium citrate. *Kidney international* 30: 422-428, 1986.

64. **Pak CY, Sakhaee K, Peterson RD, Poindexter JR, and Frawley WH**. Biochemical profile of idiopathic uric acid nephrolithiasis. *Kidney international* 60: 757-761, 2001.

65. **Pithon-Curi TC, De Melo MP, and Curi R**. Glucose and glutamine utilization by rat lymphocytes, monocytes and neutrophils in culture: a comparative study. *Cell biochemistry and function* 22: 321-326, 2004.

66. **Rapoport A, Crassweller PO, Husdan H, From GL, Zweig M, and Johnson MD**. The renal excretion of hydrogen ion in uric acid stone formers. *Metabolism: clinical and experimental* 16: 176-188, 1967.

67. **Remer T, and Manz F**. Estimation of the renal net acid excretion by adults consuming diets containing variable amounts of protein. *The American journal of clinical nutrition* 59: 1356-1361, 1994.

68. **Rogers S, Gavin JR, 3rd, and Hammerman MR**. Phorbol esters inhibit gluconeogenesis in canine renal proximal tubular segments. *The American journal of physiology* 249: F256-262, 1985.

69. **Sakhaee K, Adams-Huet B, Moe OW, and Pak CY**. Pathophysiologic basis for normouricosuric uric acid nephrolithiasis. *Kidney international* 62: 971-979, 2002.

70. **Sakhaee K, Nicar M, Hill K, and Pak CY**. Contrasting effects of potassium citrate and sodium citrate therapies on urinary chemistries and crystallization of stone-forming salts. *Kidney international* 24: 348-352, 1983.

71. **Sastrasinh S, and Sastrasinh M**. Renal mitochondrial glutamine metabolism during K+ depletion. *The American journal of physiology* 250: F667-673, 1986.

72. **Sclafani A, and Springer D**. Dietary obesity in adult rats: similarities to hypothalamic and human obesity syndromes. *Physiology & behavior* 17: 461-471, 1976.

73. **Sechi LA**. Mechanisms of insulin resistance in rat models of hypertension and their relationships with salt sensitivity. *Journal of hypertension* 17: 1229-1237, 1999.

74. **Slot C**. Plasma creatinine determination. A new and specific Jaffe reaction method. *Scandinavian journal of clinical and laboratory investigation* 17: 381-387, 1965.

75. **Solbu TT, Boulland JL, Zahid W, Lyamouri Bredahl MK, Amiry-Moghaddam M, Storm-Mathisen J, Roberg BA, and Chaudhry FA**. Induction and targeting of the glutamine transporter SN1 to the basolateral membranes of cortical kidney tubule cells during chronic metabolic acidosis suggest a role in pH regulation. *J Am Soc Nephrol* 16: 869-877, 2005.

76. **Stamatelou KK, Francis ME, Jones CA, Nyberg LM, and Curhan GC**. Time trends in reported prevalence of kidney stones in the United States: 1976-1994. *Kidney international* 63: 1817-1823, 2003.

77. **Sundberg BE, Waag E, Jacobsson JA, Stephansson O, Rumaks J, Svirskis S, Alsio J, Roman E, Ebendal T, Klusa V, and Fredriksson R**. The evolutionary history and tissue mapping of amino acid transporters belonging to solute carrier families SLC32, SLC36, and SLC38. *J Mol Neurosci* 35: 179-193, 2008.

78. **Tannen RL**. Relationship of renal ammonia production and potassium homeostasis. *Kidney international* 11: 453-465, 1977.

79. **Taylor EN, Stampfer MJ, and Curhan GC**. Diabetes mellitus and the risk of nephrolithiasis. *Kidney international* 68: 1230-1235, 2005.

80. **Tong J, Harrison G, and Curthoys NP**. The effect of metabolic acidosis on the synthesis and turnover of rat renal phosphate-dependent glutaminase. *The Biochemical journal* 233: 139-144, 1986.

81. **Trinchieri A, Coppi F, Montanari E, Del Nero A, Zanetti G, and Pisani E**. Increase in the prevalence of symptomatic upper urinary tract stones during the last ten years. *European urology* 37: 23-25, 2000.

82. **Verlander JW, Miller RT, Frank AE, Royaux IE, Kim YH, and Weiner ID**. Localization of the ammonium transporter proteins RhBG and RhCG in mouse kidney. *American journal of physiology* 284: F323-337, 2003.

83. **Vinay P, Gougoux A, and Lemieux G**. Isolation of a pure suspension of rat proximal tubules. *The American journal of physiology* 241: F403-411, 1981.

84. **Welbourne TC**. Interorgan glutamine flow in metabolic acidosis. *The American journal of physiology* 253: F1069-1076, 1987.

85. **Wesson DE, Nathan T, Rose T, Simoni J, and Tran RM**. Dietary protein induces endothelin-mediated kidney injury through enhanced intrinsic acid production. *Kidney international* 71: 210-217, 2007.

86. **Wild S, Roglic G, Green A, Sicree R, and King H**. Global prevalence of diabetes: estimates for the year 2000 and projections for 2030. *Diabetes care* 27: 1047-1053, 2004.

87. **Wu MS, Biemesderfer D, Giebisch G, and Aronson PS**. Role of NHE3 in mediating renal brush border Na+-H+ exchange. Adaptation to metabolic acidosis. *The Journal of biological chemistry* 271: 32749-32752, 1996.

88. **Yanez AJ, Nualart F, Droppelmann C, Bertinat R, Brito M, Concha, II, and Slebe JC**. Broad expression of fructose-1,6-bisphosphatase and phosphoenolpyruvate carboxykinase provide evidence for gluconeogenesis in human tissues other than liver and kidney. *Journal of cellular physiology* 197: 189-197, 2003.

VI. Characterization of a novel ENU-mutated mouse model of SNAT3 (Slc38a3)

VI.1 Introduction

N-ethyl-*N*-nitrosourea (ENU) is a chemical widely used in murine mutagenesis models to induce random changes in single nucleotides by alkylation of nucleic acids (63). It is injected into male mice, inducing changes in spermatogonial stem cells. Male mice are subsequently bred with wildtype females, and can produce countless litters. ENU mutagenesis is an efficient method of causing loss-of-function mutations in mice. There are many advantages to using ENU mutagenesis. The occurrence of ENU mutagenesis-derived single nucleotide polymorphisms (SNPs) is approximately 100 times higher than spontaneous mutations, making ENU mutagenesis a useful tool in the laboratory in order to rapidly screen many genes. Additionally, the mutagenesis occurs in spermatogonial stem cells, allowing treated males to continue to breed and generate mutated offspring (55, 117). ENU mutagenesis can induce one new loss-of-function mutation in every 700 gametes of ENU-treated male mice (55). Of importance, this form of mutagenesis is a useful way to learn more about already discovered genes, or to identify new genes in an unbiased fashion based on phenotype alone (12). ENU mutagenesis simulates mutations that would otherwise occur naturally, and give rise to better understanding of how SNPs can regulate gene function (106).

As with many murine mutagenesis models, there are some disadvantages and limitations in using ENU mutagenesis for phenotyping. It is at times difficult to assess a mutant phenotype as opposed to simply a normal variant, and analysis must be performed in numerous mice to insure the phenotype is legitimate (12). Additionally, analyses of multifaceted neurological or behavioral phenotypes are relatively difficult and require prudence and many phenotypic variants are often missed at first glance (12, 87). Further, the likelihood of identifying more than one mutation for a particular phenotype increases using ENU mutagenesis. In such cases, it is important to backcross the mutant strain over several generations to “dilute” possible bystander mutations. .

For this study, we used a novel ENU-mutagenesis murine model expressing the mutation "SLC38a3-Q263X" (Stoeger, C; Ingenium Pharmaceuticals AG, Germany). The aim of this portion of the study was to characterize SNAT3 in various murine tissues and to understand the role of SNAT3 *in vivo*.

VI.2 Material and methods

Animals

Male mice were treated with the potent mutagen, N-ethyl-N-nitrosourea (ENU), resulting in offspring carrying a single nucleotide polymorphism. This mutation was a "C" to "T" mutation, known as "SLC38a3-Q263X", causing a premature stop codon deleting the second half of the protein. The breeding scheme included back-crossing over 4 - 7 generations into C57BL/6J mice. Pups were sacrificed after intraperitoneal injection of ketamine/xylazine (n=52) at postnatal day 15-18. Organs were removed and immediately flash-frozen for further analysis. Blood and spot urine was collected. Pups had not yet been weaned from their mothers, and were housed in climate controlled and 12 h light-cycled rooms. All animal experiments were conducted according to the Swiss animal welfare laws and approved by the Swiss local animal authority, Zurich, Switzerland.

Genotyping

Tail clippings were made and genomic DNA was extracted for genotyping. Genomic DNA was sent for initial sequencing to confirm primer specificity (Microsynth, Balgach, Switzerland). Mice were subsequently genotyped using the tetra-primer ARMS-PCR method, used specifically to identify single nucleotide polymorphisms using a Biometra TGradient thermocycler (Goettingen, Germany) (154). This method employs a two primer pair system to identify two different alleles, for example, the "C" or "T" nucleotide. The pair of inner primers recognizes two deliberate mismatches; one located at the 3' terminal base of the inner primer and the template, and the other located two positions from the 3' terminus. PCR products (30 ng) were loaded onto a 12% DNA polyacrylamide gel and run at 90 mV. Gels were incubated with the nucleic acid stain, Gel-Red™ (Biotium, Hayward, CA, USA) and visualized under UV light. Alleles were easily identified and distinguishable as single bands; "T" allele was visualized at 194 kb, while the "C" allele was visualized at 172 kb. Outer primers, identifying the entire target sequence were visualized at 309 kb.

Quantitative Real-time RT PCR

Previously frozen kidneys were homogenized using a Rotor-stator homogenizer, and RNA was immediately extracted using Qiagen RNeasy Mini Kit (Qiagen; Hilden, Germany). DNase digestion was performed using the RNase-free DNase Set (Qiagen; Hilden, Germany). Total RNA extractions were analyzed using the NanoDrop ND-1000 spectophotometer (Wilmington, DE, USA). cDNA was prepared from diluted RNA samples (100 ng/µl) using the TaqMan Reverse Transcriptase Reagent Kit containing 10X RT buffer, $MgCl_2$, random hexamers, dNTPs, RNase inhibitors and Multiscribe reverse transcription enzyme (Applied Biosystems/Roche; Forster City, CA, USA). Thermocycling conditions for reverse transcription were set at 25ºC for 10 min, 48ºC for 30 min, and 95ºC for 5 min (Biometra TGradient thermocycler, Goettingen, Germany). Real-time RT-PCR was used to determine relative mRNA expression (7500 Fast Real-Time PCR system, Applied Biosystems). Thermocycling conditions were set at: 50ºC (2 min), 95ºC (10 min), 95ºC (15 sec; 40 cycles) and 60ºC (1 min). Forward and reverse primer concentration was 25 µM; probe concentration was 5 µM. TaqMan Universal PCR master mix 2X (Applied Biosystems/Roche) was used as the Taq polymerase. Primers and probes for SNAT3, SNAT2, arginase II, phosphate-dependent glutaminase (PDG), phosphoenolpyruvate carboxykinase (PEPCK), Rhesus glycoprotein (Rhcg) and Hypoxanthine-guanine phosphoribosyltransferase (HPRT) were generated using the Primer Express software from Applied Biosystems and synthesized at Microsynth (Balgach, Switzerland) as described previously (91, 102). The primer and probe sequences for Rhcg: 5'-GTT GGA GAA GAA GCG CAA GAA-3', forward; 5'-CGA AGA CCA TGG CGT GTA CA-3', reverse; 5'-TTA CTA TCG CTA CCC GAG CTT CCA G-3', probe. Probes were generated with the reporter dye FAM at the 5' end and TAMRA at the 3' end. Each sample was run in triplicate including a negative control (without Multiscribe reverse transcription enzyme). The cycle threshold (C_t) values obtained were ultimately compared to C_t values of the endogenous gene HPRT. Relative mRNA expression ratios were calculated as $R=2^{[Ct(HPRT)-Ct(gene\ of\ interest)]}$.

Immunoblotting

Total membrane and cytosolic protein preparations were prepared from whole, non-perfused kidney and liver using a K-HEPES buffer composed of 200 mM mannitol, 80 mM HEPES, 41 mM KOH, along with the protease inhibitors, PMSF, K-EDTA, and leupeptin (pH 7.5). Organs were homogenized in 200 µl of ice-cold K-HEPES buffer using a tip sonicator and immediately centrifuged at 2000 rpm for 20 min (4ºC). The supernatant was aspirated and placed in an ultracentrifuge (Sorvall, Thermo Fischer Scientific) for 1 h at 41,000 rpm 4ºC. The supernatant containing cytosolic protein from this second centrifugation step was removed and the pellet containing membrane protein was resuspended in K-HEPES buffer and sonicated to evenly distribute proteins. The BioRad Dc Protein assay was used to measure protein concentration (Bio-Rad; Hercules, CA, USA). Total membrane (75 µg) or cytosolic (50 µg) protein containing Laemmli sample buffer and loaded onto a 10% polyacrylamide gel and SDS-PAGE was performed. Proteins were transferred to polyvinylidene difluoride membranes (PVDF; Immobilon-P, Millipore, Bedford, MA, USA). Membranes were blocked with Tris-buffered saline / 0.1% Tween and 5% non-fat dry milk for 1 h. Primary antibodies were applied for 2 h at RT or overnight at 4ºC. The primary antibodies used for this study were: phosphate-dependent glutaminase (PDG), which recognizes both the rat (KGA) and human (GAC) kidney-type isoforms of PDG forming the mature PDG protein (66 and 68 kDa; a kind gift from N. Curthoys, Colorado State University, USA; diluted 1:500) (33); anti-PEPCK polyclonal antibody (63 kDa; Cayman Chemical, Ann Arbor, MI, USA; diluted 1:1,000), and mouse monoclonal antibody against β-actin (42 kDa; Sigma, St. Louis, MO, USA; diluted 1:5,000). The anti-Slc38a3 antibody (1:500) was generated as previously described (91). The glutamine synthetase antibody was detected at 45 kDa and diluted 1:5000. The secondary antibodies used were donkey anti-rabbit horseradish peroxidase conjugated diluted 1:12,000, anti-rabbit alkaline phosphatase conjugated diluted 1:5,000, and anti-mouse IgG alkaline phosphatase conjugated diluted 1:5,000. After a series of washing steps and blocking, membranes were treated with alkaline phosphatase or horseradish peroxidase conjugated developing solution and exposed to the Diana III chemiluminescence detection system (Raytest). Specific bands on PVDF membranes were later quantified using AIDA Image analyzer version 3.44.

Membranes were stripped and reprobed for anti-β-actin and subsequent analysis of the protein of interest was determined relative to β-actin quantification and reported as relative protein abundance (ratio of β-actin/protein of interest).

Immunohistochemistry

For immunohistochemical studies on kidney, liver and brain slices, mice were perfused through the left ventricle with phosphate-buffered saline (PBS) followed by a paraformaldehyde-cacodylate fixative containing a mixture of three buffers: 1) a sodium-cacodylate-Sucrose buffer (100 mM sodium-cacodylate, 100 mM sucrose); 2) a sodium-cacodylate-HAES fixative containing (60% of final volume of buffer 1, 40% HAES-10%, 3.24 mM $MgCl_2$ x 6 H_2O, 4.36 mM picric acid) and a 3) 25% paraformaldehyde solution (final concentration 3%), pH 7.4). Organs were flushed with PBS, removed, cut into slices, washed three times with PBS, and frozen in liquid propane cooled with liquid nitrogen. The immunostaining procedure was carried out as previously described (131). Briefly, 5 µm cryosections were incubated with 0.5% SDS for 5 min, washed three times with PBS, and incubated with PBS containing 1% BSA for 15 min before application of the primary antibodies. The primary antibodies (rabbit anti-SNAT3 affinity purified 1:200 (91), goat anti 4F2hc 1:400, Santa Cruz Biotechnology, CA, USA) were diluted in PBS and applied either for 75 min at RT or overnight at 4°C. Sections were washed twice with PBS + 2.7% NaCl for 5 min, once with PBS, and incubated for 1 h at RT with their respective secondary antibodies (donkey anti-rabbit Alexa 594 and donkey anti-goat Alexa 488 diluted 1:1000, Invitrogen, Basel, Switzerland). Sections were then washed twice with PBS + 2.7% NaCl and once with PBS before mounting with Dako Glycergel Mounting Media (Dako North America Inc., Carpenteria, CA, USA). All sections were viewed using a confocal microscope (Leica CLSM). Pictures were overlaid using Adobe Photoshop software.

Brush border membrane preparations and acridine orange quenching experiments

Kidney brush border membrane preparations were prepared as previously described (90). Briefly, (perfused/ non-perfused) kidneys were cut into small sections and homogenized using a Polytron homogenizer with a fine rod for 2 minutes in a buffer

containing: 300 mM mannitol, 5 mM EGTA and 12 mM Tris-HCl, pH 7.1. A fraction of the homogenates was stored at -20 ºC for immunoblotting, while 1 M $MgCl_2$ was added to the remaining homogenate and allowed to precipitate on ice for 15 minutes. The sample was then centrifuged at 4500 rpm for 15 minutes. The supernatant was aspirated and centrifuged at 18000 rpm for 30 minutes. The pellet was resuspended in membrane buffer consisting of: 300 mM mannitol, 20 mM HEPES-Tris, pH 7.4. The resuspended samples were then centrifuged at 18500 rpm for 30 minutes. Brush border membrane vesicles were resuspended in vesicle buffer containing: 280 mM mannitol, 5 mM MES/N-methyl-D-glutamine and 2 mM $MgCl_2$, pH 5.5. Protein concentration was measured using the BioRad fast method.

Acridine orange quenching measurements were performed as previously described (56). Briefly, BBMV suspensions (30 µl) and 6 µM of acridine orange dye were added to a spectrofluometer cuvette held at 25ºC. Excitation occurred at 493 nm and emission at 530 nm. NHE activity was calculated as the as the Δ pH per minute over *Q*, where *Q* represents the quenching of acridine orange detected upon addition of sodium gluconate to the cuvette (2 M).

Statistical analyses were performed using unpaired Student's *t*-test, and results with $p \leq 0.05$ were considered statistically significant. Data are presented as means ± SEM.

VI.3 Preliminary results

After back-crossing mice between 4-7 generations, pups (n= 52) were sacrificed on postnatal-day 15-18 and tail clips were taken for genotyping mice. The target sequences are shown in figure 1 A. ENU-mutagenesis produced a "C" to "T" mutation in offspring, which was clearly detected using a tetra-primer ARMS-PCR genotyping system and DNA polyacrylamide electrophoresis (figure 1 B). To confirm our genotyping results, samples were sent to Microsynth (Balgach, Switzerland) for sequencing of genomic DNA (figure 2 A-C). The sequencing data was visualized using Chromas software (Technelysium Pty Ltd). Analysis of a small number of pups suggests that the ratio of genotypes obtained follows Mendelian inheritance.

	Male	**Female**
Wildtype	*n = 4 (19 %)*	*n = 4(13 %)*
Heterozygous	*n =12(57 %)*	*n = 17(55 %)*
Mutant	*n = 5(24 %)*	*n = 10(32 %)*

Table 1. Gene distribution between genders.

SNAT3 protein is undetectable in kidney and liver of mutant mice

Whole, non-perfused kidney and liver samples were homogenized in preparation for immunoblotting or RNA extraction and quantitative real-time RT-PCR. Using both C-(not shown) and N-terminal antibodies, we were unable to detect SNAT3 protein in the kidney or liver samples of mutant mice, demonstrating that the mutation indeed leads to ablation of the SNAT3 protein (figure 3 B and 4 B, respectively). On the mRNA level, renal SNAT3 mRNA expression was significantly reduced in mutant mice in comparison to littermates (figure 3 A). Similarly, SNAT3 mRNA expression in liver samples of mutant mice was minimal, while wildtype and heterozygous mice showed strong expression (figure 4 A).

Phenotyping SNAT3 mutant mice

Once genotyping results were confirmed, phenotypic analysis could be performed. Mutant mice were easily distinguishable by eye; they were growth retarded and displayed mild forms of ataxia and neurological disturbances (unpublished observations). Mutant mice weighed significantly less than their wildtype or heterozygote littermates (figure 5 A). After postnatal day 15-18, spot urines were collected, and mice were sacrificed; blood and organs were removed and immediately flash frozen for further analysis. Mean relative organ weights were taken in comparison to body weight. Mean relative kidney weight was comparable among littermates. Mean relative brain weight was significantly larger and mean relative liver weight significantly smaller in mutants in comparison to both wildtype and heterozygous littermates (figure 5 B).

SNAT3 deletion causes reduced urinary ammonia and urea excretion and elevated serum urea in mutant mice

Urine samples were obtained as spot urines, given that it is impossible to collect 24 h urine samples from two-week old pups. Spot urine was analyzed for urinary NH_4^+ and urea concentration. Serum urea was also analyzed from blood samples collected upon sacrifice of animals. Urinary NH_4^+ excretion was significantly reduced in mutant mice in comparison to both wildtype and heterozygous mice (figure 6). Urinary urea in mutants decreased in parallel (figure 7 A). Serum urea, on the other hand, increased substantially in mutant mice relative to littermates (figure 7 B).

PDG and PEPCK are not affected by SNAT3 deletion

mRNA expression of PDG and PEPCK were determined in kidney samples taken from wildtype, heterozygous or mutant mice. Renal PDG and PEPCK mRNA expression was unremarkable among groups, however differences were observed after immunoblotting for PDG (figure 8 A-C). Mutant mice appear to express more PDG protein than wildtype or heterozygous mice (figure 8 C), while PEPCK remained unchanged among littermates.

Mutant mice exhibit enhanced mRNA expression of liver glutamine synthetase

Liver samples were prepared for quantitative real-time RT-PCR. Glutamine synthetase is an important enzyme involved in the conversion of glutamate and ammonia to glutamine in the liver during ammonia detoxification. Mutant mice showed strong upregulation of glutamine synthetase (Glu1) mRNA in comparison to wildtype and heterozygous littermates (figure 9 A). Glu1 protein was detected in all groups by immunoblotting, however no changes were observed among littermates (figure 9 B).

Compensatory glutamine transporting mechanisms are not present in SNAT3 mutant mice

SNAT2, a member of System A transport, is highly expressed in the kidney and could potentially compensate for the loss of SNAT3 function in mutant mice. We tested kidney samples for SNAT2 mRNA expression, and could not detect changes among wildtype, heterozygous, or mutant mice (figure 10 A).

To rule out changes in distal tubule NH_4^+ handling, mRNA expression of the Rhesus glycoprotein, Rhcg, was examined in all mice. Rhcg is primarily expressed in the connecting tubule and the collecting duct, and plays an important role in apical NH_4^+ extrusion into the final urine (13, 22) . Mutant mice did not show changes in renal mRNA expression of Rhcg, in comparison to wildtype or heterozygous mice (figure 10 B).

Heterozygous mice show differences in ammonium handling after an acid challenge

Differences in SNAT3 protein abundance were observed in both kidney and liver samples of heterozygote and wildtype mice, which prompted further investigation. We sought to determine if, under control conditions or after an acid challenge, heterozygote mice exhibited any differences in comparison to wildtype mice. Wildtype and heterozygote mice were placed in metabolic cages, and mice were divided into acid-loaded groups. The acid load consisted of 0.28 M NH_4Cl added to the drinking water for 48 h. Urine was collected and kidneys harvested upon sacrifice.

Both wildtype and heterozygous mice, with or without an acid load, showed appropriate responses to the acid challenge; total urinary NH_4^+ excretion increased while urinary pH decreased (figure 11, A-C).

On the mRNA level, renal SNAT3, PDG and PEPCK were significantly enhanced in heterozygote mice after acid-loading in comparison to wildtype mice. This observation suggests that perhaps heterozygous mice compensate for the partial defect in the SNAT3 protein by upregulation of SNAT3, PDG and PEPCK mRNA expression (figure 12 A-C).

It has been previously shown that Na^+/H^+ exchanger isoform 3 (NHE3) is present on the apical brush border membrane of renal proximal tubule cells, and is critical for luminal NH_4^+ transport. We sought to determine if heterozygote mice exhibited altered NHE3 activity in comparison to wildtype mice, in the presence or absence of an acid-challenge. Brush border membrane vesicle acridine orange quenching experiments were performed. We observed a significant increase in NHE3 activity in acid-loaded heterozygous mice in comparison to controls (figure 13).

VI.4 Discussion

The preliminary results of this SNAT3 mutant study reveal interesting findings regarding the role and regulation of SNAT3 *in vivo*. Deletion of SNAT3 is lethal. Mutants die within the first 3 weeks after birth, and appear to suffer from severe neurological disturbances. Our data suggest that SNAT3 plays a significant role in the regulation of glutamine flux in kidney and liver and most likely brain, since major defects were observed on the functional level.

SNAT3 is highly expressed in brain astrocytes, and is purported to play a role in the glutamine-glutamate cycling involved in neurotransmission (15, 25). The lethargy and altered, uncoordinated gait observed in mutant mice could largely be due to SNAT3 deletion in the brain, affecting neurotransmission. Preliminary immunohistochemical studies revealed SNAT3-related staining in wildtype and heterozygous but not mutant brain slices (not shown). Further studies will be performed in order to more accurately localize SNAT3 in brain tissue, as well as identify other transport mechanisms that could be compensatory in these animals, such localization and expression of the glial glutamate transporter EAAT2, the neuronal glutamate transporter excitatory amino acid carrier-1 EAAC1, and other glutamine transporting members of the SLC38 family.

SNAT3 deletion in the kidney reveals important regulatory roles of SNAT3 in renal ammoniagenesis and gluconeogenesis. We and others have shown that SNAT3 mRNA and protein increase in response to metabolic acidosis (25, 68, 91, 102, 127). These studies show strong evidence that SNAT3 is an important glutamine influx mechanism in proximal tubule cells for ammoniagenesis. Our mutant mice clearly show reduced urinary NH_4^+ excretion, indicative of a reduced capacity either to generate or excrete NH_4^+. The fact that there are no compensatory changes in SNAT2 mRNA, (a glutamine transporter highly expressed in the kidney), suggests that changes in this transporter do not account for changes observed in urinary NH_4^+ excretion, and implies that SNAT3 is crucial for renal ammoniagenesis. Enhanced glutamine transport via SNAT3 would stimulate increases in PDG expression and activity, (as we have previously shown in both Aim I and II) enhancing ammoniagenesis, while generating more available substrate for gluconeogenesis (α-ketoglutarate). Increased α-

ketoglutarate, subsequently in the presence of PEPCK, produces both glucose and bicarbonate. We did not, however, observe changes in PDG and PEPCK on mRNA level. PDG protein in mutant mice did appear to be enhanced. Changes in mRNA stabilization could account for upregulation of PDG protein in mutants; however, this remains to be examined.

It would be interesting to examine changes in other rate-limiting gluconeogenic enzymes, such as fructose 1,6-bisphosphatase and fructose 2,6-bisphosphatase (FBP1 and FBP2, respectively). FBP1 catalyzes the conversion of fructose 1,6-bisphosphate to fructose 6-phosphate and inorganic phosphate, and has been recently immunolocalized to PT cells in human kidney (153). In Aim II, we discussed changes in both FBP1 and FBP2 in obese-glucose intolerant (O-GI) mice after an acid challenge, revealing regulation of both enzymes. These studies are planned in wildtype, heterozygous and mutant kidneys.

A distal defect NH_4^+ excretion, particularly secondary to changes in the expression of the Rhesus glycoprotein, Rhcg, could be another compensatory mechanism for SNAT3 mutant mice. Rhcg, however, was unchanged in mutant mice, further supporting our hypothesis that SNAT3 is the important regulatory mechanism in NH_4^+ handling.

Further, the kidney plays a role in the excretion of urea generated by the liver during NH_4^+ detoxification. Urea is both reabsorbed and secreted in the kidney. Mutant mice show significantly reduced urinary urea excretion, relative to wildtype and heterozygous littermates. Based on our results, we are unable to confirm whether the primary defect lies in hepatic urea production or the renal transport/absorption of urea. Further, the physiological status of the mouse at the time of urine collection could also play a role. Several isoforms of the epithelial urea transporter family "UT-A" exists in the kidney, and reduced urea excretion could be due to changes in these transport mechanisms (138). It is more likely, however, that hepatic urea production is altered, since SNAT3 is highly expressed in the liver and its primary role is to participate in glutamine influx for detoxification of NH_4^+ to urea (53). We hypothesize that less glutamine transport into periportal hepatocytes would result in reduced NH_4^+ production from the catabolism of glutamine to glutamate in periportal hepatocyte mitochondria, and

thus less NH_4^+ available for ureagenesis (53). Indeed, we found upregulation of arginase II mRNA in liver suggesting upregulation of enzymes involved in ureagenesis. In parallel, lack of SNAT3 mediated efflux of glutamine into the blood from perivenous hepatocytes may suggest a reduction in NH_4^+ detoxification and glutamine synthesis from glutamate. More experiments, however, are required to dissect the role of SNAT3 in hepatocytes.

An interesting observation in heterozygous mice led us to test whether a partial defect in SNAT3 could be functionally relevant during an oral acid challenge. Heterozygous and wildtype mice were given NH_4Cl in the drinking water for 48 h to induce acidosis. Heterozygous mice showed appropriate and similar changes in urinary pH and NH_4^+ excretion similar to wildtype mice. Surprisingly, differences in regulation were observed on mRNA level. Heterozygous mice showed stronger increases in SNAT3, PDG and PEPCK mRNA expression, suggesting that perhaps an enhancement in mRNA expression is part of a compensatory mechanism in these animals. Furthermore, increases in NHE3 activity was observed in acid-loaded heterozygous mice which could reflect the need for enhanced NH_4^+ extrusion secondary to the increased metabolic acid load.

In sum, preliminary work using our SNAT3 mutagenesis model suggests that SNAT3 is important in normal brain, kidney and liver function. Further work needs to be done in order to characterize the exact mechanisms of the defects associated with SNAT3 deletion.

VI.5 Figure legends

Figure 1. The genomic DNA sequences of both wildtype and mutant mice. Mutant mice exhibit a single nucleotide polymorphism in the SNAT3 sequence in exon 10 where a "C" to "T" mutation is observed in ENU mutants leading to an early stop codon at position Q263X and removing the last 5 of 11 transmembrane helixes (A). Allelic discrimination was easily determined among littermates using tetra-primer ARMS-PCR. Original 12 % DNA polyacrylamide gel imaged under UV light (B). The "C" or wildtype allele had the expected band size of 194 kb, while the mutant "T" allele was 172 kb. Outer primer bands are not displayed.

Figure 2. Tetra-primer ARMS-PCR genotyping results were confirmed by genomic DNA sequencing. Genomic DNA samples from previously genotyped mice were sequenced to confirm genotyping results obtained by the tetra-primer ARMS PCR method. Original sequencing results from wildtype (A); homozygous mutant (B); and heterozygous mutant (C) mice. Sequencing results were viewed using the Chromas software.

Figure 3. SNAT3 protein is not detected in mutant mice confirming deletion of the protein. mRNA expression of SNAT3 was determined in kidneys using quantitative real-time RT PCR (A). Total membranes were extracted from whole, non-perfused kidney, and PVDF membranes were probed with an N-terminal antibody against SNAT3 and reprobed after stripping for β-actin to control for equal loading (B). Original blots are depicted. $^{**}P \leq 0.01$, $^{*}P \leq 0.05$.

Figure 4. SNAT3 is highly expressed on both mRNA and protein level in liver of wildtype and heterozygous mice, but is nearly absent in mutant mice. mRNA expression of SNAT3 was determined in liver using quantitative real-time RT PCR (A). Total membranes were extracted from whole, non-perfused liver, and original blots are shown after being probed with an N-terminal antibody against SNAT3 and reprobed after stripping for β-actin to control for equal loading (B). $^{**}P \leq 0.01$.

Figure 5. Mutant mice were smaller and exhibited changes in relative organ weights in comparison to wildtype and heterozygous littermates. Mutant mice weighed significantly less than littermates (A). Mean relative organ weight per gram body weight revealed that mutant mice had significantly larger brains and smaller livers than littermates (B). Values are means ± SE of results, ***$P \leq 0.001$.

Figure 6. Mutant mice show reduced urinary NH_4^+ excretion. Spot urines were collected for NH_4^+ analysis. Mutant mice showed significantly less urinary NH_4^+ excretion than wildtype or heterozygous littermates. **$P \leq 0.01$, *$P \leq 0.05$.

Figure 7. Mutant mice exhibit disturbances in urinary urea and serum urea values. Mutant mice showed significantly less urinary urea excretion in comparison to littermates. Serum urea, however, was significantly increased in mutant mice, suggesting a defect in ureagenesis or excretion. **$P \leq 0.01$, *$P \leq 0.05$.

Figure 8. PDG and PEPCK are unaltered in mutant mice on mRNA level. mRNA expression of PDG and PEPCK was determined in kidney using quantitative real-time RT PCR (A). Cytosolic membrane fractions were extracted from whole, non-perfused kidneys, and original blots are shown (B). No differences in PDG and PEPCK mRNA expression were detected among groups; however, PDG protein abundance appeared to be slightly increased in mutant mice in comparison to wildtype and heterozygous littermates.

Figure 9. Glutamine synthetase mRNA is highly upregulated in mutant mice, despite changes in protein abundance. mRNA expression of glutamine synthetase (A) or arginase II (C) was determined in liver using quantitative real-time RT PCR. Total membrane fractions were extracted from whole, non-perfused livers; original blots are shown (B). Glutamine synthetase mRNA was substantially upregulated in mutant mice, while no differences were detected on protein level. *$P \leq 0.05$, **$P \leq 0.01$, and ***$P \leq 0.001$.

Figure 10. Reduced ammonium excretion observed in mutant mice is not likely due to alterations in distal renal ammonium transport. mRNA expression was determined in kidney samples using quantitative real-time RT-PCR. mRNA expression of SNAT2 (A) and Rhcg (B) was unremarkable between groups.

Figure 11. Heterozygous mice show appropriate responses to an acid load. Wildtype and heterozygous mice were challenged with an oral acid load, and subsequently placed in metabolic cages. Both wildtype and heterozygous mice displayed appropriate responses to an NH_4Cl load; urinary pH (A) decreased substantially in NH_4Cl treated mice, while NH_4^+ excretion per 24 hour urine volume (B) and relative to creatinine (C) increased substantially. $^{**}P \leq 0.01$, $^{***}P \leq 0.001$.

Figure 12. Acid-loaded heterozygous mice showed the greatest increases in SNAT3, PDG and PEPCK mRNA expression in comparison to wildtype mice. mRNA expression was determined in kidneys of control and acid-loaded wildtype and heterozygous mice using quantitative real-time RT-PCR. Acid-challenged heterozygous mice showed substantial increases in SNAT3, PDG and PEPCK mRNA expression. $^{*}P \leq 0.05$, $^{**}P \leq 0.01$, $^{***}P \leq 0.001$.

Figure 13. Sodium/hydrogen exchange activity is increased in BBMV from acid-loaded heterozygous mice. BBMV preparations were made and acridine orange quenching experiments were performed. Heterozygous mice given an NH_4Cl load had enhanced NHE3 activity relative to wildtype mice suggesting that increased ammoniagenesis observed in these mice leads to enhanced NH_4^+ transport, perhaps as a compensatory mechanism due to the partial defect in SNAT3 in heterozygous mice. $^{*}P \leq 0.05$.

Figure 1

A.

Wildtype

TTCTAATCTTGACTGTGGCTTCCAAGTCCCGTTGCCGACAGCTCTGCCTG
ACTCTGACACTCACGCTTCTCCACCCCAGGTCATCTATAAGAAGTTCCAAG
TTCCTTGCCCATTGGCACACAACCTGGCCAATGCCACCGGCAACTTCAGC
CACATGGTGGTGGCAGAGGAGAAGGCA***C***AGCTGCAGGGCGAGCCTGAC
GCTGCTGCTGAGGCCTTCTGTACCCCAAGCTACTTCACCCTCAACTCACA
GGTTCCAACAGGCCAAGCCGGGCCAGGGGAGCGGGGAAGGGCTTGGTG
GGGAGGGGCTGCCTTGACATAGTCCTTTGTGTCTCCAGACAGCATACACC
ATCCCCATCATGGCTTTCGCCTTCGTCTGCCACCCTGAGGTGCTGCCCAT
ATATACAGAGCTCAAGGAGTAGGTGTCTGTGGCTGGGAGAGGGACAGCG
GCTGCCTTGAGT**TGGTCTGGAGAGAATAGATGTGA**

Mutant:

TTCTAATCTTGACTGTGGCTTCCAAGTCCCGTTGCCGACAGCTCTGCCTG
ACTCTGACACTCACGCTTCTCCACCCCAGGTCATCTATAAGAAGTTCCAAG
TTCCTTGCCCATTGGCACACAACCTGGCCAATGCCACCGGCAACTTCAGC
CACATGGTGGTGGCAGAGGAGAAGGCA***T***AGCTGCAGGGCGAGCCTGACG
CTGCTGCTGAGGCCTTCTGTACCCCAAGCTACTTCACCCTCAACTCACAG
GTTCCAACAGGCCAAGCCGGGCCAGGGGAGCGGGGAAGGGCTTGGTGG
GGAGGGGCTGCCTTGACATAGTCCTTTGTGTCTCCAGACAGCATACACCA
TCCCCATCATGGCTTTCGCCTTCGTCTGCCACCCTGAGGTGCTGCCCATA
TATACAGAGCTCAAGGAGTAGGTGTCTGTGGCTGGGAGAGGGACAGCGG
CTGCCTTGAGT**TGGTCTGGAGAGAATAGATGTGA**

B.

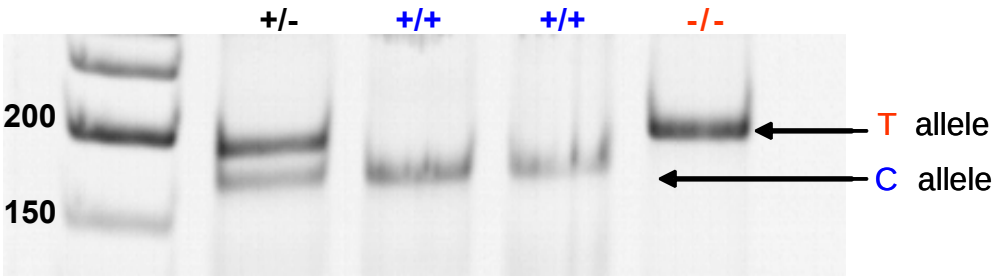

Figure 2

A.

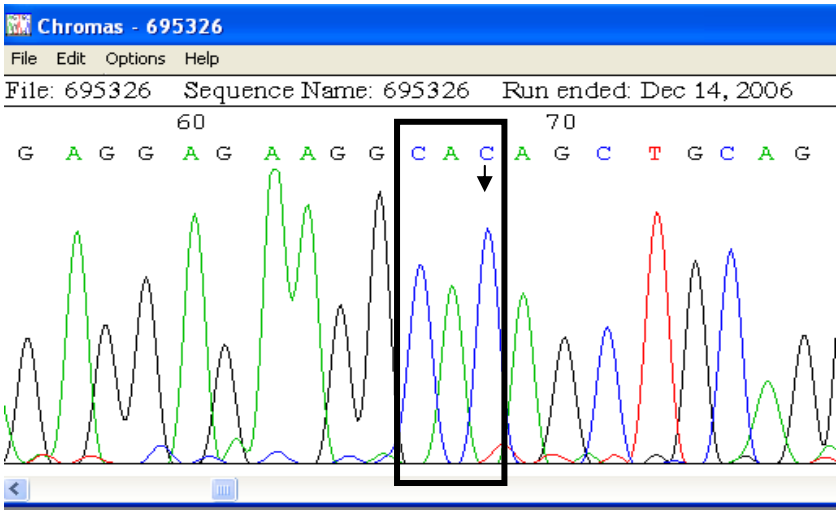

wildtype

B.

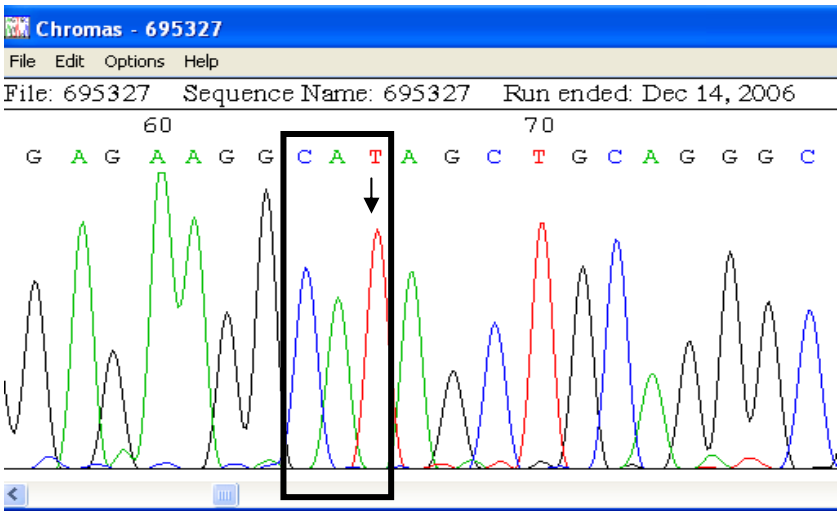

homozygous mutant

C.

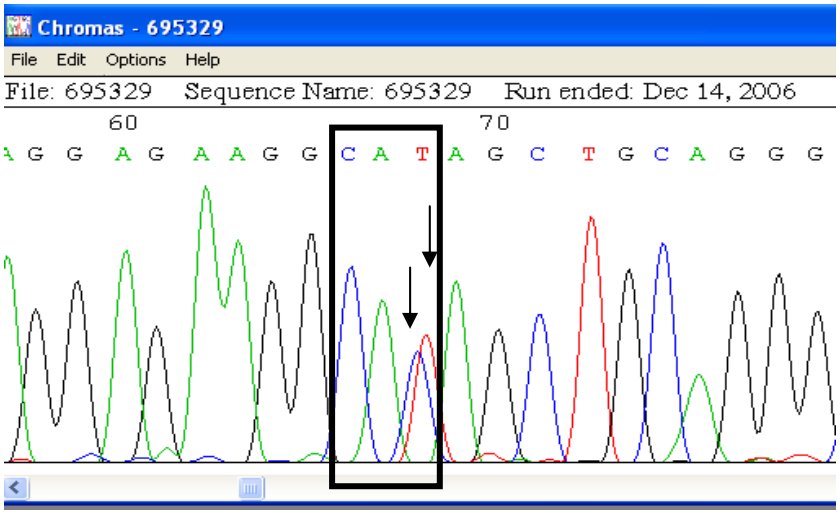

heterozygous mutant

Figure 3

A.

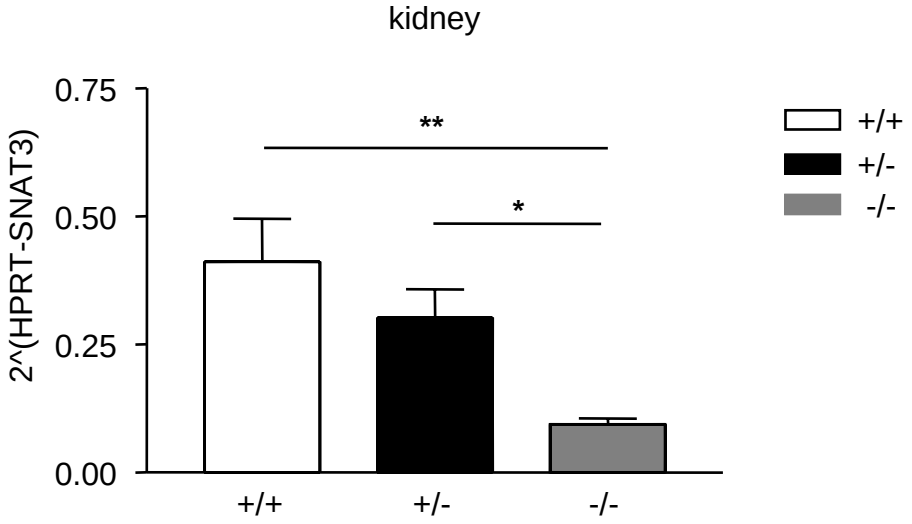

B.

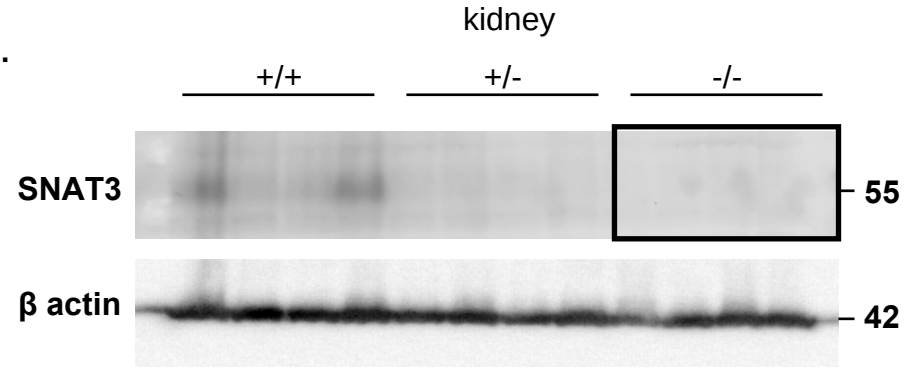

Figure 4

A.

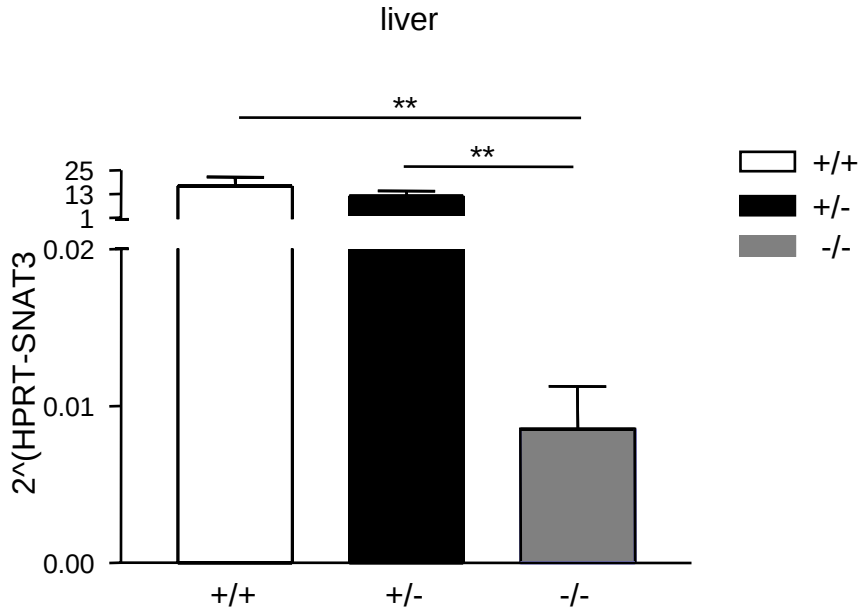

B.

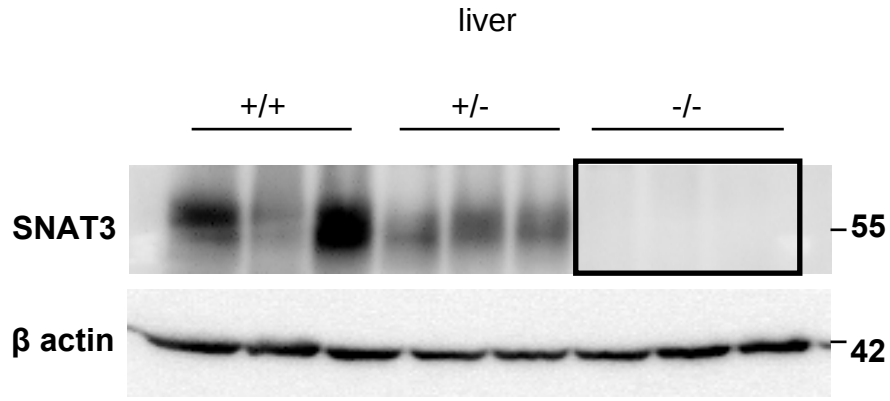

Figure 5

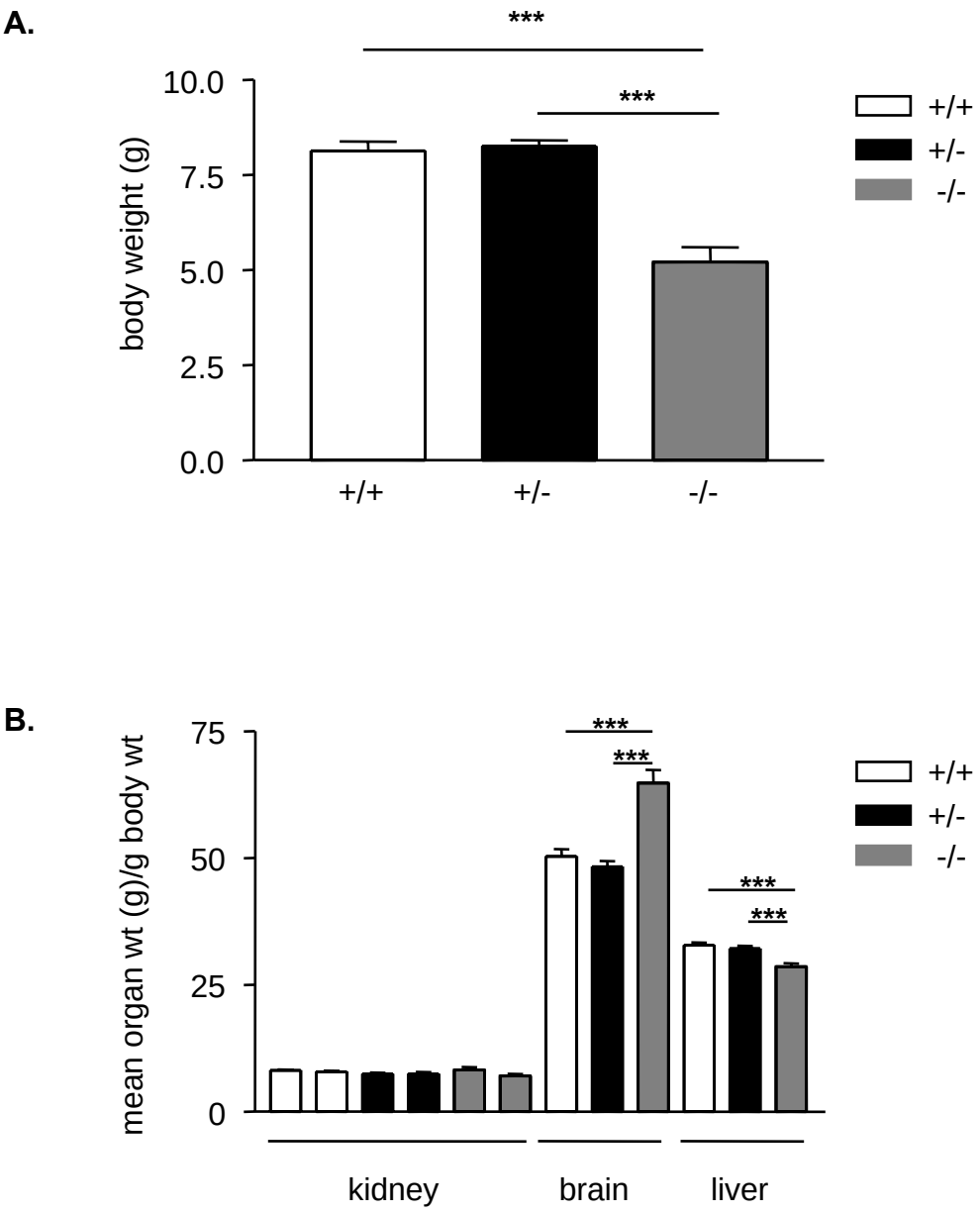
A.
***
***
10.0
7.5
5.0
2.5
0.0
body weight (g)
+/+
+/-
-/-
+/+
+/-
-/-
B.
75
50
25
0
mean organ wt (g)/g body wt
***
***
***
***
+/+
+/-
-/-
kidney
brain
liver

Figure 6

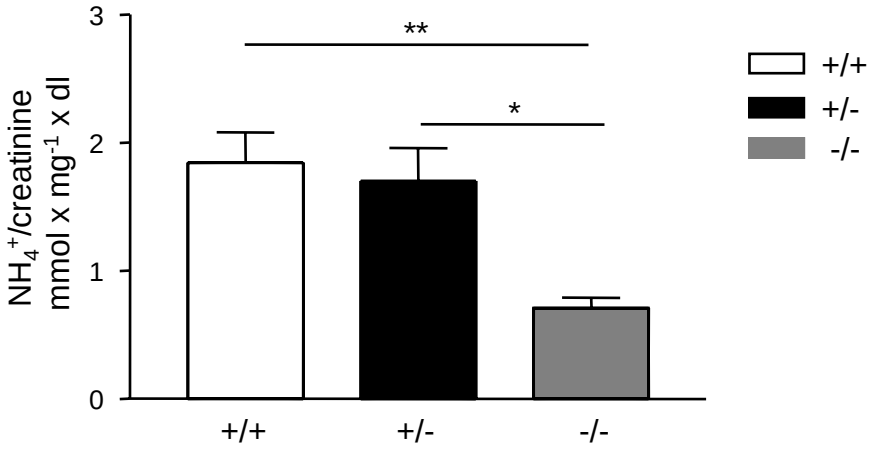

Figure 7

A.

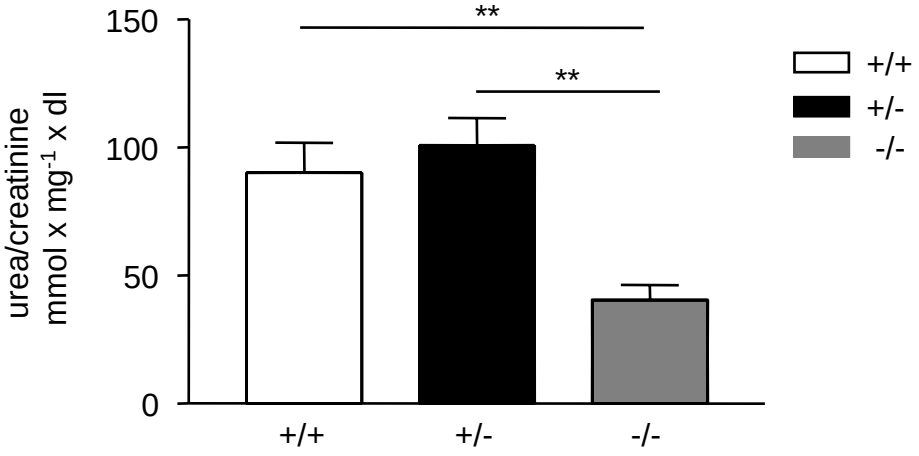
150
100
50
0
**
**
urea/creatinine
mmol x mg-1 x dl
+/+
+/-
-/-
+/+
+/-
-/-

B.

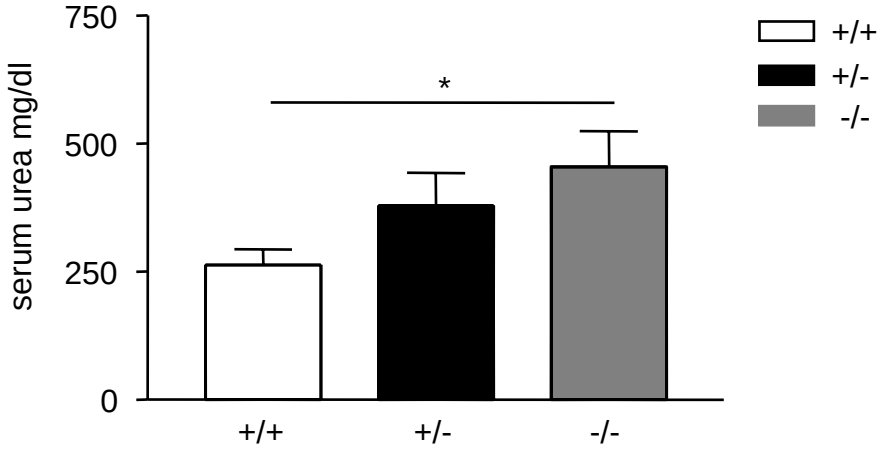
750
500
250
0
*
serum urea mg/dl
+/+
+/-
-/-
+/+
+/-
-/-

Figure 8

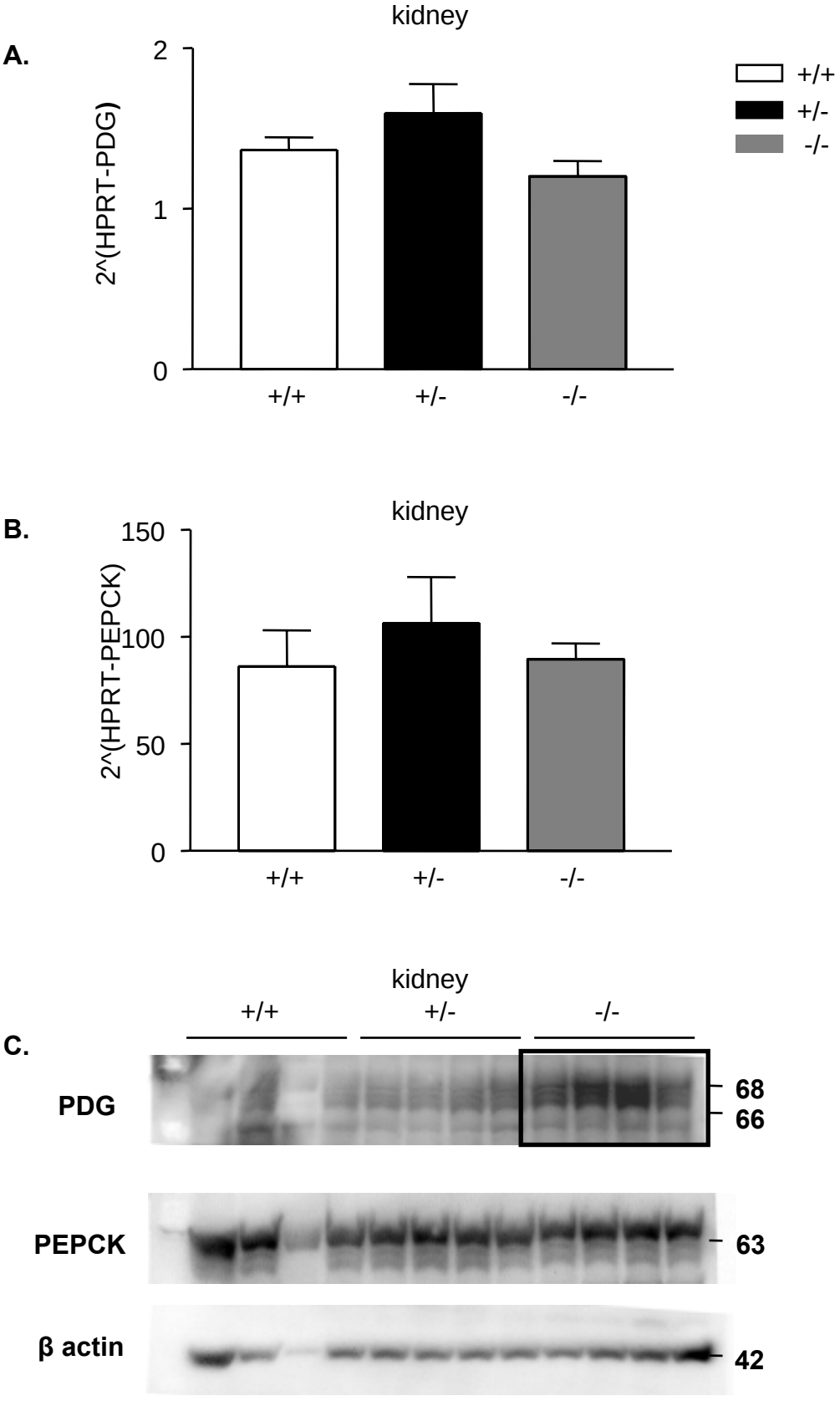
A.
kidney
2^(HPRT-PDG)
2
1
0
+/+
+/-
-/-
+/+
+/-
-/-
B.
kidney
2^(HPRT-PEPCK)
150
100
50
0
+/+
+/-
-/-
C.
kidney
+/+
+/-
-/-
PDG
68
66
PEPCK
63
β actin
42

Figure 9

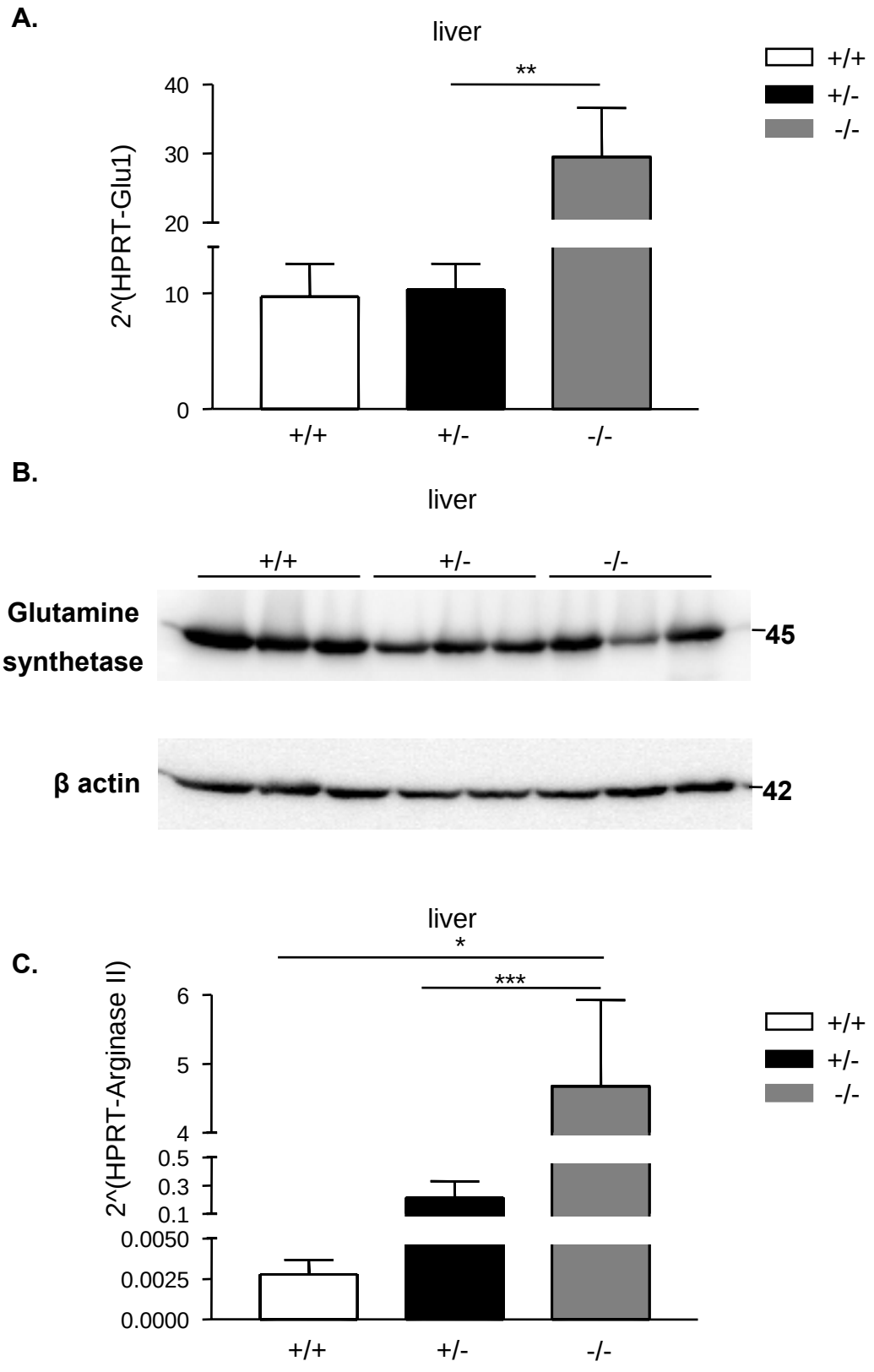
A.
liver
**
+/+
+/-
-/-
2^(HPRT-Glu1)
40
30
20
10
0
+/+
+/-
-/-
B.
liver
+/+
+/-
-/-
Glutamine synthetase
45
β actin
42
C.
liver
*
***
2^(HPRT-Arginase II)
6
5
4
0.5
0.3
0.1
0.0050
0.0025
0.0000
+/+
+/-
-/-

Figure 10

A.

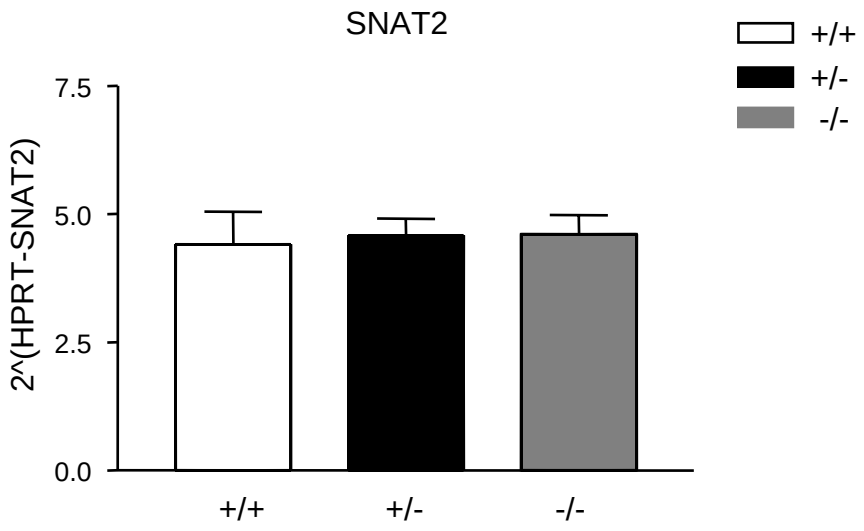

B.

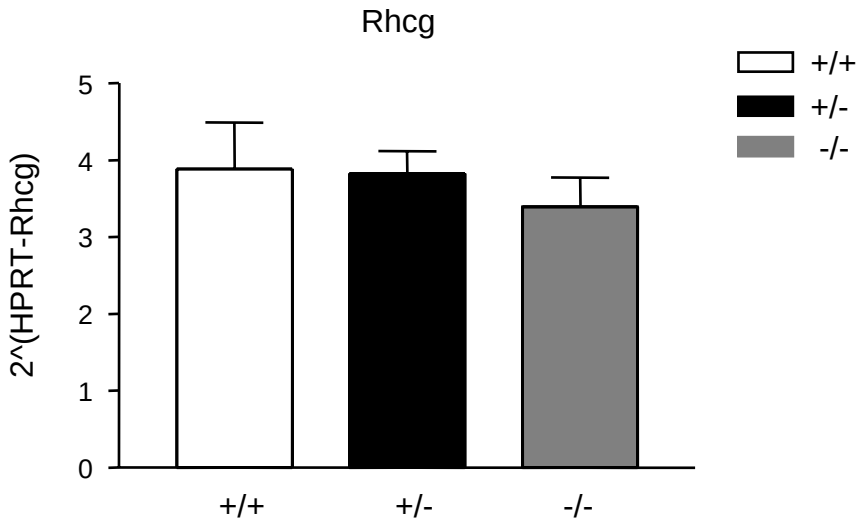

Figure 11

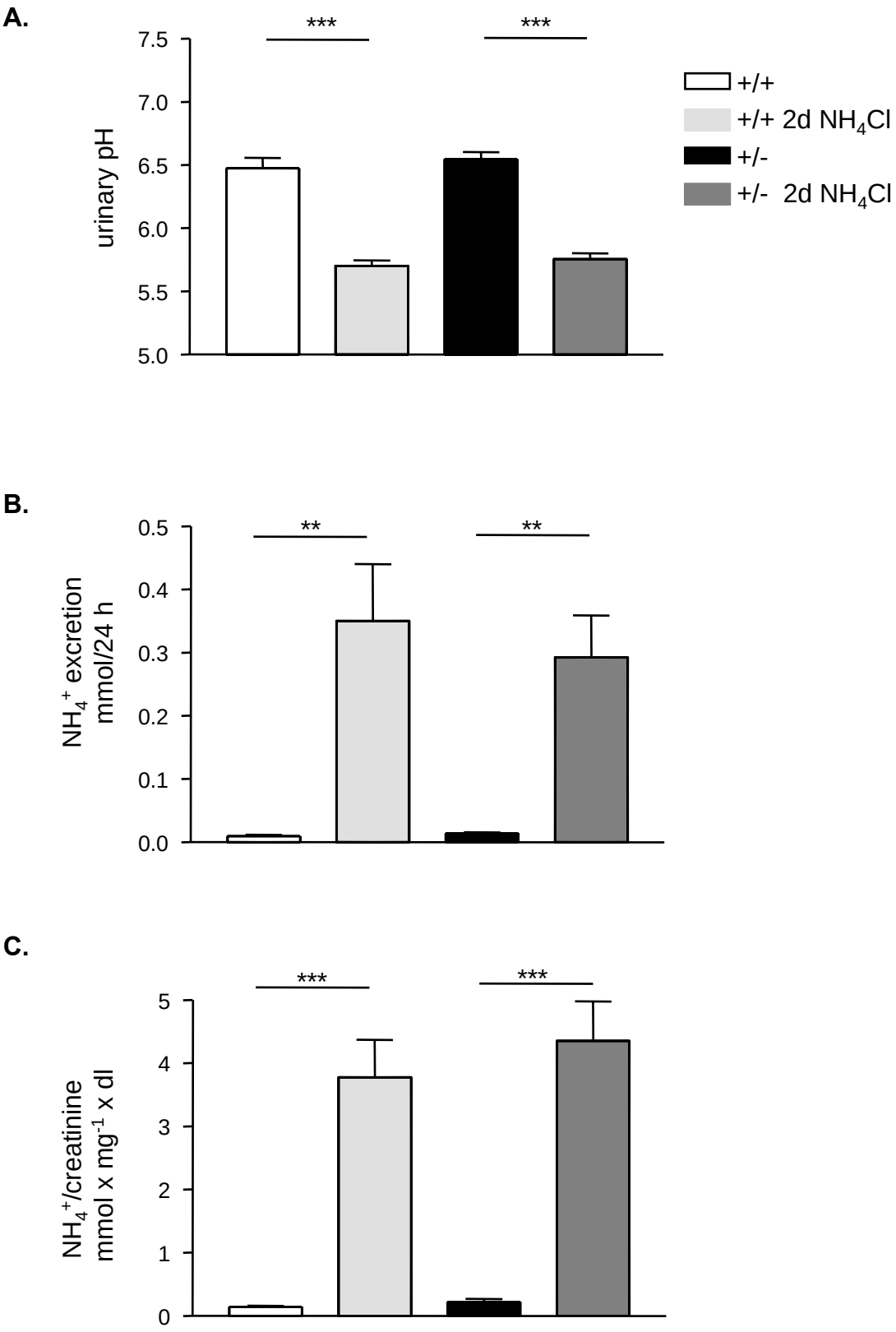
A.
***
***
7.5
7.0
6.5
6.0
5.5
5.0
urinary pH
+/+
+/+ 2d NH4Cl
+/-
+/- 2d NH4Cl
B.
**
**
0.5
0.4
0.3
0.2
0.1
0.0
NH4+ excretion
mmol/24 h
C.
***
***
5
4
3
2
1
0
NH4+/creatinine
mmol x mg-1 x dl

Figure 12

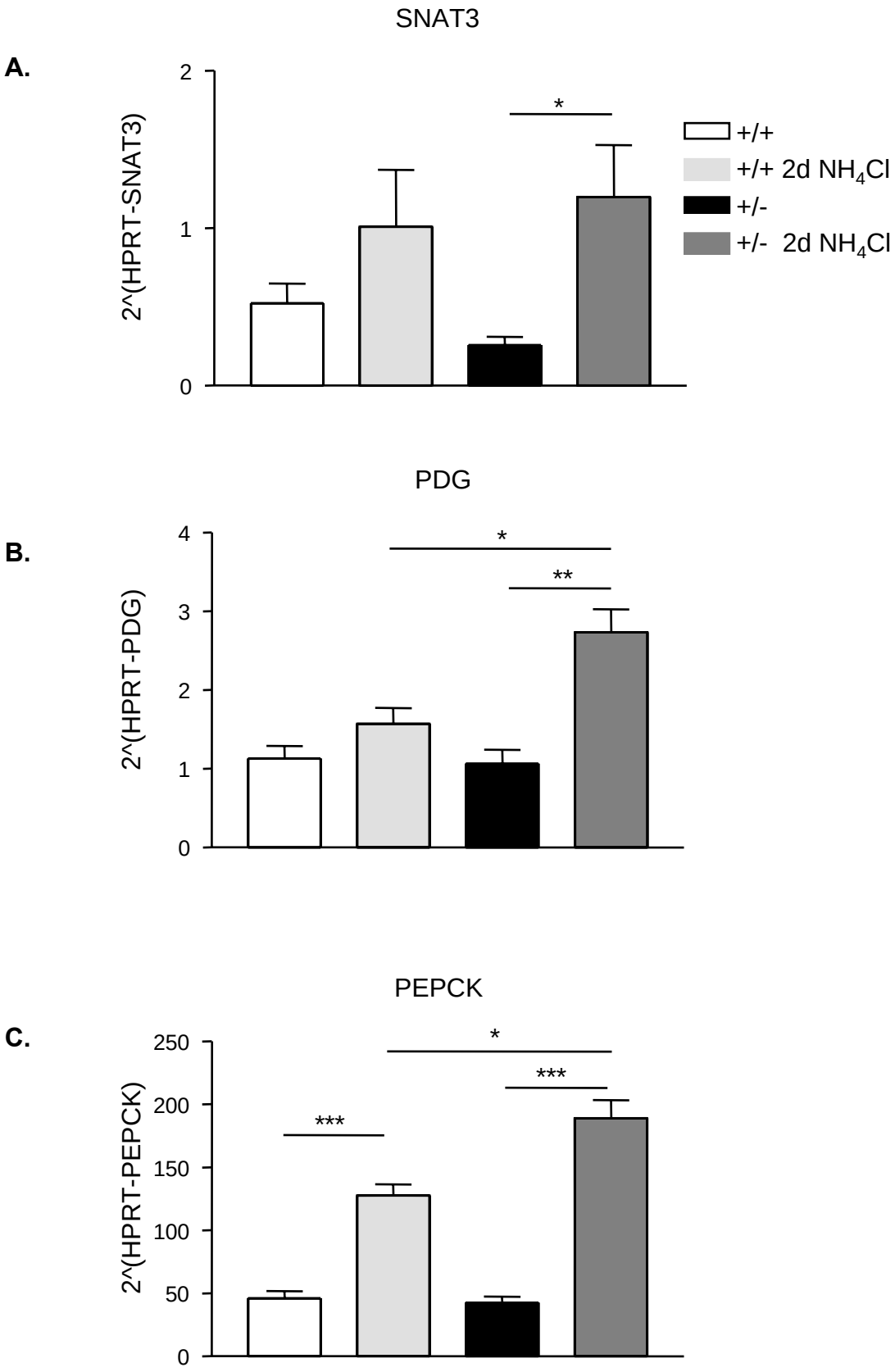
A.
SNAT3
2^(HPRT-SNAT3)
2
1
0
*
+/+
+/+ 2d NH4Cl
+/-
+/- 2d NH4Cl
B.
PDG
2^(HPRT-PDG)
4
3
2
1
0
*
**
C.
PEPCK
2^(HPRT-PEPCK)
250
200
150
100
50
0
*
***
***

Figure 13

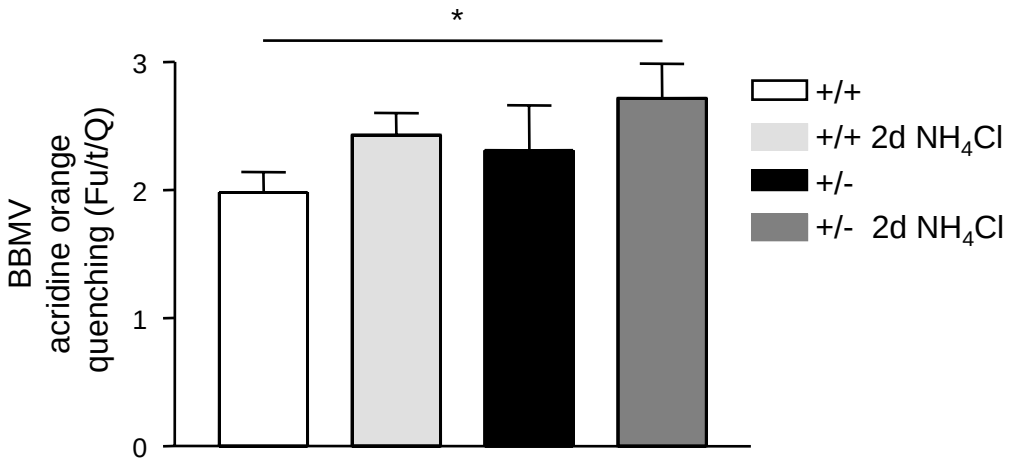

VII. Dissertation discussion

The research presented herein describes developments in understanding the regulation of SNAT3 and other transporters and enzymes involved in renal ammoniagenesis and gluconeogenesis. This work is a continuation of much past and present research in renal acid-base homeostasis and gluconeogenesis. Three different studies are described in this dissertation, and are designated as specific aims; Aim I, II and III. Aim I, discussed the role of SNAT3 during dietary potassium restriction, high protein intake and metabolic acidosis. Using a mouse model of diet-induced obesity in Aim II, we were able to show regulation of SNAT3 by obesity and glucose intolerance. An ENU-mutagenesis model of SNAT3 was utilized in Aim III, to elucidate the physiological role of SNAT3 in various organ systems and during metabolic acidosis. Taken together, this work highlights the importance of SNAT3 in the kidney, under various dietary treatments, mouse models of disease and in absence of SNAT3 *in vivo*.

The renal proximal tubule cell houses all the necessary machinery required to respond to changes in daily acid-base balance, due to localization of various transport proteins and enzymes, namely SNAT3, PDG and PEPCK. Ammonium and bicarbonate production and excretion, coupled with proton secretion are byproducts of reactions involving glutamine influx via SNAT3 and activities of PDG and PEPCK; leading to the restoration of acid-base balance in response to an acid load. These processes are indeed complex and are not fully understood.

Evidence for a role of SNAT3 in renal acid-base balance comes from a variety of observations. Renal extraction of glutamine is substantially increased during acidosis and is redirected from splanchnic pools to the kidney (35, 125, 149). A specialized transport mechanism must be in place to support the increased glutamine usage by the kidney. A dietary acid load, as observed with low K^+ or high protein intake or the oral administration of NH_4Cl, results in significant changes in proximal tubular transport mechanisms (61, 88, 115, 123, 135, 136, 150). Although the mechanisms involved vary with different treatments, the outcome is similar; acid loading, of any variety, results in a remarkable increase in SNAT3 mRNA expression and protein abundance. Localization of SNAT3 to the basolateral aspect of the proximal tubule cell provides support for a role in acid-base balance, in particular, as the glutamine influx mechanism during acidosis.

Low K^+ or high protein intake, and metabolic acidosis generated by an oral acid load leads to increases in urinary NH_4^+ excretion with a concomitant increase in SNAT3 abundance. Immunohistochemical localization showed SNAT3-like staining in S1, S2 and S3 segments in response to K^+ restriction, high protein intake and acidosis.

Cafeteria style feeding produced two cohorts of mice, based on weight and glucose intolerance; obese, glucose-intolerant (O-GI) mice and moderate weight, less glucose intolerant non-responders (NR). Challenging both groups with an acid load revealed several defects in renal ammoniagenesis which were not seen at baseline. O-GI mice, despite reduced NH_4^+ excretion and a more alkaline urinary pH, had massive increases in SNAT3 mRNA and protein expression in comparison to NR mice, suggesting potential dysregulation of SNAT3 with high-fat feeding. Our data suggest that perhaps insulin, glucose intolerance or circulating free fatty acids as observed in obesity may play a role in regulating SNAT3 and ammoniagenesis.

Finally, an ENU-mutagenesis model of SNAT3 revealed that deletion of this transporter is lethal. Apart from reduced urinary defects such as reduced NH_4^+ and urea excretion, these mice exhibit neurological disturbances and stunted growth. More work is needed to examine both brain and liver disturbances in these mice.

In conclusion, our results show strong evidence that SNAT3 is a crucial if not the primary glutamine transporter, not only in the kidney, but in the brain and liver. It appears to play an important role in renal ammoniagenesis and gluconeogenesis, and is regulated under various dietary conditions known to elicit acidosis.

VIII. References

1. **Abate N, Chandalia M, Cabo-Chan AV, Jr., Moe OW, and Sakhaee K**. The metabolic syndrome and uric acid nephrolithiasis: novel features of renal manifestation of insulin resistance. *Kidney international* 65: 386-392, 2004.

2. **Adam WR, Koretsky AP, and Weiner MW**. 31P-NMR in vivo measurement of renal intracellular pH: effects of acidosis and K+ depletion in rats. *The American journal of physiology* 251: F904-910, 1986.

3. **Alleyne GA, and Scullard GH**. Renal metabolic response to acid base changes. I. Enzymatic control of ammoniagenesis in the rat. *The Journal of clinical investigation* 48: 364-370, 1969.

4. **Ambuhl PM, Amemiya M, Danczkay M, Lotscher M, Kaissling B, Moe OW, Preisig PA, and Alpern RJ**. Chronic metabolic acidosis increases NHE3 protein abundance in rat kidney. *The American journal of physiology* 271: F917-925, 1996.

5. **Amemiya M, Tabei K, Kusano E, Asano Y, and Alpern RJ**. Incubation of OKP cells in low-K+ media increases NHE3 activity after early decrease in intracellular pH. *The American journal of physiology* 276: C711-716, 1999.

6. **Armitage FE, and Wingo CS**. Luminal acidification in K-replete OMCDi: inhibition of bicarbonate absorption by K removal and luminal Ba. *The American journal of physiology* 269: F116-124, 1995.

7. **Asplin JR**. Uric acid stones. *Seminars in nephrology* 16: 412-424, 1996.

8. **Association AD**. http://www.diabetes.org/diabetes-statistics/prevalence.jsp. [March 31, 2009

9. **Attmane-Elakeb A, Mount DB, Sibella V, Vernimmen C, Hebert SC, and Bichara M**. Stimulation by in vivo and in vitro metabolic acidosis of expression of rBSC-1, the Na+-K+(NH4+)-2Cl- cotransporter of the rat medullary thick ascending limb. *The Journal of biological chemistry* 273: 33681-33691, 1998.

10. **Bailey MA, Fletcher RM, Woodrow DF, Unwin RJ, and Walter SJ**. Upregulation of H+-ATPase in the distal nephron during potassium depletion: structural and functional evidence. *The American journal of physiology* 275: F878-884, 1998.

11. **Bank N, and Aynediian HS**. A micropuncture study of the effect of parathyroid hormone on renal bicarbonate reabsorption. *The Journal of clinical investigation* 58: 336-344, 1976.

12. **Beier DR**. ENU mutagenesis: a work in progress. *Physiological genomics* 11: 111-113, 2002.

13. **Biver S, Belge H, Bourgeois S, Van Vooren P, Nowik M, Scohy S, Houillier P, Szpirer J, Szpirer C, Wagner CA, Devuyst O, and Marini AM**. A role for Rhesus factor Rhcg in renal ammonium excretion and male fertility. *Nature* 456: 339-343, 2008.

14. **Bobulescu IA, Dwarakanath V, Zou L, Zhang J, Baum M, and Moe OW**. Glucocorticoids acutely increase cell surface Na+/H+ exchanger-3 (NHE3) by activation of NHE3 exocytosis. *American journal of physiology* 289: F685-691, 2005.

15. **Boulland JL, Osen KK, Levy LM, Danbolt NC, Edwards RH, Storm-Mathisen J, and Chaudhry FA**. Cell-specific expression of the glutamine transporter SN1 suggests differences in dependence on the glutamine cycle. *The European journal of neuroscience* 15: 1615-1631, 2002.

16. **Boulland JL, Rafiki A, Levy LM, Storm-Mathisen J, and Chaudhry FA**. Highly differential expression of SN1, a bidirectional glutamine transporter, in astroglia and endothelium in the developing rat brain. *Glia* 41: 260-275, 2003.

17. **Broer A, Albers A, Setiawan I, Edwards RH, Chaudhry FA, Lang F, Wagner CA, and Broer S**. Regulation of the glutamine transporter SN1 by extracellular pH and intracellular sodium ions. *The Journal of physiology* 539: 3-14, 2002.

18. **Buerkert J, Martin D, and Trigg D**. Ammonium handling by superficial and juxtamedullary nephrons in the rat. Evidence for an ammonia shunt between the loop of Henle and the collecting duct. *The Journal of clinical investigation* 70: 1-12, 1982.

19. **Burch HB, Narins RG, Chu C, Fagioli S, Choi S, McCarthy W, and Lowry OH**. Distribution along the rat nephron of three enzymes of gluconeogenesis in acidosis and starvation. *The American journal of physiology* 235: F246-253, 1978.

20. **Capasso G, Jaeger P, Giebisch G, Guckian V, and Malnic G**. Renal bicarbonate reabsorption in the rat. II. Distal tubule load dependence and effect of hypokalemia. *The Journal of clinical investigation* 80: 409-414, 1987.

21. **Capasso G, Kinne R, Malnic G, and Giebisch G**. Renal bicarbonate reabsorption in the rat. I. Effects of hypokalemia and carbonic anhydrase. *The Journal of clinical investigation* 78: 1558-1567, 1986.

22. **Chambrey R, Goossens D, Bourgeois S, Picard N, Bloch-Faure M, Leviel F, Geoffroy V, Cambillau M, Colin Y, Paillard M, Houillier P, Cartron JP, and Eladari D**. Genetic ablation of Rhbg in the mouse does not impair renal ammonium excretion. *American journal of physiology* 289: F1281-1290, 2005.

23. **Chan YL, Biagi B, and Giebisch G**. Control mechanisms of bicarbonate transport across the rat proximal convoluted tubule. *The American journal of physiology* 242: F532-543, 1982.

24. **Chaudhry FA, Krizaj D, Larsson P, Reimer RJ, Wreden C, Storm-Mathisen J, Copenhagen D, Kavanaugh M, and Edwards RH**. Coupled and uncoupled proton movement by amino acid transport system N. *The EMBO journal* 20: 7041-7051, 2001.

25. **Chaudhry FA, Reimer RJ, Krizaj D, Barber D, Storm-Mathisen J, Copenhagen DR, and Edwards RH**. Molecular analysis of system N suggests novel physiological roles in nitrogen metabolism and synaptic transmission. *Cell* 99: 769-780, 1999.

26. **Chobanian MC, and Hammerman MR**. Insulin stimulates ammoniagenesis in canine renal proximal tubular segments. *The American journal of physiology* 253: F1171-1177, 1987.

27. **Chobanian MC, and Julin CM**. Angiotensin II stimulates ammoniagenesis in canine renal proximal tubule segments. *The American journal of physiology* 260: F19-26, 1991.

28. **Choe H, Sackin H, and Palmer LG**. Permeation properties of inward-rectifier potassium channels and their molecular determinants. *The Journal of general physiology* 115: 391-404, 2000.

29. **Christensen HN**. Organic ion transport during seven decades. The amino acids. *Biochimica et biophysica acta* 779: 255-269, 1984.

30. **Christensen HN**. Role of amino acid transport and countertransport in nutrition and metabolism. *Physiological reviews* 70: 43-77, 1990.

31. **Curthoys NP**. Renal ammonium ion production and excretion. In: *Seldin and Giebisch's The Kidney Physiology and Pathophysiology*, edited by Alpern RJ, and Hebert SC Elsevier, 2008, p. 1601-1619.

32. **Curthoys NP, and Gstraunthaler G**. Mechanism of increased renal gene expression during metabolic acidosis. *American journal of physiology* 281: F381-390, 2001.

33. **Curthoys NP, Kuhlenschmidt T, Godfrey SS, and Weiss RF**. Phosphate-dependent glutaminase from rat kidney. Cause of increased activity in response to acidosis and identity with glutaminase from other tissues. *Archives of biochemistry and biophysics* 172: 162-167, 1976.

34. **Curthoys NP, and Lowry OH**. The distribution of glutaminase isoenzymes in the various structures of the nephron in normal, acidotic, and alkalotic rat kidney. *The Journal of biological chemistry* 248: 162-168, 1973.

35. **Curthoys NP, and Watford M**. Regulation of glutaminase activity and glutamine metabolism. *Annual review of nutrition* 15: 133-159, 1995.

36. **Daudon M, Lacour B, and Jungers P**. High prevalence of uric acid calculi in diabetic stone formers. *Nephrol Dial Transplant* 20: 468-469, 2005.

37. **Daudon M, Traxer O, Conort P, Lacour B, and Jungers P**. Type 2 diabetes increases the risk for uric acid stones. *J Am Soc Nephrol* 17: 2026-2033, 2006.

38. **Drewnowsk KD, Craig MR, Digiovanni SR, McCarty JM, Moorman AF, Lamers WH, and Schoolwerth AC**. PEPCK mRNA localization in proximal tubule and gene regulation during metabolic acidosis. *J Physiol Pharmacol* 53: 3-20, 2002.

39. **Eladari D, Cheval L, Quentin F, Bertrand O, Mouro I, Cherif-Zahar B, Cartron JP, Paillard M, Doucet A, and Chambrey R**. Expression of RhCG, a new putative NH(3)/NH(4)(+) transporter, along the rat nephron. *J Am Soc Nephrol* 13: 1999-2008, 2002.

40. **Faus MJ, Lupianez A, Vargas A, and Sanchez-Medina F**. Induction of rat kidney gluconeogenesis during acute liver intoxication by carbon tetrachloride. *The Biochemical journal* 174: 461-467, 1978.

41. **Fei YJ, Sugawara M, Nakanishi T, Huang W, Wang H, Prasad PD, Leibach FH, and Ganapathy V**. Primary structure, genomic organization, and functional and

electrogenic characteristics of human system N 1, a Na+- and H+-coupled glutamine transporter. *The Journal of biological chemistry* 275: 23707-23717, 2000.

42. **Good DW**. Ammonium transport by the thick ascending limb of Henle's loop. *Annual review of physiology* 56: 623-647, 1994.

43. **Good DW, and Burg MB**. Ammonia production by individual segments of the rat nephron. *The Journal of clinical investigation* 73: 602-610, 1984.

44. **Good DW, and Watts BA, 3rd**. Functional roles of apical membrane Na+/H+ exchange in rat medullary thick ascending limb. *The American journal of physiology* 270: F691-699, 1996.

45. **Gu S, Roderick HL, Camacho P, and Jiang JX**. Identification and characterization of an amino acid transporter expressed differentially in liver. *Proceedings of the National Academy of Sciences of the United States of America* 97: 3230-3235, 2000.

46. **Gu S, Villegas CJ, and Jiang JX**. Differential regulation of amino acid transporter SNAT3 by insulin in hepatocytes. *The Journal of biological chemistry* 280: 26055-26062, 2005.

47. **Guder WG, and Schmidt U**. The localization of gluconeogenesis in rat nephron. Determination of phosphoenolpyruvate carboxykinase in microdissected tubules. *Hoppe-Seyler's Zeitschrift fur physiologische Chemie* 355: 273-278, 1974.

48. **Gullans SR, Brazy PC, Dennis VW, and Mandel LJ**. Interactions between gluconeogenesis and sodium transport in rabbit proximal tubule. *The American journal of physiology* 246: F859-869, 1984.

49. **Guntupalli J, Onuigbo M, Wall S, Alpern RJ, and DuBose TD, Jr.** Adaptation to low-K+ media increases H(+)-K(+)-ATPase but not H(+)-ATPase-mediated pHi recovery in OMCD1 cells. *The American journal of physiology* 273: C558-571, 1997.

50. **Gutman AB, and Yue TF**. Urinary Ammonium Excretion in Primary Gout. *The Journal of clinical investigation* 44: 1474-1481, 1965.

51. **Halperin ML, and Jungas RL**. Metabolic production and renal disposal of hydrogen ions. *Kidney international* 24: 709-713, 1983.

52. **Hansen WR, Barsic-Tress N, Taylor L, and Curthoys NP**. The 3'-nontranslated region of rat renal glutaminase mRNA contains a pH-responsive stability element. *The American journal of physiology* 271: F126-131, 1996.

53. **Haussinger D**. Nitrogen metabolism in liver: structural and functional organization and physiological relevance. *The Biochemical journal* 267: 281-290, 1990.

54. **Henneman PH, Wallach S, and Dempsey EF**. The metabolism defect responsible for uric acid stone formation. *The Journal of clinical investigation* 41: 537-542, 1962.

55. **Hitotsumachi S, Carpenter DA, and Russell WL**. Dose-repetition increases the mutagenic effectiveness of N-ethyl-N-nitrosourea in mouse spermatogonia. *Proceedings of the National Academy of Sciences of the United States of America* 82: 6619-6621, 1985.

56. **Honegger KJ, Capuano P, Winter C, Bacic D, Stange G, Wagner CA, Biber J, Murer H, and Hernando N**. Regulation of sodium-proton exchanger isoform 3 (NHE3) by PKA and exchange protein directly activated by cAMP (EPAC). *Proceedings of the National Academy of Sciences of the United States of America* 103: 803-808, 2006.

57. **Hwang JJ, and Curthoys NP**. Effect of acute alterations in acid-base balance on rat renal glutaminase and phosphoenolpyruvate carboxykinase gene expression. *The Journal of biological chemistry* 266: 9392-9396, 1991.

58. **Indiveri C, Abruzzo G, Stipani I, and Palmieri F**. Identification and purification of the reconstitutively active glutamine carrier from rat kidney mitochondria. *The Biochemical journal* 333 (Pt 2): 285-290, 1998.

59. **Iynedjian PB, and Hanson RW**. Increase in level of functional messenger RNA coding for phosphoenolpyruvate carboxykinase (GTP) during induction by cyclic adenosine 3':5'-monophosphate. *The Journal of biological chemistry* 252: 655-662, 1977.

60. **Iynedjian PB, and Hanson RW**. Messenger RNA for renal phosphoenolpyruvate carboxykinase (GTP). Its translation in a heterologous cell-free system and its regulation by glucocorticoids and by changes in acid-base balance. *The Journal of biological chemistry* 252: 8398-8403, 1977.

61. **Jaeger P, Karlmark B, and Giebisch G**. Ammonium transport in rat cortical tubule: relationship to potassium metabolism. *The American journal of physiology* 245: F593-600, 1983.

62. **Joseph PK, and Subrahmanyam K**. Effect of growth hormone, insulin, thyroxine and cortisone on renal gluconeogenesis. *Archives of biochemistry and biophysics* 127: 288-291, 1968.

63. **Justice MJ, Carpenter DA, Favor J, Neuhauser-Klaus A, Hrabe de Angelis M, Soewarto D, Moser A, Cordes S, Miller D, Chapman V, Weber JS, Rinchik EM, Hunsicker PR, Russell WL, and Bode VC**. Effects of ENU dosage on mouse strains. *Mamm Genome* 11: 484-488, 2000.

64. **Kahn AM, Dolson GM, Hise MK, Bennett SC, and Weinman EJ**. Parathyroid hormone and dibutyryl cAMP inhibit Na+/H+ exchange in renal brush border vesicles. *The American journal of physiology* 248: F212-218, 1985.

65. **Kamel KS, Cheema-Dhadli S, and Halperin ML**. Studies on the pathophysiology of the low urine pH in patients with uric acid stones. *Kidney international* 61: 988-994, 2002.

66. **Karim Z, Attmane-Elakeb A, Sibella V, and Bichara M**. Acid pH increases the stability of BSC1/NKCC2 mRNA in the medullary thick ascending limb. *J Am Soc Nephrol* 14: 2229-2236, 2003.

67. **Karinch AM, Lin CM, Meng Q, Pan M, and Souba WW**. Glucocorticoids have a role in renal cortical expression of the SNAT3 glutamine transporter during chronic metabolic acidosis. *American journal of physiology* 292: F448-455, 2007.

68. **Karinch AM, Lin CM, Wolfgang CL, Pan M, and Souba WW**. Regulation of expression of the SN1 transporter during renal adaptation to chronic metabolic acidosis in rats. *American journal of physiology* 283: F1011-1019, 2002.

69. **Khanna A, Simoni J, Hacker C, Duran MJ, and Wesson DE**. Increased endothelin activity mediates augmented distal nephron acidification induced by dietary protein. *J Am Soc Nephrol* 15: 2266-2275, 2004.

70. **Khanna A, Simoni J, and Wesson DE**. Endothelin-induced increased aldosterone activity mediates augmented distal nephron acidification as a result of dietary protein. *J Am Soc Nephrol* 16: 1929-1935, 2005.

71. **Khatchadourian J, Preminger GM, Whitson PA, Adams-Huet B, and Pak CY**. Clinical and biochemical presentation of gouty diathesis: comparison of uric acid versus pure calcium stone formation. *The Journal of urology* 154: 1665-1669, 1995.

72. **Kida K, Nakajo S, Kamiya F, Toyama Y, Nishio T, and Nakagawa H**. Renal net glucose release in vivo and its contribution to blood glucose in rats. *The Journal of clinical investigation* 62: 721-726, 1978.

73. **Kilberg MS, Handlogten ME, and Christensen HN**. Characteristics of an amino acid transport system in rat liver for glutamine, asparagine, histidine, and closely related analogs. *The Journal of biological chemistry* 255: 4011-4019, 1980.

74. **Kinsella JL, and Aronson PS**. Interaction of NH4+ and Li+ with the renal microvillus membrane Na+-H+ exchanger. *The American journal of physiology* 241: C220-226, 1981.

75. **Kinsella JL, Freiberg JM, and Sacktor B**. Glucocorticoid activation of Na+/H+ exchange in renal brush border vesicles: kinetic effects. *The American journal of physiology* 248: F233-239, 1985.

76. **Knepper MA, Good DW, and Burg MB**. Ammonia and bicarbonate transport by rat cortical collecting ducts perfused in vitro. *The American journal of physiology* 249: F870-877, 1985.

77. **Krivosikova Z, Spustova V, and Dzurik R**. Participation of P-dependent and P-independent glutaminases in rat kidney ammoniagenesis and their modulation by metabolic acidosis, hippurate and insulin. *Physiological research / Academia Scientiarum Bohemoslovaca* 47: 177-183, 1998.

78. **Laterza OF, and Curthoys NP**. Specificity and functional analysis of the pH-responsive element within renal glutaminase mRNA. *American journal of physiology* 278: F970-977, 2000.

79. **Laterza OF, Hansen WR, Taylor L, and Curthoys NP**. Identification of an mRNA-binding protein and the specific elements that may mediate the pH-responsive induction of renal glutaminase mRNA. *The Journal of biological chemistry* 272: 22481-22488, 1997.

80. **Lemieux G, Berkofsky J, and Lemieux C**. Renal tissue metabolism in the rat during chronic metabolic alkalosis: importance of glycolysis. *Canadian journal of physiology and pharmacology* 64: 1419-1426, 1986.

81. **Lemieux G, Kiss AL, Lemieux C, Ibanez RJ, and Aranda MR**. Renal tubular biochemistry during acute and chronic metabolic alkalosis in the dog. *Kidney international* 27: 908-918, 1985.

82. **Lloyd-Jones D, Adams R, Carnethon M, De Simone G, Ferguson TB, Flegal K, Ford E, Furie K, Go A, Greenlund K, Haase N, Hailpern S, Ho M, Howard V, Kissela B, Kittner S, Lackland D, Lisabeth L, Marelli A, McDermott M, Meigs J, Mozaffarian D, Nichol G, O'Donnell C, Roger V, Rosamond W, Sacco R, Sorlie P, Stafford R, Steinberger J, Thom T, Wasserthiel-Smoller S, Wong N, Wylie-Rosett J, and Hong Y**. Heart disease and stroke statistics--2009 update: a report from the American Heart Association Statistics Committee and Stroke Statistics Subcommittee. *Circulation* 119: e21-181, 2009.

83. **Lupianez JA, Dileepan KN, and Wagle SR**. Interrelationship of somatostatin, insulin, and calcium in the control of gluconeogenesis in kidney cortex slices. *Biochemical and biophysical research communications* 90: 1153-1158, 1979.

84. **Maalouf NM, Cameron MA, Moe OW, and Sakhaee K**. Novel insights into the pathogenesis of uric acid nephrolithiasis. *Current opinion in nephrology and hypertension* 13: 181-189, 2004.

85. **May RC, Kelly RA, and Mitch WE**. Metabolic acidosis stimulates protein degradation in rat muscle by a glucocorticoid-dependent mechanism. *The Journal of clinical investigation* 77: 614-621, 1986.

86. **McIntire SL, Reimer RJ, Schuske K, Edwards RH, and Jorgensen EM**. Identification and characterization of the vesicular GABA transporter. *Nature* 389: 870-876, 1997.

87. **McKerlie C**. Cause and effect considerations in diagnostic pathology and pathology phenotyping of genetically engineered mice (GEM). *ILAR journal / National Research Council, Institute of Laboratory Animal Resources* 47: 156-162, 2006.

88. **McKinney TD, and Davidson KK**. Effect of potassium depletion and protein intake in vivo on renal tubular bicarbonate transport in vitro. *The American journal of physiology* 252: F509-516, 1987.

89. **Meydan N, Barutca S, Caliskan S, and Camsari T**. Urinary stone disease in diabetes mellitus. *Scandinavian journal of urology and nephrology* 37: 64-70, 2003.

90. **Moran A, Stange G, and Murer H**. Sodium-hydrogen exchange system in brush border membranes from cortical and medullary regions of the proximal tubule. *Biochemical and biophysical research communications* 163: 269-275, 1989.

91. **Moret C, Dave MH, Schulz N, Jiang JX, Verrey F, and Wagner CA**. Regulation of renal amino acid transporters during metabolic acidosis. *American journal of physiology* 292: F555-566, 2007.

92. **Nagami GT**. Ammonia production and secretion by the proximal tubule. *Am J Kidney Dis* 14: 258-261, 1989.

93. **Nagami GT**. Effect of angiotensin II on ammonia production and secretion by mouse proximal tubules perfused in vitro. *The Journal of clinical investigation* 89: 925-931, 1992.

94. **Nagami GT**. Effect of bath and luminal potassium concentration on ammonia production and secretion by mouse proximal tubules perfused in vitro. *The Journal of clinical investigation* 86: 32-39, 1990.

95. **Nagami GT**. Effect of luminal angiotensin II on ammonia production and secretion by mouse proximal tubules. *The American journal of physiology* 269: F86-92, 1995.

96. **Nagami GT**. Luminal secretion of ammonia in the mouse proximal tubule perfused in vitro. *The Journal of clinical investigation* 81: 159-164, 1988.

97. **Nagami GT**. Renal ammonia production and excretion. In: *The Kidney Physiology and Pathophysiology*, edited by Seldin D, Giebisch, GLippincott Williams & Wilkins, 2000, p. 1995-2013.

98. **Nagami GT**. Role of angiotensin II in the enhancement of ammonia production and secretion by the proximal tubule in metabolic acidosis. *American journal of physiology* 294: F874-880, 2008.

99. **Nagami GT, Sonu CM, and Kurokawa K**. Ammonia production by isolated mouse proximal tubules perfused in vitro. Effect of metabolic acidosis. *The Journal of clinical investigation* 78: 124-129, 1986.

100. **Nagaraja TN, and Brookes N**. Glutamine transport in mouse cerebral astrocytes. *Journal of neurochemistry* 66: 1665-1674, 1996.

101. **Nonoguchi H, Takehara Y, and Endou H**. Intra- and inter-nephron heterogeneity of ammoniagenesis in rats: effects of chronic metabolic acidosis and potassium depletion. *Pflugers Arch* 407: 245-251, 1986.

102. **Nowik M, Lecca MR, Velic A, Rehrauer H, Brandli AW, and Wagner CA**. Genome-wide gene expression profiling reveals renal genes regulated during metabolic acidosis. *Physiological genomics* 32: 322-334, 2008.

103. **Owen OE, Felig P, Morgan AP, Wahren J, and Cahill GF, Jr.** Liver and kidney metabolism during prolonged starvation. *The Journal of clinical investigation* 48: 574-583, 1969.

104. **Pak CY, Sakhaee K, and Fuller C**. Successful management of uric acid nephrolithiasis with potassium citrate. *Kidney international* 30: 422-428, 1986.

105. **Pak CY, Sakhaee K, Peterson RD, Poindexter JR, and Frawley WH**. Biochemical profile of idiopathic uric acid nephrolithiasis. *Kidney international* 60: 757-761, 2001.

106. **Papathanasiou P, and Goodnow CC**. Connecting mammalian genome with phenome by ENU mouse mutagenesis: gene combinations specifying the immune system. *Annual review of genetics* 39: 241-262, 2005.

107. **Pitts RF**. Renal excretion of acid. *Federation proceedings* 7: 418-426, 1948.

108. **Pitts RF, Pilkington LA, MacLeod MB, and Leal-Pinto E**. Metabolism of glutamine by the intact functioning kidney of the dog. Studies in metabolic acidosis and alkalosis. *The Journal of clinical investigation* 51: 557-565, 1972.

109. **Puschett JB, Zurbach P, and Sylk D**. Acute effects of parathyroid hormone on proximal bicarbonate transport in the dog. *Kidney international* 9: 501-510, 1976.

110. **Quentin F, Eladari D, Cheval L, Lopez C, Goossens D, Colin Y, Cartron JP, Paillard M, and Chambrey R**. RhBG and RhCG, the putative ammonia transporters, are expressed in the same cells in the distal nephron. *J Am Soc Nephrol* 14: 545-554, 2003.

111. **Rapoport A, Crassweller PO, Husdan H, From GL, Zweig M, and Johnson MD**. The renal excretion of hydrogen ion in uric acid stone formers. *Metabolism: clinical and experimental* 16: 176-188, 1967.

112. **Rector FC, Jr., and Orloff J**. The effect of the administration of sodium bicarbonate and ammonium chloride on the excretion and production of ammonia; the absence of alterations in the activity of renal ammonia-producing enzymes in the dog. *The Journal of clinical investigation* 38: 366-372, 1959.

113. **Rector FC, Jr., Seldin DW, and Copenhaver JH**. The mechanism of ammonia excretion during ammonium chloride acidosis. *The Journal of clinical investigation* 34: 20-26, 1955.

114. **Reimer RJ, Chaudhry FA, Gray AT, and Edwards RH**. Amino acid transport system A resembles system N in sequence but differs in mechanism. *Proceedings of the National Academy of Sciences of the United States of America* 97: 7715-7720, 2000.

115. **Remer T, and Manz F**. Estimation of the renal net acid excretion by adults consuming diets containing variable amounts of protein. *The American journal of clinical nutrition* 59: 1356-1361, 1994.

116. **Rogers S, Gavin JR, 3rd, and Hammerman MR**. Phorbol esters inhibit gluconeogenesis in canine renal proximal tubular segments. *The American journal of physiology* 249: F256-262, 1985.

117. **Russell WL, Kelly EM, Hunsicker PR, Bangham JW, Maddux SC, and Phipps EL**. Specific-locus test shows ethylnitrosourea to be the most potent mutagen in the mouse. *Proceedings of the National Academy of Sciences of the United States of America* 76: 5818-5819, 1979.

118. **Sagne C, El Mestikawy S, Isambert MF, Hamon M, Henry JP, Giros B, and Gasnier B**. Cloning of a functional vesicular GABA and glycine transporter by screening of genome databases. *FEBS letters* 417: 177-183, 1997.

119. **Sajo IM, Goldstein MB, Sonnenberg H, Stinebaugh BJ, Wilson DR, and Halperin ML**. Sites of ammonia addition to tubular fluid in rats with chronic metabolic acidosis. *Kidney international* 20: 353-358, 1981.

120. **Sakhaee K, Adams-Huet B, Moe OW, and Pak CY**. Pathophysiologic basis for normouricosuric uric acid nephrolithiasis. *Kidney international* 62: 971-979, 2002.

121. **Sakhaee K, Nicar M, Hill K, and Pak CY**. Contrasting effects of potassium citrate and sodium citrate therapies on urinary chemistries and crystallization of stone-forming salts. *Kidney international* 24: 348-352, 1983.

122. **Sastrasinh S, and Sastrasinh M**. Glutamine transport in submitochondrial particles. *The American journal of physiology* 257: F1050-1058, 1989.

123. **Sastrasinh S, and Sastrasinh M**. Renal mitochondrial glutamine metabolism during K+ depletion. *The American journal of physiology* 250: F667-673, 1986.

124. **Schneider HP, Broer S, Broer A, and Deitmer JW**. Heterologous expression of the glutamine transporter SNAT3 in Xenopus oocytes is associated with four modes of uncoupled transport. *The Journal of biological chemistry* 282: 3788-3798, 2007.

125. **Schrock H, and Goldstein L**. Interorgan relationships for glutamine metabolism in normal and acidotic rats. *The American journal of physiology* 240: E519-525, 1981.

126. **Seney FD, Jr., and Marver D**. Protein intake and cation transport in the loop of Henle. *The Journal of laboratory and clinical medicine* 114: 587-594, 1989.

127. **Solbu TT, Boulland JL, Zahid W, Lyamouri Bredahl MK, Amiry-Moghaddam M, Storm-Mathisen J, Roberg BA, and Chaudhry FA**. Induction and targeting of the glutamine transporter SN1 to the basolateral membranes of cortical kidney tubule cells during chronic metabolic acidosis suggest a role in pH regulation. *J Am Soc Nephrol* 16: 869-877, 2005.

128. **Soleimani M, Bergman JA, Hosford MA, and McKinney TD**. Potassium depletion increases luminal Na+/H+ exchange and basolateral Na+:CO3=:HCO3- cotransport in rat renal cortex. *The Journal of clinical investigation* 86: 1076-1083, 1990.

129. **Stamatelou KK, Francis ME, Jones CA, Nyberg LM, and Curhan GC**. Time trends in reported prevalence of kidney stones in the United States: 1976-1994. *Kidney international* 63: 1817-1823, 2003.

130. **Star RA, Kurtz I, Mejia R, Burg MB, and Knepper MA**. Disequilibrium pH and ammonia transport in isolated perfused cortical collecting ducts. *The American journal of physiology* 253: F1232-1242, 1987.

131. **Stehberger PA, Schulz N, Finberg KE, Karet FE, Giebisch G, Lifton RP, Geibel JP, and Wagner CA**. Localization and regulation of the ATP6V0A4 (a4)

vacuolar H+-ATPase subunit defective in an inherited form of distal renal tubular acidosis. *J Am Soc Nephrol* 14: 3027-3038, 2003.

132. **Stetson DL, Wade JB, and Giebisch G**. Morphologic alterations in the rat medullary collecting duct following potassium depletion. *Kidney international* 17: 45-56, 1980.

133. **Sugawara M, Nakanishi T, Fei YJ, Huang W, Ganapathy ME, Leibach FH, and Ganapathy V**. Cloning of an amino acid transporter with functional characteristics and tissue expression pattern identical to that of system A. *The Journal of biological chemistry* 275: 16473-16477, 2000.

134. **Sundberg BE, Waag E, Jacobsson JA, Stephansson O, Rumaks J, Svirskis S, Alsio J, Roman E, Ebendal T, Klusa V, and Fredriksson R**. The evolutionary history and tissue mapping of amino acid transporters belonging to solute carrier families SLC32, SLC36, and SLC38. *J Mol Neurosci* 35: 179-193, 2008.

135. **Tannen RL**. Relationship of renal ammonia production and potassium homeostasis. *Kidney international* 11: 453-465, 1977.

136. **Tannen RL, and McGill J**. Influence of potassium on renal ammonia production. *The American journal of physiology* 231: 1178-1184, 1976.

137. **Taylor EN, Stampfer MJ, and Curhan GC**. Diabetes mellitus and the risk of nephrolithiasis. *Kidney international* 68: 1230-1235, 2005.

138. **Terris JM, Knepper MA, and Wade JB**. UT-A3: localization and characterization of an additional urea transporter isoform in the IMCD. *American journal of physiology* 280: F325-332, 2001.

139. **Trinchieri A, Coppi F, Montanari E, Del Nero A, Zanetti G, and Pisani E**. Increase in the prevalence of symptomatic upper urinary tract stones during the last ten years. *European urology* 37: 23-25, 2000.

140. **Vallon V, Grahammer F, Volkl H, Sandu CD, Richter K, Rexhepaj R, Gerlach U, Rong Q, Pfeifer K, and Lang F**. KCNQ1-dependent transport in renal and gastrointestinal epithelia. *Proceedings of the National Academy of Sciences of the United States of America* 102: 17864-17869, 2005.

141. **Varoqui H, and Erickson JD**. Selective up-regulation of system a transporter mRNA in diabetic liver. *Biochemical and biophysical research communications* 290: 903-908, 2002.

142. **Verlander JW, Miller RT, Frank AE, Royaux IE, Kim YH, and Weiner ID**. Localization of the ammonium transporter proteins RhBG and RhCG in mouse kidney. *American journal of physiology* 284: F323-337, 2003.

143. **Vinay P, Gougoux A, and Lemieux G**. Isolation of a pure suspension of rat proximal tubules. *The American journal of physiology* 241: F403-411, 1981.

144. **Wall SM, Davis BS, Hassell KA, Mehta P, and Park SJ**. In rat tIMCD, NH4+ uptake by Na+-K+-ATPase is critical to net acid secretion during chronic hypokalemia. *The American journal of physiology* 277: F866-874, 1999.

145. **Wall SM, Fischer MP, Mehta P, Hassell KA, and Park SJ**. Contribution of the Na+-K+-2Cl- cotransporter NKCC1 to Cl- secretion in rat OMCD. *American journal of physiology* 280: F913-921, 2001.

146. **Wang D, Zhang H, Lang F, and Yun CC**. Acute activation of NHE3 by dexamethasone correlates with activation of SGK1 and requires a functional glucocorticoid receptor. *Am J Physiol Cell Physiol* 292: C396-404, 2007.

147. **Welbourne TC**. Acidosis activation of the pituitary-adrenal-renal glutaminase I axis. *Endocrinology* 99: 1071-1079, 1976.

148. **Welbourne TC**. Glucocorticoid and acid-base homeostasis: effects on glutamine metabolism and transport. *Am J Kidney Dis* 14: 293-297, 1989.

149. **Welbourne TC**. Interorgan glutamine flow in metabolic acidosis. *The American journal of physiology* 253: F1069-1076, 1987.

150. **Wesson DE, Nathan T, Rose T, Simoni J, and Tran RM**. Dietary protein induces endothelin-mediated kidney injury through enhanced intrinsic acid production. *Kidney international* 71: 210-217, 2007.

151. **Wingo CS**. Active proton secretion and potassium absorption in the rabbit outer medullary collecting duct. Functional evidence for proton-potassium-activated adenosine triphosphatase. *The Journal of clinical investigation* 84: 361-365, 1989.

152. **Wright PA, and Knepper MA**. Phosphate-dependent glutaminase activity in rat renal cortical and medullary tubule segments. *The American journal of physiology* 259: F961-970, 1990.

153. **Yanez AJ, Nualart F, Droppelmann C, Bertinat R, Brito M, Concha, II, and Slebe JC**. Broad expression of fructose-1,6-bisphosphatase and phosphoenolpyruvate carboxykinase provide evidence for gluconeogenesis in human tissues other than liver and kidney. *Journal of cellular physiology* 197: 189-197, 2003.

154. **Ye S, Dhillon S, Ke X, Collins AR, and Day IN**. An efficient procedure for genotyping single nucleotide polymorphisms. *Nucleic acids research* 29: E88-88, 2001.

155. **Young JA, and Freedman BS**. Renal tubular transport of amino acids. *Clinical chemistry* 17: 245-266, 1971.

IX. Acknowledgements

I would like to thank the Zurich Center for Integrative Human Physiology for their financial support throughout my PhD studies.

I would like to acknowledge Professor Dr. C. A. Wagner for his kind support and fruitful discussions throughout my PhD studies.

To my friends and family, without you, I could not have gotten this far.

And to my husband, Dr. Thomas F. Fiorito Jr., for his love and constant encouragement; I am forever grateful.

X. Curriculum Vitae

Surname: **BUSQUE**
Name: **Stephanie Marie**
Date of birth: **19.01.79**
Nationality: **American**

Current address: Universitaetstrasse 100
8006 Zurich, Switzerland
Telephone: 011 41 79 600 6428
Email: stephfiorito@gmail.com

EDUCATION

PhD candidate **June 2006-August 2009**
University of Zurich/ETH, Institute of Physiology, Zurich Center for Integrative Human Physiology (ZIHP), Life Science Zurich Graduate School, Zurich, Switzerland
Dissertation: The role and regulation of Slc38a3 (SNAT3) glutamine transporter in the mouse.

Master of Science **May 2003-May 2005**
University of Connecticut, School of Allied Health, Storrs, Connecticut USA
Graduate Assistantship awardee
Dean's list
Master's Dissertation: Amino acids stimulate gastric acid secretion in parietal cells of isolated gastric glands via allosteric activation of the Calcium Sensing Receptor and a novel L-type amino acid transporter.
Research performed at Yale University School of Medicine, Departments of Endocrinology, Gastroenterology and Surgery

Bachelor of Science-Dietetics **August 1997-May 2003**
University of Connecticut, School of Allied Health, Storrs, Connecticut USA
Coordinated Dietetics Program, 900 hours of supervised clinical practice
Dean's list

High School Diploma **July 1997**
Nathan Hale-Ray High School, East Haddam, Connecticut USA

EXPERIENCE

PhD candidate June 2006-present
University of Zurich
Knowledgeable in molecular basic science methodologies, to include: metabolic cage studies, genotyping and phenotyping genetically modified mice, RT-PCR, real-time Quantitative RT-PCR, immunoblotting, immunohistochemistry, urine and serum metabolite analysis. Assisted in physiology laboratory courses for medical students. Knowledgeable and competent in writing and presenting research papers, abstracts, poster and oral communications.

Research Associate 2004-2006
Yale University School of Medicine, Departments of Gastroenterology and Surgery
Performed microsurgical hand dissection of mouse, rat and human gastric, intestinal and colonic epithelia. Performed fluorescence microscopy measurements with an emphasis on intracellular pH and ion transport, and identification of epithelial transporter activity and function. Responsibilities included: presided over the lab and its members, procurement and maintenance of lab materials and equipment, supervision and teaching of students lab members, data analysis and interpretation of results.

Certified Registered Dietitian 2004-present

Research Assistant 2002
Yale University General Clinical Research Center (GCRC)
Assisted in human clinical trials on dietary protein and calcium effects on bone health. Performed nutritional analyses of meals prepared in the GCRC, prepared calcium isotopes for administration of subjects. Assisted in subject assessments, scheduling of experiments, data analysis and interpretation of results.

PROFESSIONAL ACTIVITIES

- Member of American Physiological Society
- Member of American Dietetic Association with national and international affiliation
- Member of Swiss Physiological Society
- Graduate Program in Allied Health Award for Excellence in Research- University of Connecticut 2004
- NIH certification on Human Participants Protection Education for Research Teams- 2004
- Fluent in French, conversational Spanish, currently studying German

XI. List of Publications (*denotes first author publication)

1. Busque SM* and Wagner CA. (2009) Potassium restriction, high protein intake, and metabolic acidosis increase expression of the glutamine transporter SNAT3 (Slc38a3) in mouse kidney. *Am J Physiol Renal.* Article in press.

2. Busque SM*, Kosiek O, Foeller M, Shcheynikov N, Kirchhoff P, Bleich M, et al. (2007). SLC26a7 can function as a chloride-loading mechanism in parietal cells. *Pflugers Arch,* 454(6):989-98.

3. Remy C, Kirchhoff P, Hafner P, **Busque SM**, Müller M, Geibel JP, et al. (2007). Stimulatory pathways of the Calcium-sensing receptor on acid secretion in freshly isolated human gastric glands. *Cell Physiol Biochem,* 19(1-4):33-42.

4. Roepke TK, Anantharam A, Kirchhoff P, **Busque SM**, Young JB, Geibel JP, et al. (2006) The KCNE2 potassium channel ancillary subunit is essential for gastric acid secretion. *J Biol Chem*, 18;281(33):23740-7.

5. Kirchhoff P, Dave MH, Remy C, Kosiek O, **Busque SM**, Dufner M, et al. (2006). An amino acid transporter involved in gastric acid secretion. *Pflugers Arch*, 451(6)738-48.

6. Busque, SM*, Kerstetter JE, Geibel JP, Insogna K. (2005) L-type amino acids stimulate gastric acid secretion by activation of the calcium-sensing receptor in parietal cells. *Am J Physiol Gastrointest Liver Physiol,* 289(4):G664-9.

ABSTRACT PUBLICATIONS: Oral presentations (* denotes presenting author)

1. Busque SM*, Stoeger C and Wagner CA. "Loss of function of the glutamine transporter Slc38a3 is lethal in mice". American Society of Nephrology annual conference, Philadelphia, Pennsylvania, 2008.

2. Busque SM*, Stange G and Wagner CA. "Dysregulation of Slc38a3 and ammoniagenic enzymes in obese insulin-resistant mice". American Society of Nephrology annual conference, Philadelphia, Pennsylvania, 2008.

3. Busque SM*, Mihailova M and Wagner CA. "Dietary potassium, protein intake, and metabolic acidosis alter Slc38a3 in mouse kidney". Swiss Physiological Society annual conference, Bern, Switzerland, 2007, Asher-Hess Poster Prize contestant, accompanied by poster presentation.

4. Busque SM*, Mihailova M and Wagner CA. "Dietary K^+ and protein, and metabolic acidosis alter Slc38a3 expression in kidney". Deutsche Physiologisches Gesellschaft annual meeting, Hannover, Germany, 2007.

5. Busque SM*, Insogna K and Geibel JP. "Amino acids stimulate and enhance gastric acid secretion via two novel pathways". American Gastroenterological Association annual conference, Chicago, Illinois, 2005.

6. Busque SM*, Kerstetter JE, Insogna K and Geibel JP. "A cellular mechanism for dietary protein-induced increases in calcium absorption". American Society for Bone and Mineral Research annual conference, Seattle, Washington, 2004.

ORAL COMMUNICATIONS

7. Busque, SM*, Kerstetter JE, Insogna K and Geibel JP. "Rodent models of dietary protein-induced hypercalciuria". Yale University School of Medicine Core Center for Musculoskeletal Disorders Annual Research Forum, New Haven, Connecticut, 2005.

8. Busque SM*, Insogna K and Geibel JP. "Nutrient sensing by the Calcium Sensing Receptor". Yale University School of Medicine Department of Surgery annual meeting, New Haven, Connecticut, 2005.

9. Busque, SM*, Kerstetter JE, Insogna K and Geibel JP. "A cellular mechanism for dietary protein-induced increases in calcium absorption". Yale University School of Medicine Department of Surgery annual meeting, New Haven, Connecticut, 2004.

ABSTRACT PUBLICATIONS: Poster presentations (* denotes presenting author)

1. Busque SM*, Stoeger C and Wagner CA. “Loss of function of the glutamine transporter Slc38a3 is lethal in mice”. Transporters biannual conference Murten, Switzerland, 2008.

2. Busque SM*, Stange G and Wagner CA. “Dysregulation of Slc38a3 and ammoniagenic enzymes in obese insulin-resistant mice”. Transporters biannual conference Murten, Switzerland, 2008.

3. Busque SM*, Stoeger C and Wagner CA. “Loss of function of the glutamine transporter Slc38a3 is lethal in mice”. German Physiological Society annual meeting, Cologne, Germany, 2008 and Zurich Center for Integrative Human Physiology Annual Symposium, Zurich, Switzerland, 2008.

4. Busque SM*, Mihailova M and Wagner CA. “Dietary K^+ and protein, and metabolic acidosis alter Slc38a3 expression in kidney”. Zurich Center for Integrative Human Physiology Annual Symposium, Zurich, Switzerland, 2007.

5. Busque SM*, Mihailova M and Wagner CA. “Dietary potassium, protein intake and metabolic acidosis alter Slc38a3 expression in mouse kidney”. American Society of Nephrology annual conference, San Francisco, California, 2007.

6. Busque SM*, Mihailova M and Wagner CA. “Dietary potassium, protein intake, and metabolic acidosis alter Slc38a3 in mouse kidney”. Swiss Physiological Society annual conference, Bern, Switzerland, 2007, Asher-Hess Poster Prize contestant.

7. Busque SM*, Geibel JP. “Concomitant activation of the Calcium-sensing receptor (CaSR) and the H2 receptor results in inhibition of acid secretion in isolated rat gastric glands”. American Gastroenterological Association annual conference 2006.

8. Abdulnour-Nakhoul SM, Busque SM, Geibel JP. “Intracellular pH and calcium measurements in mouse esophagus.” American Gastroenterological Association annual conference 2006.

9. Busque SM*, Osigweh JM, Dudrick SJ, Geibel JP. "Functional identification of gastric type H^+,K^+-ATPase in rat gastric fundus glands". American Gastroenterological Association annual conference 2005.

10. Busque SM*, Osigweh JM, Dudrick SJ, Geibel JP. "Calcium Sensing Receptor modulates fundic gland acid secretion". American Gastroenterological Association annual conference 2005.

11. Busque SM*, Kerstetter JE, Insogna K and Geibel JP. "A cellular mechanism for dietary protein-induced increases in calcium absorption". Connecticut Dietetic Association annual meeting, Hartford, Connecticut 2004.